The nonavian theropod quadrate II: systematic usefulness, major trends and cladistic and phylogenetic morphometrics analyses

Christophe Hendrickx[1,2]

[1] Universidade Nova de Lisboa, Departamento de Ciências da Terra, Faculdade de Ciências e Tecnologia, Quinta da Torre, 2829-516, Caparica, Portugal.

[2] Museu da Lourinhã, 9 Rua João Luis de Moura, 2530-158, Lourinhã, Portugal.

chritophe.hendrickx@hotmail.com

Ricardo Araújo[2,3,4,5]

[2] Museu da Lourinhã, 9 Rua João Luis de Moura, 2530-158, Lourinhã, Portugal.

[3] Huffington Department of Earth Sciences, Southern Methodist University, PO Box 750395, 75275-0395, Dallas, Texas, USA.

[4] Instituto de Plasmas e Fusão Nuclear, Instituto Superior Técnico,Universidade de Lisboa, Portugal.

[3] Museum für Naturkunde, Berlin, Germany.

rmaraujo@smu.edu

Octávio Mateus[1,2]

[1] Universidade Nova de Lisboa, Departamento de Ciências da Terra, Faculdade de Ciências e Tecnologia, Quinta da Torre, 2829-516, Caparica, Portugal.

[2] Museu da Lourinhã, 9 Rua João Luis de Moura, 2530-158, Lourinhã, Portugal.

omateus@fct.unl.pt

ABSTRACT

26

27   The skull-bone quadrate in nonavian theropods is very diverse morphologically

28 alongside the disparity of the group as a whole. However this disparity has been

29 underestimated for taxonomic purposes. In order to evaluate the phylogenetic potential and

30 investigate the evolutionary transformations of the quadrate, we conducted a Catalano-

31 Goloboff phylogenetic morphometric analysis as well as a cladistic analysis using 98 discrete

32 quadrate related characters. The cladistic analysis provides a fully resolved tree mirroring to

33 some degree the classification of nonavian theropods.

34   The quadrate morphology by its own provides a wealth of data with strong

35 phylogenetic signal and allows inference of major trends in the evolution of this bone.

36 Important synapomorphies include: for Abelisauroidea, a lateral ramus extending to the

37 ectocondyle; for Tetanurae, the absence of the lateral process; for Spinosauridae, a medial

38 curvature of the ventral part of the pterygoid ramus occurring just above the mandibular

39 articulation; for Avetheropoda, an anterior margin of the pterygoid flange formed by a

40 roughly parabolic margin; and for Tyrannosauroidea, a semi-oval pterygoid flange shape in

41 medial view. The Catalano-Goloboff phylogenetic morphometric analysis reveals two main

42 morphotypes of the mandibular articulation of the quadrate linked to function. The first

43 morphotype, characterized by an anteroposteriorly broad mandibular articulation with two

44 ovoid/subcircular condyles roughly subequal in size, is found in Ceratosauria,

45 Tyrannosauroidea and Oviraptorosauria. This morphotype allows a very weak displacement

46 of the mandible laterally. The second morphotype is characterized by an elongate and

47 anteroposteriorly narrow mandibular articulation and a long and parabolic/sigmoid

48 ectocondyle. Present in Megalosauroidea, Carcharodontosauridae and Dromaeosauridae, this

49 morphotype permits the lower jaw rami to be displaced laterally when the mouth opened.

50

INTRODUCTION

In theropods and non-mammalian tetrapods in general, the quadrate is a paired bone located in the posterior part of the skull, allowing the lower jaw to articulate with the cranium (Brusatte, 2012). The nonavian theropod quadrate always displays a common anatomical architecture: a ventrodorsally elongated body, an anteriorly-oriented pterygoid flange, a mandibular articulation with two condyles separated by a furrow, a lateral articulation with the quadratojugal, and a dorsal condyle, or quadrate head, articulated with the cotylus of the squamosal. Nevertheless, the quadrate morphology and each quadrate sub-units change conspicuously among different clades of theropods (Maryańska and Osmólska, 1997; Sereno et al., 2008) so that this cranial bone shows great taxonomic potential (Elzanowski et al., 2001; Currie, 2006). Yet, no thorough study has tried to evaluate the phylogenetic value of the quadrate bone in nonavian theropods. Quadrate-related cladistic characters are minimal in most cladistic analyses performed in nonavian theropods, with a maximum of eight characters in (Choiniere et al., 2014) data matrices. Maryańska and Osmólska (1997) and Currie (2006) were the first quadrate-driven articles that investigated the morphological differences among nonavian theropod quadrates; however the later considered only five characters in order to determine theropod relationships. In essence, the paucity of characters that have been used underestimates the morphological diversity among the various clades of nonavian theropods. Here, we conduct a cladistic analysis based on a datamatrix of 98 quadrate-related characters coded for 56 taxa belonging to the majority of clades of nonavian theropods. We also performed a phylogenetic morphometric analysis (Catalano et al., 2010; Goloboff and Catalano, 2011) based on quasi homologous landmark configurations of a sub-sample of 23 taxa out of the 56 taxa above.

Institutional Abbreviations

76   **AMNH FARB,** American Museum of Natural History, collection of fossil reptiles,

77   amphibians and birds, New York, USA; **BMNH,** The Natural History Museum, London, UK;

78   **BYUVP,** Brigham Young University Vertebrate Paleontology, Provo, Utah, USA; **CMNH,**

79   Carnegie Museum, Pittsburgh, Pennsylvania, USA; **FMNH,** Field Museum of Natural

80   History, Chicago, Illinois, USA; **FRDC-GS,** Fossil Research and Development Center, Gansu

81   Bureau of Geology and Mineral Resources Exploration, Lanzhou, China; **GR,** Ghost Ranch

82   Ruth Hall Museum of Paleontology, Ghost Ranch, New Mexico, USA; **IGM,** Mongolian

83   Institute of Geology, Ulaan Bataar, Mongolia; **IPFUB,** Institute for Paleontology of the Freie

84   Universität, Berlin, Germany; **IVPP,** Institute for Vertebrate Paleontology and

85   Paleoanthropology, Beijing, China; **LACM,** Los Angeles County Museum of Natural History,

86   Los Angeles, California, USA; **MACN,** Museo Argentino de Ciencias Naturales, Buenos

87   Aires, Argentina; **MB**, Museum für Naturkunde der Humboldt Universität, Berlin, Germany;

88   **MCF PVPH,** Museo Municipal Carmen Funes, Paleontologia de Vertebrados, Plaza Huincul,

89   Argentina; **MCNA,** Museo de Ciencias Naturales y Antropológicas de Mendoza, Mendoza,

90   Argentina; **MIWG,** Dinosaur Isle, Isle of Wight Museum Services, Sandown, UK; **ML,**

91   Museu da Lourinhã, Lourinhã, Portugal; **MNHN,** Muséum national d'Histoire naturelle,

92   Paris, France; **MNA,** Museum of Northern Arizona, Flagstaff, Arizona, USA; **MNN,** Musée

93   National du Niger, Niamey, Niger; **MSNM,** Museo di Storia Naturale di Milano, Milan, Italy;

94   **MUCPv,** Museo de Ciencias Naturales de la Universidad Nacional de Comahue, Neuquén,

95   Argentina; **MWC,** Museum of Western Colorado, Fruita, Colorado, USA; **NCSM,** North

96   Carolina Museum of Natural Sciences, Raleigh, NC, USA; **OUMNH,** Oxford University

97   Museum, Oxford, UK; **PIN,** Paleontological Institute of the Russian Academy of Sciences,

98   Moscow, Russia; **PULR,** Paleontología, Universidad Nacional de La Rioja, La Rioja, Spain.;

99   **PST,** Paleontological and Stratigraphic Section of the Geological Institute, Mongolian

100   Academy of Sciences, Ulaan Baatar, Mongolia; **PVSJ,** Instituto y Museo de Ciencias

101   Naturales, San Juan, Argentina; **SMA,** Sauriermuseum Aathal, Aathal, Switzerland; **SMNS,**

102   Staatliches Museum für Naturkunde, Stuttgart, Germany; **IGM,** Paleontology and

103   Stratigraphy Section of the Geological Institute, Ulan Baatar, Mongolia; **RTMP,** Royal

104   Tyrrell Museum of Palaeontology, Drumheller, Alberta, Canada; **UCMP,** University of

105   California Museum of Paleontology, Berkeley, California, USA; **UC,** University of Chicago

106   Paleontological Collection, Chicago, USA; **UMNH,** Utah Museum of Natural History, Salt

107   Lake City, Utah, USA; **USNM,** United State National Museum Vertebrate Paleontology,

108   Washington D. C., USA; **UUVP,** Utah Museum of Natural History, Salt Lake City, Utah,

109   USA; **ZPAL,** Instytut Paleobiologii PAN, Warsaw, Poland; **WDC,** Wyoming Dinosaur

110   Center, Thermopolis, USA

111

MATERIAL AND METHODS

113   Table 1

114   **Cladistic Analysis**

115   In order to assess the evolution and taxonomic value of the quadrate bone in nonavian

116   theropods, a datamatrix including quadrate-related characters only was created and scored in

117   55 nonavian theropod taxa and one outgroup taxa (Table 1, Appendix 1). Quadrates

118   pertaining to most clades of nonavian Theropoda have been examined and coded from 1)

119   first-hand observations (35 taxa equivalent to 62.5% of the dataset) 2) high-resolution

120   photographs (16 taxa equivalent to 28.5%), and 3) by using full descriptions and illustrations

121   of the bone in the literature for 5 taxa (Table 1). Most nonavian theropods with well-preserved

122   and well-visible quadrates were included in the analysis and coded at the species level. Due to

123   the weak variation of quadrate morphology among oviraptorid taxa and the exhaustive

124   description of their anatomy in a single paper (Maryańska and Osmólska, 1997), the clade of

125   Oviraptoridae was coded at the "family" level as operational taxonomic units (OTU).

126   Likewise, troodontid quadrates were also coded at the "family" level due to the scarcity of

127   information on their morphology, gleaned from several published and unpublished specimens,

128   and the absence of a single complete and well-illustrated troodontid in the literature.

129   Compsognathidae were not included in the cladistic analysis due to lack of

130   information of the quadrate morphology and bad preservations of this bone. Indeed, the

131   quadrates of all compsognathids such as *Compsognathus corallestris* (Ostrom, 1978; Peyer,

132   2006), *Juravenator starki* (Chiappe and Göhlich, 2010), *Scipionyx samniticus* (Dal Sasso and

133   Signore, 1998; Dal Sasso and Maganuco, 2011), *Huxiagnathus orientalis* (Hwang et al.,

134   2004), *Sinocalliopteryx gigas* (Ji et al., 2007) and *Sinosauropteryx prima* (Currie and Chen,

135   2001) have been flattened by post mortem deformation and are either poorly preserved or

136   obscured by other bones.

137   The data matrix encompasses 98 equally weighted discrete morphological characters

138   related to the quadrate (Appendices 1 & 2) and allowing to test and propose several quadrate

139   synapomorphies for the 56 taxa coded (Appendix 3.1; Figure S5). A combination of 18

140   characters are taken from the literature and 80 characters (81 %) are new. Among the 54

141   multistate characters, twelve were treated as ordered (Appendix 1), and most quadrate related

142   characters are illustrated in the appendices (Figures S1-S3). *Eoraptor lunensis*, considered to

143   be either a basal sauropodomorph (Martinez et al., 2011; Sereno et al., 2013) or a basal

144   theropod (e.g., Nesbitt et al., 2009; Nesbitt, 2011; Sues et al., 2011) in the most recent

145   cladistic studies, was treated as the outgroup. In order to constrain all major theropod clades

146   and visualize the quadrate-based synapomorphies for each clades, a second analysis was

147   performed on a supermatrix combining our quadrate-based data matrix to six recent datasets

148   on non-avian theropods based on the whole skeleton (Choiniere, Xu, et al., 2010; Brusatte,

149   Norell, et al., 2010; Martinez et al., 2011; Carrano et al., 2012; Pol and Rauhut, 2012), and

150   from which all quadrate-related characters were removed. The resulting supermatrix includes

151   1889 characters and only twelve quadrate related characters were treated as ordered

152   (Appendix 3.2).

153   TNT v1.1 (Goloboff et al., 2008) was employed to search for most-parsimonious trees

154   (MPTs). The matrix and supermatrix were analyzed under the 'New Technology Search' with

155   the 'driven search' option (TreeDrift, Tree Fusing, Ratchet, and Sectorial Searches selected

156   with default parameters), and stabilizing the consensus twice with a factor of 75. The

157   consistency and retention indices as well as the Bremer supports (Bremer, 1994) were

158   calculated using the "stats" and "aquickie" commands, respectively, and a bootstrap analysis

159   was performed with the standard options.

160   The dataset was also analyzed with WinClada 1.00.08 (Nixon, 2002) after making

161   characters non-additive (fitch) and trees were searched for using the Ratchet (Island Hopper)

162   option with default settings.

163

164   **Phylogenetic Morphometrics Analysis**

165   The phylogenetic morphometrics (hereinafter phylo-morpho) analysis approach is

166   based on Catalano et al. (2010) and Goloboff and Catalano (2011) method. This method

167   extends the parsimony criteria for characters like landmark data that change in more than one

168   dimension. The method calculates the score of landmark configurations on a tree as the sum

169   of the difference (weighted or not) in landmark position of each of its landmarks along all the

170   branches of the tree. A different landmark configuration (i.e., set of quasi-homologous points

171   that describes the structure under analysis) is therefore regarded as a different character. For

172   example, the same set of landmarks of the anterior view of the quadrate is considered a

173   character. Several configurations can be included in a single phylogenetic analysis and

174   landmark data can also be analyzed in combination with alternative sources of evidence like

175   traditional morphological characters or molecules. In that case the tree score is the sum of the

176 scores for each landmark configuration plus the score for each traditional character. We ran

177 two different sets of analyses: 1) each individual phylo-morpho character alone; and 2) a

178 combination of all phylo-morpho characters (Appendices 6-7). This array of analysis allowed

179 us to understand the influence of the phylo-morpho characters on resolving the phylogeny of

180 nonavian theropod quadrates and, to provide a substantial basis for discretization of

181 morphotypes that can be observed with the naked eye, but are hard to define verbally (e.g.,

182 outline of the posterior view of the nonavian theropod quadrate).

183   The phylo-morpho analysis comprised a sample of 23 taxa out of the 56 used in the

184 traditional cladistic analysis (Table 1; Appendix 6). The selection of a smaller sample of

185 nonavian theropod quadrates was based on the following criteria, the quadrate 1) had to be

186 complete, 2) could not be post-mortem deformed, 3) had to be isolated from the cranium, and

187 4) all views had to be well-preserved. Two quadrate morphotypes were included for

188 *Allosaurus* (*A*. *fragilis* and *A*. '*jimmadseni*') and *Ceratosaurus* (*C*. '*magnicornis*' and *C*.

189 '*dentisulcatus*' sensu Madsen and Welles, 2000). In our analysis we used three different

190 phylo-morpho characters of the quadrate: outline of the medial view (character 1; 8

191 landmarks), outline of the ventral view (character 2; 8 landmarks) and outline of the posterior

192 view (character 3; 12 landmarks). The rationale for the position of the landmarks is

193 summarized in Appendix 5 Figure S6 and detailed below. The outline of the anterior and

194 dorsal views was not used. Not only some of the landmarks visible anteriorly are also visible

195 posteriorly (i.e., it would imply overweighting certain landmarks) but also, in the dorsal view,

196 because it was hard to find homologous landmarks through taxa due to the lack of reference

197 points of the quadrate head in nonavian theropods. Pictures from different taxa were sorted

198 and compiled for each character individually using tpsUtil (Tps geometric morphometrics

199 software is available for free download at http://life.bio.sunysb.edu/morph/soft-utility.html).

200 The digitization of the landmarks on the pictures was done with tpsDig2. The resulting file

201 was taken to tpsRelw were only the alignment was saved by using "Save aligned specimens"

202 option. The resulting *.tps file had to be parsed in order to run in TNT v1.1 (Goloboff et al.,

203 2008). A pre-requisite for the analysis of landmark data is the superimposition of the

204 configurations (= alignment). This is accomplished by superimposition methods, i.e., rotation,

205 translation and sizing. Because different alignments can produce different phylogenetic

206 results, we generated two different dataset, the first aligned using RFTRA (Rho-Theta

207 Resistant-fit Analysis, see Siegel and Benson, 1982; Rohlf and Slice, 1990) and the second

208 performing an ordinary superimposition by minimizing the sum of linear distances of each

209 configuration against a reference configuration (Catalano and Goloboff, 2012).

210   In order to reconstruct a phylogeny departing from landmark data alone, we used the

211 landsch.run TNT script. To run the combined search we used the TNT script

212 landcombsch.run. The latter allows running a combined analysis of traditional and phylo-

213 morpho characters in an analogous way as two (or more) different gene sequences can be

214 analyzed together where each one contributes to the resolution of a phylogeny. Both scripts

215 are available at http://tnt.insectmuseum.org/index.php/Scripts. The phylogenetic searches

216 were re-run considering four different levels of search thoroughness (the scripts pre-defined

217 levels 0, 1, 2 and 3). The parameters that define a "level of thoroughness" are: number of

218 replicates, termpoints (i.e., inclusion of the geometric medians as a possible point for an

219 ancestral landmark position), number of cell in the grid (i.e., the higher number of cells the

220 more points available for reconstruction of the ancestral positions), nesting level (i.e., a grid

221 can be nested within another grid in order to allow a more precise, and computationally-

222 efficient, reconstruction of the landmark ancestral positions), and neighbors level (i.e.,

223 number of neighboring cells included in the nesting level). The score of each configuration

224 were rescale in all the analysis is such a way that the contribution of one landmark

225 configuration character is similar to a traditional character (TNT default option). For analysis

226 3 the driven search option of TNT was used considering Sectorial search, tree drifting, tree

227 fusing, and ratchet algorithms, and finishing the search upon consensus stabilization. The

228 exact same characters used in analysis 4 were used in analysis 3. For the analysis of the

229 traditional characters TBR (tree bisection and reconnection) and 116 non-additive characters

230 were employed. The resulting tree score is the sum of the tree length and the scaled weighted

231 score for the phylo-morpho characters (see Goloboff and Catalano, 2011, p. 47). On this

232 analysis, both ordinary superimposition minimization and RFTRA datasets, the tree scores

233 converge to an asymptote at the level 2 of thoroughness. This implies that the optimality of

234 the trees can be correctly established with a thoroughness level 2. Thus, we selected the tree

235 that would mirror more accurately present day knowledge on nonavian theropod phylogeny.

236 A more accurate tree is the one that recovers a higher number of known clades in the analysis.

237 In our analysis that was the case for level 2, re-aligned using RFTRA. The criterion used for

238 picking between different trees was based on the tree score; the lowest the tree scores the

239 more parsimonious the tree topology (see Catalano et al., 2010 for an explanation of the tree

240 score calculation).

241

242 **Landmark configurations.** The landmark configuration schemes chosen (Appendix 5,

243 Figure S6) attempt to capture as much information possible that can depict accurately the

244 evolutionary processes on the nonavian theropod quadrate (Zelditch et al., 2009). The

245 landmarks chosen were selected manually and are all of Bookstein's type 2, i.e., tip of a bony

246 process or local curvature minima or maxima (Bookstein, 1997).

247 *Medial view (Character 1; Figure S6.1).* Landmark 1 is the apex of the curvature of

248 the mandibular articulation. Landmark 2 is the apex of the curvature of the dorsal quadrate

249 head. Landmark 3 is the mid-distance between the apices of the dorsal quadrate head and the

250 mandibular articulation. Landmark 4 is the dorsal intersection between the quadrate ridge and

the pterygoid flange. Landmark 5 is the dorsal kink of the pterygoid flange. Landmark 6 is the

ventral kink of the pterygoid flange. Landmark 7 is the apex of the curvature of the ventral

portion of the pterygoid flange. Landmark 8 is the ventral intersection of the quadrate ridge

and the pterygoid flange.

Ventral view (Character 2; Figure S6.2). Landmark 1 is the anterior point on the semi-

major axis of the ellipse formed by the entocondyle. Landmark 2 is the posterior point on the

semi-major axis of the ellipse formed by the entocondyle. Landmark 3 is the medial point on

the semi-minor axis of the ellipse formed by the entocondyle. Landmark 4 is the lateral point

on the semi-minor axis of the ellipse formed by the entocondyle. Landmark 5 is the medial

point on the semi-major axis of the ellipse formed by the ectocondyle. Landmark 6 is the

lateral point on the semi-major axis of the ellipse formed by the ectocondyle. Landmark 7 is

the anterior point on the semi-minor axis of the ellipse formed by the ectocondyle. Landmark

8 is the posterior point on the semi-minor axis of the ellipse formed by the ectocondyle.

Posterior view (Character 3; Figure S6.3). Landmark 1 is the ectocondyle curvature

apex and landmark 2 is the curvature apex of the entocondyle, while landmark 3 is the dorsal

quadrate head curvature apex. Landmark 4 is on the lateral margin of the photographic plane

at the level of the mid-height of the quadrate, and the landmark 5 is on the medial margin.

Landmark 6 is the dorsalmost point of the ventral quadratojugal contact. Landmark 7 is the

ventralmost point of the ventral quadratojugal contact. Landmark 8 is the apex of the

concavity formed by the quadrate foramen. Landmark 9 is the dorsalmost point of the

quadrate foramen. Landmark 10 is the ventralmost point of the quadrate foramen. Landmark

11 is located on the lateral-most point of the posterodorsal margin of the ectocondyle.

Landmark 12 is located on the medial-most point of the posterodorsal margin of the

entocondyle.

276

277 Figure 1 and 2

278 **Cladistic Analysis**

279   The cladistic analysis of the data matrix of quadrate-based characters and including 56

280 theropod taxa yielded 40 most parsimonious trees (MPTs), in which the strict consensus trees

281 (Length = 592 steps; CI = 0.271, RI = 0.536) resulted in a few polytomies affecting clades of

282 no more than three taxa (see Appendix 4 Figure S4). Although the consensus tree poorly

283 mirrors the current classification of nonavian theropods, many theropod clades such as

284 Noasauridae, Megalosauridae, Spinosauridae, Allosauridae, Carcharodontosauridae,

285 Tyrannosauridae, Ornithomimosauria, Therizinosauroidea, Oviraptorosauria and

286 Dromaeosauridae were found resolved. As it was noted for teeth (Hwang, 2007; Hendrickx

287 and Mateus, 2014), quadrate-related characters are good at recovering individual clades, but

288 not at resolving the relationship between those clades. Nevertheless, the deletion of *Eoraptor*,

289 *Abelisaurus* and *Irritator*, from which few information on the quadrate can be extracted (55%,

290 46% and 64% of missing data, respectively), gave a different tree topology. The cladistic

291 analysis performed on the datamatrix of 53 taxa yielded, this time, 19 MPTs in which the

292 consensus tree (Length = 580 steps; CI = 0.285, RI = 0.554; Figure 1) recovered to a much

293 better degree the general topology of theropod classification with the usual major clades (e.g.,

294 Neotheropoda, Averostra, Ceratosauria, Tetanurae, Megalosauroidea). Indeed, when rooting

295 *Herrerasaurus* as the outgroup, *Eodromaeus*, *Tawa*, *Dilophosaurus* and the clade of

296 coelophysoids (*Liliensternus* + *Syntarsus*) were correctly retrieved as the most-basal

297 theropods, Neotheropoda and Averostra were found monophyletic and the latter includes both

298 Ceratosauria and Tetanurae. Likewise, Megalosauroidea was retrieved as a clade closely

299 related to the basal tetanuran *Monolophosaurus* (Carrano et al., 2012) and correctly includes

300 Megalosauridae and Spinosauridae.

301   Nevertheless, the Tetanurae clade does not correspond to the general idea of the

302   classification of these derived averostrans (Figure 1) as the common clades of Allosauroidea,

303   Avetheropoda, Coelurosauria and Maniraptora were not resolved. For instance, non-

304   carcharodontosaurids allosauroids were found closely related to Therizinosauria,

305   Carcharodontosauridae forms the sister clade of Ornithomimosauria + Dromaeosauridae, and

306   non-tyrannosaurid Tyrannosauroidea, Oviraptorosauria and Troodontidae are gathered in a

307   same clade. In fact, the classification of basal theropods (i.e., non-tetanuran Theropoda) is

308   much better resolved than this of Tetanurae. This can be explained by the large sample of

309   non-coelurosaur theropods in the dataset (60% of the datamatrix), whereas coelurosaurs are

310   under-represented (21 taxa representing 36.5%) and includes one or two taxa of several

311   coelurosaur clades such as Ornithomimosauria, Alvarezsauroidea and Therizinosauria.

312   Furthermore, the clades of Oviraptoridae and Troodontidae have both been coded as a single

313   OTU and no compsognathid taxa were incorporated in the datamatrix. It is therefore likely

314   that the inclusion of more coelurosaur taxa into the datamatrix of quadrate-based characters in

315   the future will allow mirroring to a better degree the current classification of Tetanurae and

316   Coelurosauria. Interestingly, the quadrate of megalosauroids and allosauroids are relatively

317   similar as members of those two clades were found closely related, giving some support to a

318   monophyletic Carnosauria (Megalosauroidea + Allosauroidea) as it was previously suggested

319   (Kurzanov 1989; Currie 1995; Rauhut 2003).

320   With a high decay index, Spinosauridae (Bremer support of 5), Allosauridae (Bremer

321   support of 4), Tyrannosauridae (Bremer support of 4) and Ornithomimosauria (Bremer

322   support of 4) are the best supported clades and all possess a highly diagnostic quadrate. The

323   quadrate of non-carcharodontosaurid Allosauroidea (here gathered in a monophyletic group),

324   Therizinosauria and Dromaeosauridae, all with a Bremer support of 3, is also easily

325   recognizable in these theropods. In fact, the cladistic analysis performed on the supermatrix of

326 56 taxa, and yielding 34 MPTs (Length = 3616 steps; CI = 0.562; RI = 0.631; Figure 2), has

327 shown that many theropod clades can be defined by using a combination of ambiguous and

328 unambiguous quadrate-based synapomorphies (Figure 2, Appendix 4 Figures S5A-B). Among

329 the best resolved clades, Spinosauridae are supported by 10 synapomorphies (with five

330 unambiguous), and eight synapomorphies define the clades of Ceratosauria and

331 Carcharodontosauridae. Clades of more than three quadrate synapomorphies include

332 Abelisauroidea (4), Averostra (5), Megalosauridae (5), Avetheropoda (5), Allosauroidea (6),

333 Allosauridae (4), Tyrannosauridae (5) and Ornithomimosauria (6). Coelophysoidea,

334 Abelisauridae and Dromaeosauridae are the only clade of theropods that are not define by a

335 single quadrate synapomorphy.

336

337 Figure 3

338 **Phylogenetic Morphometrics Analysis**

339   The two most interesting results concerning the phylogenetic morphometric analysis

340 performed character by character is the dichotomy retrieved when character 2 and 3 are run

341 independently (Figure 3; Appendix 6). For the posterior view (character 3; Figure 3.1), this

342 consists essentially on a 'coelurosaurian' (Morphotype A) *versus* a 'ceratosaurian' type

343 (Morphotype B). The distinction of these two morphotypes lies essentially on the clear

344 differences of the morphology of the quadrate foramen (landmarks 6-10) and the robustness

345 of the quadrate body (landmarks 1,2 and 3). In morphotype A, the quadrate is low and stout

346 comparatively to the tall and slender bone in morphotype B. Also the quadrate foramen of

347 morphotype A is well-delimited and relatively broad lateromedially, but it is shallow,

348 lateromedially narrow or completely absent in morphotype B. The latter morphotype can be

349 found in ceratosaurian taxa, as well as in megalosaurids and carcharodontosaurids theropods

350 (Appendix 7, Figure S8). On the other hand, morphotype A is present in all coelurosaurians

351 and *Dilophosaurus*, non-carcharodontosaurid allosauroids and Spinosauridae. The basal

352 placement of *Sinraptor* and *Acrocanthosaurus* in each 'morphoclade' reveals the clear

353 transition from one morphotype to the other during the evolution of Allosauroidea.

354   For the ventral view (character 2; Figure 3.2), the dichotomy divides a ceratosaurian

355 *versus* a megalosauroid type, although this result is more blurred due to the recovery of

356 *Afrovenator* among the ceratosaurian-dominated clade.

357

ANATOMY OF THE NONAVIAN THEROPOD QUADRATE

359 Figure 4

Non-neotheropod Theropoda

361   *Eoraptor lunensis* (PVSJ 512; Sereno et al., 2013; Figure 4.5)*, Herrerasaurus*

362 *ischigualastensis* (PVSJ 53 = *Frenguellisaurus ischigualastensis*; PVSJ 407; Figure 4.2–4.4)*,*

363 *Eodromaeus murphi* (PVSJ 562; Figure 4.5–4.10); *Daemonosaurus chauliodus* (Sues et al.,

364 2011); *Tawa hallae* (Nesbitt et al., 2009; Figure 4.11–4.16).

365   Although recent discoveries of new basal theropods have increased dramatically in the

366 last five years, information regarding the quadrate anatomy can be improved. The quadrates

367 of many basalmost theropods are still articulated in the cranium and therefore not visible in

368 anterior, ventral and dorsal views. This is the case for *Eoraptor lunensis* which most of the

369 right quadrate is covered by matrix, and *Herrerasaurus ischigualastensis* (PVSJ 407) in

370 which the mandibular condyles are still in articulation with the lower jaw (Sereno and Novas,

371 1994). Likewise, the right quadrate bone of *Daemonosaurus chauliodus* is not only badly

372 preserved, but also shows the lateral part of the bone only. Fortunately, the left quadrate of

373 *Eodromaeus murphi* and both left and right quadrates of *Frenguellisaurus ischigualastensis*

374 (PVSJ 53), now considered to be a junior synonym of *Herrerasaurus ischigualastensis*

375 (Novas, 1994), and *Tawa hallae*, the most derived form of non-neotheropod Theropoda

376 (sensu Nesbitt et al., 2009), are relatively well preserved and allow a better understanding of

377 the quadrate anatomy in non-neotheropod Theropoda.

378 The quadrate of these basalmost theropods is tall (strongly elongated ventrodorsally

379 relative to the lateromedial width of the mandibular articulation; ratio corresponding to the

380 lateromedial width of mandibular articulation divided by the ventrodorsal length from

381 entocondyle to quadrate head of less than 0.35), lateromedially narrow, and possesses a small

382 quadrate foramen (Figure 4.1, 4.5) at the lower one-third of the quadrate body in *E. lunensis*

383 and *H. ischigualastensis* (presence of a quadrate foramen in *E. murphi*, *D. chauliodus* and *T.*

384 *hallae* remains unknown). The quadrate foramen of these two taxa is mostly delimited by the

385 quadrate and only the lateral border is formed by the quadratojugal. In *H. ischigualastensis*,

386 the quadrate foramen is adjacent to the quadrate ridge (PVSJ 53, 407; Figure 4.1), whereas the

387 foramen is well-separated from the ridge in *E. lunensis* (contra Martinez and Alcober, 2009;

388 Figure 4.5) as in the basal sauropodomorph *Panphagia protos* (PVSJ 874, (Martinez and

389 Alcober, 2009).

390 The quadrate ridge in *H. ischigualastensis* and *E. murphi* is prominent, rod-shaped,

391 strongly inclined laterally and get flared above the entocondyle, at one third of the quadrate

392 body (Figure 4.1, 4.8). In *E. lunensis*, the quadrate ridge is only visible on the dorsal part of

393 the quadrate body, just below the quadrate head. Like in *H. ischigualastensis* and *E. murphi*,

394 the ridge reaches the quadrate head but, similar to *T. hallae*, it is straight and not inclined

395 laterally. In lateral view, the posterior margin of the quadrate ridge is concave in *E. lunensis*

396 (Sereno et al., 2013), *E. murphi* and *T. hallae*, but straight in *H. ischigualastensis*.

397 In *E. murphi* and *T. hallae*, the ventral quadratojugal contact is ovoid to D-shaped,

398 with an irregular articulating surface. It faces postero-laterally in *E. murphi* (Figure 4.8), and

399 laterally in *T. hallae*. The ventral quadratojugal contact is wider than the dorsal one in all non-

400 neotheropod theropods, as the dorsal quadratojugal contact corresponds to a thin line on the

401   lateral surface of the lateral process in *E. lunensis* and *H. ischigualastensis*. The ventral

402   quadratojugal contact projects slightly anteriorly in *T. hallae* (Figure 4.16), unlike *H.*

403   *ischigualastensis* and *E. murphi* in which the quadratojugal process is absent (Figure 4.4,

404   4.10).

405   Like non-tetanuran theropods, the quadrate of *H. ischigualastensis* possesses a

406   subtriangular lateral process projecting anterolaterally that joins the quadrate body at the

407   foramen level ventrally and the quadrate head dorsally. A lateral process reaching the

408   quadrate head is also present in *E. lunensis* (Sereno et al., 2013), but its lateral margin is

409   rather parabolic, and the process is relatively short and only projects laterally (Figure 4.5)

410   when compared to *H. ischigualastensis*. A parabolic lateral process also exists in *D.*

411   *chauliodus* but its dorsal extent terminates well-ventral from the quadrate head. The lateral

412   process of all non-neotheropod theropods contacts the quadratojugal and the squamosal along

413   its lateroventral and laterodorsal rims, respectively. The presence of a lateral process in *E.*

414   *murphy* and *T. hallae* cannot be determined as this part of the quadrate body is missing.

415   The pterygoid flange of basalmost theropods is subtrapezoidal in outline (i.e., the

416   anterior margin of the flange is roughly formed by three sides where the most anterior one is

417   straight and short ventrodorsally), and the most anterior point of the flange appears at mid-

418   height of the quadrate. The pterygoid flange meets the quadrate body far above the

419   mandibular condyles in *H. ischigualastensis*, *E. murphi* and *D. chauliodus*, a condition shared

420   by most other non-tetanuran theropods (pers. obs.). The angle formed by the ventral margin of

421   the pterygoid flange and the main axis of the quadrate ridge varies between 60° and 70°. The

422   flange only projects anteriorly and its anterior part does not curve medially. Nevertheless,

423   there is a weak medial curvature of the ventral margin of the flange ('horizontal shelf' sensu

424   Sereno et al., 2013), and a shallow medial fossa exists in the posteroventral part of the

425   pterygoid flange.

426   In *D. chauliodus*, the quadrate head is an extension of a cylindrical projection of the

427   quadrate shaft. It is single headed, small (Sues et al., 2011) and the posterior margin is

428   convex. The pterygoid flange reaches the quadrate body just below the anteroventral limit of

429   the quadrate head. The same condition occurs in *E. murphy* where the quadrate head is

430   globular in lateral view, and roughly subtriangular in shape with rounded corner in dorsal

431   view (Figure 4.9). The quadrate head and the dorsalmost part of the quadrate body seem to be

432   slightly posterodorsaly-oriented in *E. lunensis* but sub-horizontal in *H. ischigualastensis*, *D.*

433   *chauliodus* and *E. murphy* (contra Martinez et al., 2011, figure 1B). In *H. ischigualastensis*,

434   the quadrate head is convex, subtriangular in outline in posterior view and exposed in lateral

435   view, and a flattened medial surface below the quadrate head contacts the paroccipital process

436   (Sereno and Novas, 1994).

437   Although little information is known about the morphology of the mandibular

438   articulation in the holotypes of *E. lunensis* and *H*. *ischigualastensis*, this part of the quadrate

439   is however well-preserved in a specimen referred to *H. ischigualastensis* (PVSJ 53; Figure

440   4.5), and almost complete in *E. murphi* and *T. hallae* in which the anterior part of the

441   ectocondyle and entocondyle, respectively, is missing. Both ecto- and entocondyle are

442   subequal in size in *H. ischigualastensis* but the ectocondyle is longer in *E. murphi* and *T.*

443   *hallae*. The ectocondyle is elliptical of *H. ischigualastensis* and *E. murphi* whereas it is

444   slightly sigmoid in *T. hallae*. The entocondyle is elliptical, strongly elongated and does not

445   protrude anteriorly in both *H. ischigualastensis* (Figure 4.4) and *E. murphi* (Figure 4.10). The

446   mandibular condyles are separated by a shallow and diagonally-oriented intercondylar sulcus

447   in these two taxa, whereas the sulcus is deep and well-delimited in *T. hallae* (Figure 4.16).

448   Likewise, the angle between the main axes passing through the intercondylar sulcus and

449   mandibular articulation is lower than 135° in *H. ischigualastensis* and *E. murphi* but much

450   higher than this value in *T. hallae*.

451   Although the quadrate height of all basal theropods is subequal or below 80% of the

452 orbit height within the cranium, the quadrate inclination may have been variable among

453 primitive theropods. Indeed, the mandibular articulation lies anterior to the quadrate head in

454 *E. lunensis* (Sereno et al., 1993, 2013), at the same level in *D. chauliodus* (Sues et al., 2011),

455 and posterior to the quadrate head in *H. ischigualastensis* (Sereno and Novas, 1994).

456

457 Figure 5

458 **Coelophysoidea**

459   *Liliensternus liliensterni* (von Huene, 1934; Figure 5.1–5.6); '*Syntarsus*' *kayentakatae*

460 (Rowe, 1989; Figure 5.7–5.9); '*Syntarsus*' *rhodesiensis* (Raath, 1977); *Coelophysis bauri*

461 (CM 81765; AMNH FARB 7223, 7224,7225, 7227, 7237, 7238); *Zupaysaurus rougieri*

462 (PULR 076).

463   As in basal Theropoda, few information of the quadrate anatomy of coelophysoid

464 theropods can be extracted from the literature, as the cranial material of most coelophysoid

465 taxa are still in articulation with the skull, and cannot be observed in all views. This is the

466 case of both quadrates of '*Syntarsus*' *kayentakatae, Zupaysaurus rougieri* (in which the

467 quadrates are mostly covered by the matrix; Arcucci and Coria, 2003; Ezcurra, 2007) and all

468 specimens of *Coelophysis bauri* examined in this study (CM 81765; AMNH FARB 7223,

469 7224,7225, 7227, 7237, 7238). However, the right quadrate of '*S.*' *kayentakatae* is

470 particularly well-visible (Tykoski, 2005) in posterior view (Figure 5.7–5.8), although the

471 pterygoid flange is hidden by matrix and the mandibular articulation is still articulated to the

472 lower jaw. An incomplete non-articulated right quadrate of *Liliensternus liliensterni* (Figure

473 5.1–5.6) also gives us the opportunity to have a better understanding of the quadrate anatomy

474 of coelophysoids.

475   As seen in the earliest forms of theropods, the quadrate of coelophysoids is elongated

476   and relatively narrow lateromedially, and the posterior margin of the quadrate body is

477   lateromedially concave. A quadrate foramen seems to be present and situated at mid-height of

478   the bone in all coelophysoids. The size and limits of this foramen are however highly variable

479   in this clade, being relatively large, oval and inside the quadrate body in *Z. rougieri* (Arcucci

480   and Coria, 2003; Ezcurra, 2007), small, deeply recessed and equally surrounded by the

481   quadrate and quadratojugal in '*S.*' *rhodesiensis* (Raath, 1977, figure 3D, 4J; Yates, 2005;

482   Tykoski, 2005) and minute and largely encircled by the quadrate in '*S.*' *kayentakatae*

483   (Tykoski, 2005; Figure 5.7). A quadrate foramen has also been reported in *Liliensternus*

484   *liliensterni* (von Huene, 1934), but not in *C. bauri* (Colbert, 1989); however, according to

485   Tykoski (2005), poor preservation renders its absence uncertain in *Coelophysis*, an opinion

486   that we also follow for *L. liliensterni* as some part of the quadrate body are missing in this

487   specimen (Figure 5.3).

488   The quadrate ridge is subvertical, prominent and particularly narrow, forming a

489   shallow crest in '*S.*' *kayentakatae* (Figure 5.7). In *L. liliensterni*, the quadrate ridge is rod-

490   shaped and strongly laterally inclined (Figure 5.3). Nevertheless, the ridge extends from

491   slightly above the entocondyle in both taxa, and reaches the quadrate head in '*S.*'

492   *kayentakatae*. As some basal forms like *H. ischigualastensis*, the quadrate of coelophysoids

493   possesses a subtriangular lateral process (Colbert, 1989) extending anterolaterally from above

494   the quadrate foramen. This process is well-visible in '*S.*' *kayentakatae*, '*S.*' *rhodesiensis*

495   (Raath, 1977, figure 4j), *Z. rougieri* and *L. liliensterni* (Figure 5.2) and contacts the quadrate

496   body just beneath the quadrate head at least in '*S.*' *kayentakatae*.

497   Although the dorsal and ventral quadratojugal contacts are not visible or not preserved

498   in most coelophysoids, the ventral quadratojugal contact of *L. liliensterni* is wide, and much

499 larger than the dorsal quadratojugal contact as the latter corresponds to an elongated line on

500 the edge of lateral process (Figure 5.2).

501   A posterior fossa is well-visible in '*S.*' *kayentakatae* (Figure 5.7–5.8) and *L.*

502 *liliensterni*. This fossa is relatively small, oval and centered on the quadrate body in both taxa.

503 It does not surround the quadrate foramen at least in '*S.*' *kayentakatae* but may have bordered

504 the quadrate foramen in *L. liliensterni*.

505   The mandibular articulation is ventrally visible in '*S.*' *kayentakatae* and shows a

506 diagonal intercondylar sulcus separating a lateromedially elongated ectocondyle and a smaller

507 entocondyle. The ectocondyle of '*S.*' *kayentakatae* seems to project well-beneath the

508 quadratojugal, a feature only observed in this taxon so far. In *L. liliensterni*, the entocondyle

509 is ovoid to elliptical in outline and does not protrude anteriorly (Figure 5.6).

510   The quadrate inclination is quite variable in coelophysoids, as the quadrate is strongly

511 inclined anteriorly in '*S.*' *kayentakatae* (Figure 5.9), subvertical in *C. bauri* (pers. obs.) and

512 posteriorly inclined in *Z. rougieri* (Ezcurra, 2007); pers. obs.).

513

514 **Dilophosauridae**

515   *Dilophosaurus wetherilli* (Welles, 1984; Figure 5.10–5.15).

516   The name of Dilophosauridae was used by Charig and Milner (1990) to contain only

517 the genus type *Dilophosaurus*. It will also be used here to include this taxon as the

518 morphology of its quadrate differs significantly from this of other coelophysoids and

519 ceratosaurians. Two disarticulated quadrates are available in *Dilophosaurus wetherilli* and

520 Welles (1984) provided a relatively detailed description of them. However, they are here

521 figured for the first time (Figure 5.10–5.15) and comparison with the quadrate of other

522 theropods is here given.

523   Unlike other very basal theropods and coelophysoids, the quadrates of *D. wetherilli*

524   are moderately tall and less ventrodorsally elongated relative to the mandibular articulation

525   (ratio of 0.39). In addition, the quadrate ridge is extremely prominent, rod-shaped, strongly

526   laterally-inclined, and slightly twisted so that both ventromedial and dorsolateral margins of

527   the ridge are convex (Figure 5.12). Nevertheless, the ridge is prominent above the

528   entocondyle and terminates beneath the quadrate head without reaching it. However, the

529   quadrate ridge of *D. wetherilli* is convex in medial view (Figure 5.13), a condition also shared

530   with the megalosaurid *Dubreuillosaurus valesdunensis* (Allain, 2002).

531   The pterygoid flange of *D. wetherilli* is straight (not medially bent in its anterior part),

532   subtrapezoidal with the anteriormost margin inclined posteriorly, and does not seem to

533   possess a ventral shelf extending all along the ventral margin of the flange as other taxa such

534   as *Ceratosaurus* (Figure 6.4) and *Allosaurus* (SMA 005/02; Figure 10.4). The flange also

535   reaches the quadrate head at its anteroventral margin dorsally, and the quadrate body well

536   above the mandibular condyles ventrally (Figure 5.13). The most anterior point of the

537   pterygoid flange in *D. wetherilli* is situated at two-thirds of the bone and the ventroposterior

538   margin is slightly medially folded (pers. obs.).

539   Like more basal theropods, *D. wetherilli* possesses a subtriangular lateral process and

540   reaches the quadrate body beneath the quadrate head (Figure 5.11). This lateral process is

541   strongly anteriorly oriented and particularly well-developed in this taxon.

542   Unlike ceratosaurs and megalosaurids, a quadrate foramen is present in *D. wetherilli*

543   and its shape and position are autapomorphic to this taxon (Figure 5.12). The main axis of the

544   foramen, rather than being subparallel to the long axis of the quadrate, is sub-perpendicular to

545   the quadrate axis and the foramen has an atypical 'keyhole' shape, an autapomorphic

546   character of *D. wetherilli*. The foramen is mostly delimited by the quadrate and surrounded by

547   a deep posterior fossa (Figure 5.12). This fossa is atypical in *D. wetherilli* as it is

subtriangular in shape and deep inside the ventral part of the lateral process, delimited by the

prominent quadrate ridge medially and by an important bending of the lateral process laterally

(Figure 5.12).

Like most basal theropods, the ventral quadratojugal contact is ovoid, almost

D-shaped, and much thicker than the dorsal quadratojugal suture which, once again,

corresponds to the narrow edge of the lateral process (Figure 5.11). The anterior margin of the

ventral contact slightly projects anteriorly.

The mandibular articulation is well-preserved in the left quadrate of *D.*

wetherilli. It clearly shows a relatively narrow and sigmoid ectocondyle delimited from a

thicker, rather elliptical, and non-protuberant entocondyle by a large and shallow

intercondylar sulcus (Figure 5.15). Like megalosauroids, the ectocondyle is much longer than

the entocondyle and the angle made by the intercondylar sulcus with the long axis passing

through the mandibular articulation is around 130°. These conditions are not shared by any

ceratosaurs.

An unnamed clade encompassing *D. wetherilli*, *Dracovenator regenti* and *Z. rougieri*

was retrieved in Yates (2005) and later by Smith et al. (2007) which also includes *Sinosaurus*

triassicus (Hu, 1993; Xing, 2012; Xing et al., 2013) and *Cryolophosaurus ellioti* (Hammer

and Hickerson, 1994) but without *Z. rougieri*. The quadrates of the two latter are indeed quite

similar to those of *D. wetherilli* in many aspects such as the shape and inclination of the

quadrate ridge and the size and position of the quadrate foramen. However, *C. ellioti* does not

seem to have a lateral process and both *C. ellioti* and *Z. rougieri* possess a ventrodorsally

elongated quadrate foramen and no subtriangular posterior fossa surrounding it. While there is

no doubt that *Z. rougieri* is a coelophysoid, *C. ellioti* has also been considered to be a basal

tetanuran (Sereno et al., 1994, 1996; Carrano et al., 2012).

573   Figure 6

574   **Ceratosauridae**

575   *Ceratosaurus nasicornis* (USNM 4735; MWC 1; Madsen and Welles, 2000; Figure

576   6.1–6.5).

577   Both quadrates of the holotype of *Ceratosaurus nasicornis* USNM 4735 are in

578   articulation within the cranium and strongly distorted (Gilmore, 1920), yet the disarticulated

579   quadrates of MWC 1 (formerly known as *Ceratosaurus* '*magnicornis*') and UUVP 1646

580   (formerly known as *Ceratosaurus* '*dentisulcatus*') are relatively complete and slightly

581   deformed (Madsen and Welles, 2000), allowing to propose a full picture of their anatomy.

582   The quadrates of MWC 1 and UUVP 1646 have been briefly described by Madsen and

583   Welles (2000) and a full description of their anatomy is here given for the first time.

584   As in more basal theropods, the quadrate bone of *Ceratosaurus* is strongly

585   ventromedially elongated, the mandibular articulation is lateromedially short (Figure 6.3), and

586   the pterygoid flange is straight, subtrapezoidal and reaches the quadrate body well above the

587   mandibular condyles ventrally (Figure 6.4). In addition, the quadrate also possesses a

588   subtriangular lateral process attached to the quadrate body roughly at mid-height of the bone

589   ventrally and far beneath the quadrate head dorsally (Figure 6.3). The latter is prominent,

590   narrow and subtriangular in outline in dorsal view. The quadrate is fused to the quadratojugal

591   (Figure 6.1, 6.3), a condition seen in some derived abelisaurids such as *Carnotaurus* (Figure

592   7.14).

593   The dorsal part of the quadratojugal contact is larger than the ventral one. As in *D.*

594   *wetherilli*, the ventral margin of the pterygoid flange curves medially and there is a ventral

595   shelf. The most anterior point of the pterygoid flange is situated at two thirds of the quadrate

596   height (Figure 6.4).

597   The quadrates of the different species of *Ceratosaurus* share also together a

598   combination of characters only observed in this genus: the absence of a quadrate foramen,

599   making the quadratojugal contact of the quadrate continuous; a relatively thick, subvertical,

600   and not-well delimited quadrate ridge, becoming visible at one-third of the quadrate, well-

601   above the entocondyle, but reaching the quadrate head; a deep mesial fossa and a large

602   posterior fossa formed by both quadrate and quadratojugal and centered on the suture of these

603   two bones; a lateral process laterally oriented; and both ecto- and entocondyle are parabolic,

604   subparallel and similar in size in ventral and posterior views. The two mandibular condyles

605   are also separated by a shallow intercondylar sulcus as large as the condyles (Figure 6.5). The

606   ventral quadratojugal contact is lanceolate, and does not possess any anterior projection,

607   whereas the dorsal contact is filiform and follows the edge of the lateral process.

608

609   **Noasauridae**

610   *Masiakasaurus knopfleri* (FMNH PR 2496; Figure 6.6–6.11); *Noasaurus leali* (PVL

611   4061; Figure 6.12–6.17).

612   In noasaurids, only the right quadrates are known in *Noasaurus leali* and

613   *Masiakasaurus knopfleri*. The quadrate of the latter is incomplete (ventral part of the lateral

614   and medial rami preserved) and has recently been extensively described by Carrano et al.

615   (2011). The quadrate of *N. leali* has been only figured in medial view and very briefly

616   described by Bonaparte and Powell (1980, figure 7C).

617   *M. knopfleri* and *N. leali* quadrate morphology are similar in many aspects and

618   clearly reflects their ceratosaurian affinity. They are indeed quite similar to the quadrate of

619   *Ceratosaurus* and only differ from those of Abelisauridae on its derived features. As in

620   *Ceratosaurus*, the quadrate of *M. knopfleri* and *N. leali* possesses a sub-vertical and poorly

621   delimited ridge emerging from above the entocondyle and terminating at the quadrate head

622 (Figure 6.8, 6.14). Although incomplete, the lateral process of both noasaurids is also present,

623 mostly laterally-oriented and the dorsal margin of the process reaches the quadrate body well-

624 below the quadrate head. As in Abelisauridae, the ventral margin of the process joins the

625 quadrate body at the level of the mandibular articulation (Figure 6.8 and 6.14).

626 The pterygoid flange is straight and the posteroventral margin is medially folded in *M.*

627 *knopfleri* (Figure 6.11). A ventral shelf is absent in *N. leali* and its presence cannot be

628 determined in *M. knopfleri*. The dorsal margin of the flange reaches the quadrate head, and

629 the ventral margin attaches the quadrate body well-above the mandibular articulation in

630 noasaurids (Figure 6.7 and 6.13). Although figured as a subtriangular flange by Bonaparte and

631 Powell (1980, figure 7C), the pterygoid flange of *N. leali* is clearly subtrapezoidal, with a

632 very short anterior margin (Figure 6.15). The medial fossa of the pterygoid flange is very

633 shallow in both noasaurids, and, due to preservation, the existence of a posterior fossa cannot

634 be determined.

635 Following (Carrano et al., 2011) observation, the presence of the quadrate foramen in

636 *M. knofleri* cannot be ruled out due to poor preservation of the lateral margin of the quadrate

637 body. Likewise, the presence of a quadrate foramen in *N. leali* cannot be determined as the

638 lateral margin of the bone is badly preserved, and both ventral and dorsal parts are missing

639 (pers. obs.). Bonaparte and Powell (1980) noted the presence of the quadrate foramen in this

640 taxon and Carrano and Sampson (2008) coded it as absent in their datamatrix, therefore our

641 interpretation contradicts these observations.

642 The ventral part of the quadratojugal contact of *M. knopfleri* and *N. leali* is similar in

643 shape, and forms a ventrodorsally elongated lanceolate shape facing laterally. Although partly

644 damaged in *M. knopfleri* and completely absent in *N. leali*, the dorsal part of the quadratojugal

645 contact was most likely a very narrow line running along the lateral margin of the lateral

646 process, as observed in more basal theropods.

647　　　　　The quadrate head of *M. knopfleri* is strongly damaged but the head is well-preserved

648　　in *N. leali* and corresponds to a semi-spherical condyle with a convex dorsal margin in

649　　posterior view (Figure 6.16). The mandibular articulation of *M. knopfleri* is very similar to

650　　those of Abelisauridae in possessing a subcircular ectocondyle smaller than the ovoid

651　　entocondyle, and a narrow and deep intercondylar sulcus (Figure 6.11), two derived features

652　　absent in non-abelisauroids Ceratosauria. In *N. leali*, although incomplete, the entocondyle

653　　was obviously larger than the ectocondyle. The latter corresponds to a subcircular condyle

654　　separated from the entocondyle by a shallow and poorly delimited intercondylar sulcus

655　　(Figure 6.17).

656

657　　Figure 7

658　　**Abelisauridae**

659　　　　　*Abelisaurus comahuensis* (MPCA 11098); *Ilokelesia aguadagrandensis* (MCF PVPH

660　　35; Figure 7.1–7.6); *Aucasaurus garridoi* (MCF-PVPH 236); *Majungasaurus crenatissimus*

661　　(FMNH PR 2100; Figure 7.7–7.12); *Carnotaurus sastrei* (MACN CH 894; Figure 7.13–7.17).

662　　　　　The quadrates of *Abelisaurus comahuensis* and *Carnotaurus sastrei* have only been

663　　briefly described in the literature (e.g., Bonaparte and Novas, 1985; Bonaparte, 1991). The

664　　quadrate anatomy of *Ilokelesia aguadagrandensis*, which includes the two portion of a right

665　　quadrate, and *Majungasaurus crenatissimus*, from which the two quadrates are well-

666　　preserved, are well-known as they have been described in detail and are illustrated by Coria

667　　and Salgado (1998) and Sampson and Witmer (2007) respectively.

668　　　　　　Abelisaurid quadrates are easily recognizable by some features present in these

669　　derived ceratosaurians such as a lateral process extending below the mid-height of the

670　　quadrate body, just above the ectocondyle or reaching the latter, and, in some of them, an

671　　anterior and posterior fossae.

672   The quadrate is strongly ventrodorsally-elongated with a relatively short mandibular

673   articulation. However, the quadrate body is lateromedially wider than basal ceratosaurians as

674   they possess a lateral process attaching well beneath the quadrate head but almost joining the

675   ectocondyle ventrally, forming a tall and subtriangular flange laterally-oriented (*I.*

676   *aguadagrandensis*; Figure 7.2; *M. crenatissimus*; Figure 7.8) or lateromedially-oriented (*C.*

677   *sastrei*; Figure 7.14). Like basal ceratosaurs, there is no quadrate foramen piercing the

678   quadrate body in Abelisauridae.

679   The quadrate ridge is sub-vertical and only well-delimited at mid-height and two-

680   thirds of the quadrate bone in posterior view (Figure 7.3, 7.9, 7.15). The ridge becomes

681   noticeable at one-third of the quadrate body, well above the mandibular condyles, and gets

682   flared below the quadrate head.

683   As seen in *Ceratosaurus*, the pterygoid flange of abelisaurids is subtrapezoidal and

684   displays a ventral shelf extending all along the ventral margin of the flange (Figure 7.10,

685   7.15). The anteriormost point of this flange is situated at about two thirds of the quadrate, and

686   its ventral margin connects the quadrate body well-above the ectocondyle while the dorsal

687   margin gets attached to the quadrate body just under the ventral margin of the quadrate head.

688   The latter is subtriangular in outline in dorsal view and subvertical (no bent medially in its

689   anterior part).

690   When present, the posterior fossa is small, ovoid and situated at mid-height of the

691   quadrate body, as seen in *Aucasaurus garridoi* (MCF-PVPH 236) and *M. crenatissimus*

692   (Figure 7.9). In some abelisaurids, a second fossa occurs on the anterior surface of the

693   quadrate body, lateral to the ventralmost part of the pterygoid flange. This anterior fossa is

694   deep and well-visible in *A. comahuensis*, *M. crenatissimus* (Figure 7.7), and *C. sastrei* (Figure

695   7.13).

696   As observed in other ceratosaurians, the ventral quadratojugal contact of *M.*

697   *crenatissimus* is lanceolate and the dorsal quadratojugal contact is an elongated line following

698   the lateral edge of the lateral process (Figure 7.8). On the other hand, the ventral

699   quadratojugal contact of *I. aguadagrandensis* is hemicircular and placed on the anterolateral

700   part of the ectocondyle (Figure 7.2–7.1). Abelisaurids and noasaurids share a very similar

701   mandibular articulation in which both ecto- and entocondyle are ovoid or subcircular, and the

702   entocondyle is larger than the ectocondyle (Figure 7.6, 7.12, 7.17). The intercondylar sulcus is

703   very narrow in *M. crenatissimus* and *C. sastrei* whereas it is large and shallow in *A.*

704   *comahuensis* and *I. aguadagrandensis*. The first two taxa also possess a deep quadrate notch

705   on the anterior margin of the mandibular articulation (Figure 7L,Q).

706

Basal Tetanurae

708   *Cryolophosaurus ellioti* (Smith et al., 2007); *Monolophosaurus jiangi* (Zhao and

709   Currie, 1993; Brusatte, Benson, et al., 2010); *Marshosaurus bicentissimus* (Madsen, 1976a);

710   *Sinosaurus triassicus* (Hu, 1993; Xing, 2012).

711   Recent cladistic analyses performed on tetanurans by Benson (2010) and Carrano et

712   al. (2012) found several theropod taxa placed basally among Tetanurae, but outside the clades

713   of Megalosauria and Allosauroidea. Among those basal tetanurans, *Cryolophosaurus ellioti*,

714   *Marshosaurus bicentissimus*, *Sinosaurus triassicus* and *Monolophosaurus jiangi* have a

715   quadrate preserved, but this bone has only been well-described in *M. jiangi* (Brusatte, Benson,

716   et al., 2010). *M. jiangi* was retrieved at the base of a clade encompassing Megalosauroidea,

717   Allosauroidea, and Dromaeosauridae in the present analysis (Figure 1). *Cryolophosaurus*

718   *ellioti*, on the other hand, was found outside Tetanurae, along with Ceratosauria. As noted

719   before, *C. ellioti* was considered to be closely related to *D. wetherilli* by Smith et al. (2007)

720   but Carrano et al. (2012) analysis found it as a basalmost Tetanurae. Both quadrates of *C.*

721 *ellioti* (Hammer and Hickerson, 1994) are preserved, and only the right quadrate is well-

722 visible (Smith et al., 2007), but the mandibular condyles are still in connection with the

723 mandible and only the posterior and the lateral views of the bone can be seen. As for *S.*

724 *triassicus*, both quadrate are in articulation within the skull of two specimens (KMV 8701;

725 LDM-LCA 10), but the bone has been poorly described by Hu (1993) and a full picture of the

726 cranial anatomy of this taxon is still waited.

727   The quadrate body of basal tetanurans are moderately tall (ratio of 0.44 for *M.*

728 *jiangi* and around 0.36 for *C. ellioti*) and the mandibular articulation is positioned posterior to

729 the quadrate head. A ventrodorsally elongated quadrate foramen is present in all basal

730 tetanurans (e.g., Hue, 1993; Carrano et al., 2012). In *C. ellioti*, it is small (around 3% of the

731 dorsoventral depth of the quadrate body) and elliptical, whereas the quadrate bone of *M.*

732 *jiangi* possesses a large lanceolate quadrate foramen. However, both taxa have their quadrate

733 foramen almost equally delimited by the quadrate and quadratojugal, with the quadrate

734 contributing slightly more to the margin of the foramen than the quadratojugal (pers. obs. for

735 *C. ellioti*; Zhao and Currie 1993; Brusatte et al. 2010a, figure 1D).

736   The quadrate ridge of basal tetanurans is rod-shaped, well-delimited, diagonally-

737 oriented and slightly twisted in *C. ellioti*. The ridge seems to reach the entocondyle in *M.*

738 *jiangi* and gets flared just above the medial condyle in *C. ellioti*. The quadrate head of *M.*

739 *jiangi* only contacts the squamosal and is clearly exposed in lateral view rather than being

740 obscured by the squamosal (Zhao and Currie, 1993). The same condition exists in *S.*

741 *triassicus* (LDM-LCA 10).

742   Contrarily to most basal theropods and ceratosaurians, there is no lateral process

743 projecting from the quadrate body in *S. triassicus*, *C. ellioti* and *M. jiangi*. The pterygoid

744 flange of *M. jiangi* is moderately expanded anteroposteriorly (ratio of the pterygoid flange,

745 corresponding to the antero-posterior length of the flange divided by the ventrodorsal

746 elongation of the quadrate body, of 0.43) while the anteroposterior elongation of the pterygoid

747 flange is surprisingly important in *C. ellioti* (ratio of 0.7). As in megalosaurids and

748 spinosaurids, the anteriormost point of the flange is located at two-thirds of the quadrate in

749 basal tetanurans. However, the most anterior side of the flange is slightly inclined anteriorly

750 in *M. jiangi* and strongly inclined posteriorly in *C. ellioti*. In both taxa, a posterior fossa is

751 absent and the medial fossa is deep and located in the posteroventral corner of the pterygoid

752 flange. The posteroventral margin of the pterygoid flange deflects medially, and this fold

753 extends well anteriorly in *M. jiangi*, forming a protuberant ventral shelf. In *M. jiangi*, a small

754 concavity just above the boundary between the ento- and ectocondyles appears on the

755 posterior face of the quadrate body (Zhao and Currie, 1993, figure 1D). A concave area seems

756 to be also present at this place in *C. ellioti* but shallower than in *M. jiangi*. Similar to the non-

757 averostran condition, the quadrate of *M. jiangi* and *C. ellioti* is apneumatic (Smith et al., 2007;

758 Benson, 2010) datamatrix).

759   According to Benson (2010) datamatrix coding, the quadrate of the basal

760 megalosauroid *M. bicentissimus* is also apneumatic, lacking a quadrate foramen and

761 possessing "a small circular depression adjacent to the mandibular condyle" (Benson, 2010, p.

762 35) on the medioventral side of the quadrate and dorsal to the entocondyle. As stated by this

763 author, it "may represent incipient development" (Benson, 2010, p. 35) of the medial foramen

764 existing above the entocondyle and adjacent to the ventral margin of the pterygoid flange in

765 some derived Megalosauridae.

766

767 Figure 8

768 **Megalosauridae**

769   *Eustreptospondylus oxoniensis* (OUMNH J.13558; Figure 8.1–8.5); *Dubreuillosaurus*

770   *valesdunensis* (Allain, 2002); *Torvosaurus tanneri* (Britt, 1991; BYUVP 9246; Figure 8.6–

771   8.11); *Afrovenator abakensis* (UC OBA1; Figure 8.12–8.17);

772   The quadrate of *Eustreptospondylus oxoniensis* and *Afrovenator abakensis* are

773   complete (Sereno et al., 1994; Sadleir et al., 2008), but the right quadrate of *Torvosaurus*

774   *tanneri* has the pterygoid flange missing (Britt, 1991). Only a fossil imprint of pterygoid

775   flange of the left quadrate has been recovered in *Dubreuillosaurus valesdunensis* (Allain,

776   2002).

777   The quadrate is moderately elongated in comparison to the lateromedial width

778   of the mandibular articulation (ratio between 0.35-0.45) and slightly anteriorly-inclined in

779   lateral view. The quadrate body is significantly laterally-inclined from the horizontal axis

780   passing through the mandibular articulation (Figure 8.3, 8.8, 8.14). It has lateral and medial

781   margins subparallel in posterior view, and the posterior margin is concave except in *D.*

782   *valesdunensis* in which this margin seems to be convex (Allain, 2002). Like ceratosaurians,

783   the quadrate of megalosaurid taxa lacks a quadrate foramen, therefore the quadratojugal

784   contact extends all the way dorsoventrally. The ventral part of the quadratojugal contact is

785   subtriangular in shape and shows an anterior projection, whereas the dorsal part is an

786   elongated and narrow suture with subparallel anterior and posterior margins (Figure 8.3, 8.8,

787   8.14). The quadrate ridge is rod-shaped as in ceratosaurians, and can be either shallow and not

788   well-marked (*E. oxoniensis*; Figure 8.3) or, well-delimited at mid-height of the quadrate body

789   (*T. tanneri*; Figure 8.8; *A. abakensis*; Figure 8.14). Nevertheless, the ridge always becomes

790   visible well above the entocondyle, at one third of the bone, and reaches the quadrate head.

791   As all megalosauroids, there is no lateral process of the quadrate body.

792   The pterygoid flange is straight (no medial curvature of the anterior part),

793   subtrapezoidal and reaches the dorsal margin of the quadrate head dorsally and, not far above

794 from the entocondyle ventrally (Figure 8.2, 8.7, 8.15). The posteroventral margin of the

795 flange is medially-folded but there is no ventral shelf in the anteroventral part of the flange.

796 The medial fossa of the quadrate is shallow and there is no distinct posterior fossa, but an

797 depression ventrodorsally elongated along the quadrate body, lateral to the quadrat ridge. The

798 quadrate head projects vertically and its shape is ovoid rather than subtriangular in posterior

799 view as in other non-tetanuran theropods (Figure 8.10, 8.16).

800 The mandibular articulation is also lateromedially larger than in more basal

801 theropods. In both posterior and ventral views, the ectocondyle is longer than the entocondyle

802 and its ventral margin is slightly sigmoid in *T. tanneri* in anterior view (Figure 8.6). The

803 ectocondyle is parabolic in *T. tanneri* (Figure 8.11) and *E. oxoniensis* (Figure 8.5), but it is

804 rather elliptical in *A. abakensis* (Figure 8.17). Likewise, the anterior margin of the

805 ectocondyle is concave both in *T. tanneri* and *E. abakensis.* The entocondyle is elliptical to

806 oblong in outline, and strongly protrudes anteriorly. The intercondylar sulcus is deep and

807 well-marked in *E. oxoniensis* (Figure 8.5), but large and shallow in *T. tanneri* (Figure 8.11)

808 and *A. abakensis* (Figure 8.17).

809 In *T. tanneri*, the ventral margin of the ventral quadratojugal contact and the

810 posteroventral margin of the pterygoid flange are joined together to form a convex arc on the

811 anteroventral side of the quadrate (Figure 8.6). This taxon can also be distinguished from the

812 two other megalosaurids by having a concavity on the anteroventral margin of the quadrate,

813 ventral to the pterygoid flange and anterior to the entocondyle. A similar but larger and deeper

814 concavity has also been noted in some derived Spinosauridae (pers. obs.).

815 A subtriangular depression with a small foramen inside is present in *T. tanneri* on the

816 ventromedial part of the quadrate just above the entocondyle (Figure 8.9; Britt, 1991; Benson,

817 2010; pers. obs.). A shallow concavity with no foramen also exists at the same position in *A.*

818 *abakensis* but nothing comparable is present in *E. oxoniensis* (Benson, 2010); pers. obs.). In

819   *T. tanneri* and *A. abakensis*, a second and larger ovoid foramen also occurs at the ventralmost

820   part of the pterygoid flange, beneath the medial fossa and above the shallow fossa dorsal to

821   the entocondyle (Figure 8.9, 8.15; Benson, 2010, figure 19A). Although a medial

822   pneumatopore was noted by Sadleir et al. (2008) at the base of the pterygoid flange in *E.*

823   *oxoniensis*, no pneumatopore was observed at this place in this taxon. Instead, there is a

824   groove leading to a small foramen on the anteroventral part of the quadrate, lateral to the

825   ventral part of the pterygoid flange (Figure 8.1) but this structure might be an artifact of

826   preservation. The quadrate of megalosaurids seems therefore to be apneumatic.

827

828   Figure 9

829   **Spinosauridae**

830   *Baryonyx walkeri* (BMNH R9951; Figure 9.1–9.6); *Suchomimus tenerensis* (MNN

831   GAD 502; Figure 9.7–9.12); *Irritator challengeri* (SMNS 58022); Undescribed Spinosaurinae

832   (MSNM V6896; WDC-CSG uncatalogued; Figure 9.13–9.18).

833   Both quadrates of *Baryonyx walkeri* provide a good basis to understand the anatomy

834   of this derived clade of Megalosauroidea. An incomplete left quadrate of *Suchomimus*

835   *tenerensis*, a small portion of the lateral part of the right quadrate and the quadrate head of the

836   left quadrate in *Irritator challengeri* (Sues et al., 2002), and six indeterminate spinosaurid

837   quadrates from the Cenomanian of the Kem Kem beds (Morocco) offer further details.

838   The quadrates of *B. walkeri* have been described in detail by Charig and

839   Milner (1997) but the anatomy of the quadrate of *I. challengeri* has been very briefly given by

840   Sues et al. (2002) and that of *S. tenerensis* has not yet been described. A detailed description

841   of the six spinosaurid quadrates from Morocco and comparison with other spinosaurid

842   quadrates will be given elsewhere.

843   The Spinosauridae quadrates are highly diagnostic and differ significantly

844   from megalosaurids. The mandibular articulation is very broad lateromedially and the

845   quadrate body is short (ratio more than 0.5). It also seems that the quadrate bone was

846   posteriorly-inclined in the cranium as this configuration appears in *I. challengeri*, the only

847   reported spinosaurid taxon with an articulated quadrate.

848   In Baryonychinae, the quadrate foramen is large (thereby called the 'quadrate

849   fenestra' by Sereno et al. (1998), strongly ventrodorsally elongated and predominantly formed

850   by the quadrate (Figure 9.3 and 9.9). Indeed, the dorsal quadratojugal contact possesses a

851   short ventral projection making the dorsolateral margin of the quadrate foramen. Such feature

852   can also be observed in the quadrates of spinosaurid taxa from Morocco (Figure 9.15) but its

853   presence remains uncertain in *I. challengeri* (pers. obs.). However, the quadrate foramen of

854   Spinosaurinae is slightly to considerably smaller and also subcircular to bean-shaped when

855   compared to Baryonychinae (pers. obs.). As in Megalosauridae, there is no lateral process.

856   The quadrate ridge of spinosaurids is broad, the broadest among nonavian theropods,

857   and the quadrate body corresponds to the quadrate ridge at the level of the quadrate foramen

858   (Figure 9.3, 9.9, 9.15). The ridge is also strongly inclined laterally, becomes marked just

859   above the entocondyle and flares at two thirds of the quadrate body where, in some derived

860   spinosaurids, it can reappear more dorsally, beneath the quadrate head (pers. obs.).

861   By having a very long anteriormost margin, the pterygoid flange of the quadrate is

862   sub-rectangular in outline and such morphology is typical of spinosaurid theropods (Figure

863   9.4, 9.16). The flange attached dorsally at the level of the quadrate head and descends the

864   quadrate body to meet the entocondyle. A shallow notch occurs at one-fifth of the pterygoid

865   flange and the dorsal margin of the flange is slightly medially-folded from that point (Figure

866   9.1, 9.7). Unlike Baryonychinae, the flange is strongly medially curved in Spinosaurinae. The

867 medial fossa, located ventrally and delimited by the prominent ridge, is particularly deep in

868 comparison to other theropods (Figure 9.4, 9.16).

869   The shape of the quadrate head is highly variable among spinosaurid theropods:

870 subcircular in *B. walkeri* (Figure 9.5), subtriangular in *S. tenerensis* (Figure 9.11), and

871 diamond shaped in *I. challengeri* and an indeterminate spinosaurine (MSNM V6896; Figure

872 9.17). There is a small concavity situated on the posterior side of the quadrate body, just

873 beneath the quadrate head, a feature shared among all Spinosauridae (pers. obs.).

874   The ventral quadratojugal contact is anteroposterioly broad, reniform to D-shaped, and

875 much broader than the dorsal quadratojugal contact which is lanceolate and elongated

876 ventrodorsally (Figure 9.2, 9.8, 9.14). The suture between the quadrate and quadratojugal

877 must have been rigid as the ventral contact is deeply excavated by one or several cavities, and

878 the surface of the dorsal contact is irregular and sometimes shows a central ridge delimited by

879 two elongated grooves. The dorsal quadratojugal contact has an anterior projection and

880 always extents on to the ectocondyle (Figure 9.2, 9.14, 9.14). On the posterior side of the

881 quadrate, a shallow and recurved groove running from above the ventral quadratojugal to the

882 boundary between the ecto- and entocondyles has been observed in *B. walkeri* and other

883 spinosaurines (pers. obs.).

884   With a strongly elongated and sigmoid ectocondyle and a short entocondyle, both

885 being delimited by a diagonally-oriented intercondylar sulcus, the mandibular articulation of

886 the quadrate is also typical to the clade of Spinosauridae (Figure 9.6, 9.12, 9.18). The

887 entocondyle is subtriangular and not well-marked and the intercondylar sulcus is shallow in *B.*

888 *walkeri*, possibly due to the immaturity of the specimen (Charig and Milner, 1997). In more

889 derived spinosaurids, the entocondyle is elliptical in shape and does not protrude anteriorly.

890 The ectocondyle is much larger than the entocondyle in both posterior and anterior views. In

891   anterior view, the ventral margin of the condyle is sigmoid. The intercondylar sulcus is deep

892   and well-delimited in mature individuals of Spinosaurine (Hendrickx and Mateus, 2012).

893

894   Figure 10

895   **Non-carcharodontosaurid Allosauroidea**

896   *Allosaurus fragilis* (Madsen, 1976b; Bakker, 1998); *Allosaurus europaeus* (ML 415);

897 *Allosaurus 'jimmadseni'* (SMA 005/02; Figure 10.1–10.6); *Aerosteon riocoloradensis*

898 (Sereno et al., 2008; Figure 10.7–10.12); *Sinraptor dongi* (Currie, 2006; Figure 10M–Q).

899   The quadrate of non-carcharodontosaurid allosauroids is known in *Allosaurus fragilis*

900 (Madsen, 1976b), *Allosaurus 'jimmadseni'* (Chure, 2000), *Allosaurus europaeus* (Mateus et

901 al., 2006), *Sinraptor dongi* (Currie, 2006), and *Aerosteon riocoloradensis* (Sereno et al.,

902 2008). However, the quadrate has only been relatively well-described in *A. 'jimmadseni'* and

903 *S. dongi*. Although *Allosaurus*, *Sinraptor* and *Aerosteon* pertain to different clades of

904 allosauroids (sensu Benson et al., 2010; Carrano et al., 2012), they share many features that

905 are not seen in other theropods and Carcharodontosauridae. Thus, the quadrate of

906 Carcharodontosauridae will thereby be described and compared to other theropod taxa in the

907 next chapter.

908   The quadrate of allosaurids and *A. riocoloradensis* is moderately elongated (ratio

909 between 0.35 and 0.5; Figure 10.3) but that of *S. dongi* is notably tall (ratio is approximately

910 0.3; Figure 10.15) and similar to non-tetanuran theropods. This can be explained by the

911 relatively short mandibular articulation in *S. dongi*, whereas the mandibular articulation of

912 other allosauroids is much broader lateromedially.

913   The quadrate foramen of allosaurids and *S. dongi* is mostly delimited by the quadrate

914 (Currie, 2006; Figure 10.3), but it is completely enclosed in *A. riocoloradensis* (Figure 10.7),

915 a feature also present in the coelophysoid *Z. rougieri* (Ezcurra, 2007). In *A. riocoloradensis*,

916   the quadrate foramen is particularly large, ovoid and situated at mid-height of the bone, while

917   in allosaurids and sinraptorids, the quadrate foramen is more elliptical, smaller, slightly to

918   strongly elongated ventrodorsally, and positioned slightly ventrally from the half of the

919   quadrate body.

920   The quadrate ridge is prominent, laterally-inclined, and rod-shaped in allosaurids

921   (Figure 10.3, 10.15), and forming almost a broad crest in *A. riocoloradensis* (Figure 10.9).

922   Interestingly, the ridge is divided in two portions by a groove at one-third or one-fourth of the

923   quadrate body, instead of forming a single structure as in other nonavian theropods. This

924   groove is deep and diagonally-oriented in *A. fragilis*, *A. europaeus* and *Allosaurus*

925   '*jimmadseni*' (SMA 0005/02; Figure 10.3) and well-marked but subvertical in *A.*

926   *riocoloradensis* (Figure 10.9). In fact, in *A. riocoloradensis* the ventral part of the ridge butts

927   against the quadrate head while the remaining dorsal portion emerged well beneath the

928   quadrate head laterally, being parallel to the squamosal contact interpreted by Sereno et al.

929   (2008). In *S. dongi*, however, this feature is more superficial but it seems that the dorsal part

930   of the quadrate ridge deviates laterally beneath the quadrate head (Figure 10.15). A second

931   and much narrower ridge of *S. dongi* becomes distinct more medially at one fourth of the

932   quadrate body, and remains parallel to the other (Figure 10.15). In allosaurids, the ridges

933   forms a convex protuberance at one-third of the quadrate body and well-visible in lateral view

934   (Figure 10.2). This bump on the posterodorsal margin in the quadrate body is not unique to

935   these theropods as it has also been observed in the *C. ellioti* (Smith et al., 2007, figure 4A–B).

936   A short lateral process is present and projects laterally from the quadrate foramen to

937   the quadrate head in allosaurids (Figure 10.3) and *S. dongi* (Figure 10.15). The process

938   attaches well-below the quadrate head in these taxa, and its lateral margin is parabolic. In the

939   other hand, the lateral process projects completely anteriorly in *A. riocoloradensis*, and

940   extends entirely on the quadrate body, from the mandibular articulation ventrally to the

941   quadrate head dorsally (Figure 10.7-10.8).

942   The pterygoid flange is very slightly medially-recurved in allosaurids (Figure 10.1)

943   and *S. dongi* (Figure 10.13), and strongly arched medially in *A. riocoloradensis* (Figure 10.7).

944   However, the shape of the flange is quite similar between them, as the flange is parabolic in

945   shape with a rounded anteriormost margin instead of a straight margin present in more basal

946   theropods. The flange meets the quadrate body far above the mandibular condyles ventrally

947   while it reaches the quadrate head just below its ventral margin dorsally. The quadrate head is

948   subcircular in allosauroids and follows the curvature of the quadrate body in allosaurids and

949   *S. dongi*, whereas the dorsal fourth of the quadrate strongly bends posteriorly in *A.*

950   *riocoloradensis* (Figure 10.10).

951   The medial fossa is shallow and roughly centrally positioned in *A. riocoloradensis* and

952   *S. dongi*. This fossa is deeper and more ventrally positioned in *Allosaurus* 'jimmadseni' due to

953   a well-developed ventral shelf in this taxon (Figure 10.4). Such shelf is also present in *S.*

954   *dongi* but, instead of being projected dorsomedially like in *Allosaurus* 'jimmadseni', the shelf

955   folds medially (Figure 10.16). *A. riocoloradensis* does not have such feature. The posterior

956   fossa of *S. dongi* is deep, ventrodorsally-elongated and does not includes the quadrate

957   foramen. No similar fossa exists in allosaurids and *A. riocoloradensis*, but there is a

958   ventrodorsally-elongated depression surrounding the quadrate foramen in these allosauroids.

959   This concavity is bounded medially by the quadrate ridge and laterally by the quadratojugal

960   contact in allosaurids, and a ridge delimiting posteriorly the lateral process in *A.*

961   *riocoloradensis*.

962   The ventral quadratojugal contact of *A. fragilis* is D-shaped and faces laterally

963   whereas it is lanceolate and faces posterolaterally in *S. dongi* (Figure 10.14). Nevertheless,

964   both ventral quadratojugal contacts share a short quadratojugal process projecting anteriorly.

965   The dorsal quadratojugal contact is ventrodorsally-elongated and faces anterolaterally or

966   completely anteriorly in these taxa. Although we agree with Sereno et al. (2008) that the

967   lateral contact of *A. riocoloradensis* extends from the ectocondyle to the dorsal margin of the

968   quadrate head along the lateral process (Figure 10.8), we are giving a different interpretation

969   of the morphology of this contact. According to Sereno et al. (2008, figure 4A), the

970   quadratojugal/squamosal contact is broad, its anterior and posterior margins are subparallel,

971   its surface is regular and flattened, and the dorsal part of the lateral contact of *A.*

972   *riocoloradensis* quadrate would have been connected to the squamosal (Sereno et al., 2008,

973   figure 4). Our observation of the quadrate of *A. riocoloradensis* suggests that only the anterior

974   margin of the lateral process was contacting the quadratojugal anteriorly. The presence of a

975   deep depression on the lateroventral part of the lateral process, here interpreted as an

976   additional pneumatic fossa, seems to support this interpretation. Nevertheless, it is indeed

977   likely that the squamosal was connecting the quadrate on the dorsal surface of the lateral

978   process, as suggested by Sereno et al. (2008, figure 4A).

979   The mandibular articulation of the allosauroids *S. dongi* (Figure 10.17) and *A.*

980   *riocoloradensis* (Figure 10.12) is very similar in shape as both condyles are elliptical,

981   globular and prominent, with a relatively deep intercondylar sulcus separating them. The main

982   axis passing through the ecto- and entocondyles are medially-oriented and the ectocondyle

983   axis is slightly more inclined medially than the entocondyle one, although both axes can be

984   subparallel is some allosaurids (SMA 0005/02; Figure 10.6). All allosaurids, however, show a

985   diagnostic quadrate notch on the posterior side of the mandibular articulation.

986   Quadrate pneumaticity exists in some non-carcharodontosaurid allosauroids such as *A.*

987   *riocoloradensis* (Sereno et al., 2008; Figure 10I) where a large and deep pneumatic recess is

988   located on the posterior side of the quadrate body. Currie (2006) estimates that the deep

989   posterior fossa posteromedial to the quadrate foramen in *S. dongi* (Figure 10.15) was

990　presumably pneumatic in origin, an interpretation followed here. A depression also occurs on

991　the lateroventral surface of the lateral process in *A. riocoloradensis* (Figure 10.8) and was

992　originally pneumatic as well in this taxon.

993

994　Figure 11

995　**Carcharodontosauridae**

996　　　*Acrocanthosaurus atokensis* (NCSM 14345; Figure 11.1–11.5); *Shaochilong*

997　*maortuensis* (Brusatte et al., 2009); *Giganotosaurus carolinii* (MUCPv-CH-1; Figure 11.6–

998　11.11); *Mapusaurus roseae* (MCF PVPH-1011.102; Figure 11.12–11.17).

999　　　The quadrate of Carcharodontosauridae is relatively well-known due to its detailed

1000　description for *Acrocanthosaurus atokensis* (Eddy and Clarke, 2011), *Shaochilong*

1001　*maortuensis* (Brusatte, Chure, et al., 2010) and *Mapusaurus roseae* (Coria and Currie, 2006).

1002　The bone is moderately elongated and has an lateral process along the dorsal half of the body

1003　and a relatively broad mandibular articulation ventrally. The quadrate ridge is pronounced,

1004　strongly laterally-inclined, becomes noticeable at one-third of the quadrate and more dorsally,

1005　being completely flared on the first one-third surface of the quadrate body (Figure 11.3, 11.8,

1006　11.14). The ridge varies in width, being lateromedially large at mid-height of the quadrate and

1007　reducing in width to form a thin crest below the quadrate head in *A. atokensis* (Figure 11.3).

1008　　　The quadrate of the carcharodontosaurids retains many plesiomorphies with basal

1009　allosauroids, such as a very small quadrate foramen (less than 7% of the ventrodorsal height

1010　of the quadrate body; Figure 11.3, 11.8, 11.14) mostly delimited by the quadrate, a short

1011　lateral process between the quadrate foramen and quadrate head, and a quadrate ridge

1012　relatively narrow at two thirds of the quadrate body and divided into ventral and dorsal

1013　portions.

1014   The quadrate body shows a large posterior fossa leading to the quadrate foramen

1015   ventrally. This depression is elliptical in shape, poorly-delimited, ventrodorsally elongated

1016   and medially inclined in carcharodontosaurids (Figure 11.3, 11.8, 11.14). The narrow

1017   quadrate body of *S. maortuensis* (Brusatte, Chure, et al., 2010, figure 7b) does not show a

1018   similar posterior fossa but, according to us, the lateral part of the quadrate body is missing.

1019   Unlike more basal allosauroid taxa, the pterygoid flange is straight, with no medial

1020   curvature, and the medial fossa is rather sub-circular, centrally positioned on the flange, and

1021   very shallow. Furthermore, the flange meets the quadrate body slightly above the entocondyle

1022   and well-beneath the ventral margin of the quadrate head. Nevertheless, as other allosauroids,

1023   the pterygoid flange is sub-parabolic in medial view, with a large and rounded anterior margin

1024   (Figure 11.4). The quadrate head is subcircular in shape in dorsal view in

1025   carcharodontosaurids (Figure 11.10) and, subvertical rather than flexing posteriorly as in *A.*

1026   *riocoloradensis*.

1027   Both ventral and dorsal quadratojugal contacts of carcharodontosaurids are

1028   morphologically similar to allosaurids and *S. dongi* (Figure 11.7, 11.13). The dorsal

1029   quadratojugal contact is a narrow, elongated, and extends along the lateral process of the

1030   quadrate. Except *A. atokensis*, the ventral quadratojugal contact does not show any anterior

1031   projection like in more basal allosauroids.

1032   The mandibular articulation is broad, with an ectocondyle always lateromedially

1033   larger than the entocondyle in both anterior and posterior views (Figure 11.5, 11.11, 11.17). It

1034   is constituted of an elliptical to oblong bulged entocondyle and an elongated parabolic to

1035   sigmoid ectocondyle, usually separated by a narrow but deep intercondylar sulcus (Figure

1036   11.5, 11.11). Although the entocondyle is prominent on both anterior and posterior sides in

1037   most carcharodontosaurids, its margins are rather flared in *S. maortuensis* which also displays

1038   a very shallow intercondylar sulcus.

1039   All carcharodontosaurids but *S. maortuensis* have a pneumatic quadrate. The

1040   pneumatic quadrate of carcharodontosaurids possesses a pneumatopore at the base of the

1041   pterygoid flange, ventral to the medial fossa (Figure 11.4, 11.9, 11.15). This medial

1042   pneumatic recess is large, subcircular and divided by a septum in *A. atokensis*. In *M. roseae*,

1043   the medial pneumatopore is also relatively large but elliptical and with no septum, like in *G.*

1044   *carolinii* in which this pneumatic opening is relatively small, subcircular and more dorsally-

1045   situated on the pterygoid flange. Unlike *A. atokensis*, Giganotosaurinae taxa do not show any

1046   posterior pneumatopore inside the posterior fossa of the quadrate body. However, an anterior

1047   pneumatic aperture is present in *M. roseae* at one third of the bone, lateral to the ventral

1048   termination of the pterygoid flange (Figure 11.12).

1049

1050   **Basal Coelurosauria**

1051   *Bicentenaria argentina* (MPCA 865; Figure 14.1–14.6); *Zuolong salleei* (Choiniere,

1052   Clark, et al., 2010); *Lourinhanosaurus antunesi* (ML 565-10, 565-150; Hendrickx and

1053   Mateus, 2012); *Aorun zhaoi* (Choiniere et al., 2014).

1054   The quadrate of the basal coelurosaurs of *Zuolong salleei* (Choiniere, Clark, et al.,

1055   2010), *Lourinhanosaurus antunesi* (Hendrickx and Mateus, 2012), and *Aorun zhaoi*

1056   (Choiniere et al., 2014) are relatively well-known as a thorough description has been provided

1057   in these taxa. Nevertheless, additional information deserves to be added in *Bicentenaria*

1058   *argentina* (Novas et al., 2012) as the quadrate of this coelurosaur shows some interesting

1059   features not seen in other theropod clades.

1060   Only the ventral half of the left and right quadrates of *B. argentina* are preserved

1061   (Figure 14.1–14.6). The quadrate of this taxon displays a prominent and well-defined rod-

1062   shaped quadrate ridge extending ventro-dorsally, perpendicular to the long axis of the

1063   mandibular articulation. The quadrate ridge does not reach the mandibular articulation

1064 posteriorly but extends to the entocondyle in its medial part (Figure 14.4). The quadrate

1065 foramen is strongly ventro-dorsally oriented and ventrolaterally bounded by a short and

1066 pointed projection of the basal quadratojugal contact so that the foramen is mostly delimited

1067 by the quadrate (Figure 14.3).

1068   As seen in some tyrannosauroids, the pterygoid flange of *B. argentina* extends far

1069 anteriorly, its anterior margin is semi-oval, and the ventral margin of the flange forms a right

1070 angle with the long axis of the quadrate ridge (Figure 14.4). The pterygoid flange projects

1071 anteriorly and does not curve medially. It also reaches the quadrate body slightly above the

1072 mandibular articulation, at the level of the entocondyle, and displays a rod-like ventral shelf

1073 oriented dorsomedially in its posteroventral margin, so that the medial fossa is relatively deep.

1074 In lateral view, the ventral quadratojugal contact is elliptical in shape and slightly anteriorly

1075 inclined (Figure 14.2). The contact is concave is posterior view and does not extend on the

1076 ectocondyle laterally. The articulating surface of the ventral quadratojugal contact is smooth

1077 and slightly excavated in its central part, and its posterodorsal margin is bounded by a wide

1078 but short lateral projection.

1079   The mandibular articulation is unique in possessing two well-delimited condyles

1080 strongly diagonally oriented in which the ectocondyle is one-third longer than the entocondyle

1081 and markedly protrudes laterally in ventral view (Figure 13.6). The mandibular condyles

1082 share however a same width and both condyles are separated by a wide and deep

1083 intercondylar sulcus. The long axis of the ento-, ectocondyles and intercondylar sulcus is

1084 parallel.

1085   The most interesting features in the quadrate of the embryonic specimens of *L.*

1086 *antunesi* are the absence of a quadrate foramen and the poor delimitation of the mandibular

1087 articulation, both interpreted as ontogenetical characters. The quadrate shows some

1088 similarities with this of *B. argentina* such as a well-defined rod-shaped quadrate ridge

1089 ('quadrate shaft' sensu Hendrickx and Mateus 2012) almost reaching the entocondyle

1090 medially, a ventral quadratojugal not extending on the ectocondyle, and a pterygoid flange

1091 projecting mostly anteriorly whose the ventral margin is perpendicular to the long axis

1092 passing through the quadrate ridge.

1093   The quadrate of *Z. salleei* shows a combination of features only seen in this taxon,

1094 namely: a deep posterior fossa bounded medially by a well-delimited and rod-shaped quadrate

1095 ridge, and laterally by a strongly elongated ventral projection of the dorsal quadratojugal

1096 contact, a large medially inclined quadrate foramen showing a lenticular outline in posterior

1097 view, a ventral quadratojugal contact extending along almost one half of the quadrate body, a

1098 dorsal quadratojugal contact facing anteriorly, and two relatively small mandibular condyles

1099 separated by a wide intercondylar sulcus. The pterygoid flange projects only anteriorly and

1100 possesses a shallow medial fossa and no ventral shelf on its ventral margin. As the two other

1101 basal coelurosaurs, the ventral margin of the pterygoid flange extends perpendicular to the

1102 long axis of the quadrate shaft but the anterior margin of the flange is parabolic rather that

1103 semi-oval.

1104   The quadrate of the basal coelurosaur *A. zhaoi* significantly differs from those of *B.*

1105 *argentina* and *Z. sallei*. The pterygoid flange is autapomorphically triangular and

1106 convergently similar to this of dromaeosaurids. A vertically oriented ventral shelf ('sliver of

1107 bone' sensu Choiniere et al., 2014) seems to be present on the medial surface of the pterygoid

1108 flange, along the posteroventral margin of the flange. The quadrate foramen is large,

1109 subcircular, and entirely developed within the quadrate body at one half of the bone

1110 (Choiniere et al., 2014). A quadrate foramen with similar size, shape and occupation only

1111 occurs in the neovenatorid *Aerosteon*. Similar to basal coelurosaurs, the lateral process is

1112 absent in *A. zhaoi*, yet no pronounced and well-delimited posterior fossa surrounding the

1113 quadrate foramen is present in this taxon (Choiniere et al., 2014).

1114

1116 **Tyrannosauroidea**

1117   *Proceratosaurus bradleyi* (NHM R 4860; Rauhut et al., 2010; Figure 12.1–12.3);

1118 *Eotyrannus lengi* (MIWG, 1997.550; Figure 12.4–12.9); *Xiongguanlong baimoensis* (Li et al.,

1119 2010); *Alioramus altai* (Brusatte et al., 2012; Figure 12.10–12.15); *Albertosaurus*

1120 *sarcophagus* (Currie, 2003); *Gorgosaurus libratus* (AMNH 5336, 5664); *Daspletosaurus* sp.

1121 (Currie, 2003); *Tyrannosaurus rex* (FMNH PR2081, AMNH 5027; Molnar, 1991; Brochu,

1122 2003).

1123   Although a significant amount of work has recently been published on tyrannosauroid

1124 paleobiology and anatomy due to recent discoveries (e.g., Xu et al., 2004, 2006; Brusatte,

1125 Carr, et al., 2009; Ji et al., 2009; Sereno et al., 2009; Carr and Williamson, 2010; Averianov

1126 and Sues, 2011; Hone et al., 2011; Loewen et al., 2013), the quadrate anatomy in this

1127 important clade of theropods is not particularly well-known. Detailed descriptions are

1128 available only for four tyrannosauroid taxa: *Proceratosaurus bradleyi* (Rauhut et al., 2010),

1129 *Alioramus altai* (Brusatte et al., 2012; Gold et al., 2013), *Albertosaurus sarcophagus* (Carr,

1130 1996) and *Tyrannosaurus rex* (Molnar, 1991; Brochu, 2003).

1131   The tyrannosaurid quadrate is particularly short (ratio of more than 0.5) while in the

1132 basal forms like *P. bradleyi* and *X. baimoensis* it is moderately ventrodorsally-elongated (ratio

1133 between 0.45 and 0.5) like in basal tetanurans (Figure 12.1). In Tyrannosauridae and some

1134 basal tyrannosauroids such as *X. baimoensis*, the mandibular articulation and the quadrate

1135 body at the level of the ventral quadratojugal contact are particularly broad (Figure 12.12).

1136 However, the quadrate body is strongly constricted at the level of the quadrate foramen,

1137 giving the typical axe shape to the quadrate in posterior view (Figure 12.12).

1138   The quadrate ridge is laterally-inclined and usually distinct, and rod-shaped in basal

1139   forms like *P. bradleyi* (Figure 12.1), but forming a typical crest delimiting the medial margin

1140   of the quadrate body in some derived tyrannosauroids like *T. rex* (AMNH 5027; Larson,

1141   2008). This crest is prominent just dorsal to the entocondyle at the posteromedial portion of

1142   the quadrate, and reaches the second third of the quadrate body in *A. sarcophagus* and

1143   *Daspletosaurus* sp. (Currie, 2003, figures 10, 28) while it extends to the quadrate head in *T.*

1144   *rex* as a narrow crest. The quadrate ridge is straight in most tyrannosauroids but rather

1145   biconvex in posterior view, and strongly posteriorly-folded in medial view in *A. altai* (Figure

1146   12.13) and *T. rex*. The quadrate ridge of tyrannosaurids is also divided into two ridges

1147   separated by a small concavity at the ventral part of the ridge, just above the entocondyle,

1148   although the two ridges are rather shallow in *A. altai* (Figure 12.13) and *Daspletosaurus*

1149   (Currie, 2003, figure 10). The concavity bordered by those two ridges is deep and well-visible

1150   in *A. sarcophagus* (Currie, 2003, figure 10) and *T. rex* (AMNH 5027), and strongly baso-

1151   apically elongated, covering the basal half of the quadrate ridge, in the latter.

1152   The quadrate foramen is mostly delimited by the quadrate bone in Tyrannosauroidea

1153   (Figure 12.1, 12). In basal forms such as *P. bradleyi*, the quadrate foramen is small, elliptical

1154   and strongly ventrodorsally-elongated. It becomes larger in more derived tyrannosauroids like

1155   *X. baimoensis*, *G. libratus* and *T. rex*, in which it is lenticular or lanceolate. In tyrannosaurids,

1156   a short ventral projection of the dorsal quadratojugal contact delimits the dorsal margin of the

1157   quadrate foramen laterally.

1158   Another condition uniting most tyrannosauroid taxa is the semi-oval shape of the

1159   pterygoid flange, strongly anteroposteriorly-elongated relative to the height of the quadrate

1160   body (ratio of more than 0.8). The pterygoid flange forms an elongated subtrapezoidal shape

1161   in derived tyrannosaurids like *A. altai* (Figure 12.13), where both ventral and dorsal margins

1162   are concave and the anterior margin is rugged. In tyrannosaurids, the ventral margin of the

1163 flange is divided into two crests in which the lateral one terminates at the middle of the

1164 quadrate body, just above the intercondylar sulcus of the mandibular condyle or reaching

1165 them. The medial crest, on the other hand, meets the quadrate body at its medial margin and

1166 well-above the entocondyle. A ventral pneumatic recess is found between these two ridges of

1167 the pterygoid flange in *A*. *altai* (Figure 12.15), *A*. *sarcophagus* (Carr, 1996), *Daspletosaurus*

1168 sp. (Currie, 2003, figure 28C) and *T*. *rex* (Brochu, 2003). The lateral process of the quadrate

1169 body is absent in all tyrannosauroids.

1170   The quadrate head of some tyrannosaurids like *Daspletosaurus* sp. and *A*. *altai* is sub-

1171 circular (Currie, 2003, figure 28D; Brusatte et al., 2012), but it is slightly biconvex and almost

1172 double-headed in *T*. *rex* (Figure 12.11) and *A*. *sarcophagus* (Currie, 2003, figure 10B)*,* which

1173 possess a small concavity centrally-positioned on the quadrate head. The posterior fossa of

1174 tyrannosauroids is absent. Nonetheless, the quadrate foramen of some derived tyrannosaurids

1175 is bounded by a large depression on the quadrate shaft which is delimited dorsally by the

1176 dorsal quadratojugal contact, and laterally by the quadrate ridge. This depression is, however,

1177 not considered homologous to the posterior fossa of other theropod taxa.

1178   Most tyrannosauroids have a dorsal quadratojugal contact facing lateroposteriorly

1179 (Figure 12.12) or completely posteriorly as in *T*. *rex* (Larson, 2008). This feature is difficult to

1180 assess in the basal taxon *P*. *bradleyi* because the descending process of the squamosal covers

1181 the posterodorsal side of the quadrate. However, a dorsal quadratojugal contact on the

1182 lateroposterior margin of the quadrate body seems to be present in *X*. *baimoensis*. Unlike

1183 other tyrannosaurids, the ventral quadratojugal contact of the quadrate is broad lateromedially

1184 and lanceolate in *T*. *rex*, whereas it is more ventrodorsally-elongated and irregularly-shaped in

1185 more basal tyrannosaurids. The ventral quadratojugal contact of some Tyrannosauridae such

1186 as *Eotyrannus lengi* (Figure 12.5), *A*. *altai*, *A*. *sarcophagus*, and *T*. *baatar* is also

1187 lateroposteriorly-positioned and D-shaped or subquadrangular (Figure 12.11).

1188   The mandibular articulation in Tyrannosauroidea is composed of two ovoid and

1189 subparallel condyles obliquely-oriented, roughly similar in size, and delimited by a very broad

1190 and shallow intercondylar sulcus which is parallel to the main axis passing through the

1191 mandibular condyles (Figure 12.9, 12.15). Although the ectocondyle of *P. bradleyi* is wider

1192 posteriorly than the entocondyle (Rauhut et al., 2010), they are usually subequal in posterior

1193 view in other tyrannosauroids taxa like *E. lengi* and *T. rex*.

1194   Pneumacity is a common feature among tyrannosaurids and pneumatic foramina can

1195 also appear in a pneumatic recess in the medial fossa of the pterygoid flange such as in *A.*

1196 *sarcophagus* (Currie, 2003, figure 10B) and *T. rex* (Molnar, 1991, figure 7). Also, *T. rex* and

1197 *A. sarcophagus* possess a pneumatic foramen on the anterodorsal side of the quadrate,

1198 beneath the quadrate head (Molnar, 1991; Brochu, 2003, figure 7).

1199

1200 **Compsognathidae**

1201   *Compsognathus longipes* (MNHN CNJ 79; Ostrom, 1978; Peyer, 2006); *Scipionyx*

1202 *samnicicus* (Dal Sasso and Maganuco, 2011); *Juravenator starki* (Chiappe and Göhlich,

1203 2010); *Sinosauropteryx prima* (Currie and Chen, 2001).

1204   The quadrate anatomy of compsognathids is one of poorest known among nonavian

1205 theropods. A thorough description of the bone was only given by Dal Sasso and Maganuco

1206 (2011) for *Scipionyx samnicicus*, and the quadrate of other Compsognathidae was either

1207 briefly described, as in *Compsognathus longipes* (Ostrom, 1978; Peyer, 2006), *Juravenator*

1208 *starki* (Chiappe and Göhlich, 2010), and *Sinosauropteryx prima* (Currie and Chen, 2001), or

1209 not described at all, as in *Huxiagnathus orientalis* (Hwang et al., 2004) and *Sinocalliopteryx*

1210 *gigas* (Ji et al., 2007). Although most of compsognathid specimens with cranial material tend

1211 to be extremely well preserved and almost complete, their remains are found in two

1212 dimensions on slabs of fine grained limestone, usually in articulations with other cranial

1213   bones, or associated with them. Therefore, due to crushing, missing elements and hidden

1214   parts, few information on the compsognathid quadrate can be extracted. This is particularly

1215   the case in *J. starki* and *H. orientalis* in which only a small portion of the quadrate is visible.

1216   The quadrate of Compsognathidae is an elongated and slender bone in which the

1217   mandibular articulation is relatively narrow, so that the quadrate body is tall both in lateral

1218   and posterior views. When articulated, the quadrate lies perpendicular to the ventral margin of

1219   the cranium, then gently curves posteriorly with the results that the quadrate head is

1220   positioned posteriorly relative to the mandibular articulation. An anterior inclination of the

1221   quadrate was proposed by Dal Sasso and Maganuco (2011) for *S. samniticus* but the quadrate

1222   seems to be slightly posteriorly inclined even in articulation, as represented by these authors

1223   in the cranial reconstruction of this taxon (Dal Sasso and Maganuco, 2011, figure 175b). The

1224   posterior margin of the quadrate body is weakly concave and the lateral margin is sigmoid in

1225   *S. prima* (Currie and Chen, 2001, figure 3f).

1226   A small quadrate foramen exists at one third of the quadrate body in *S. samniticus*, but

1227   its presence cannot be determined in other compsognathids. Nevertheless, the quadrate and

1228   quadratojugal tend to be disarticulated instead of fused together, so that the presence of an

1229   quadrate foramen between the quadrate and quadratojugal seems to be likely. No quadrate

1230   ridge has been illustrated in *S. prima*, but if present, the ridge was ventro-dorsally oriented

1231   rather than medially inclined. The ventral quadratojugal contact corresponds to a lanceolate

1232   surface extending on the ectocondyle in *S. samniticus*, and the shape dorsal quadratojugal

1233   contact is unknown of this taxon and other compsognathids.

1234   The quadrate head is single headed and corresponds to a spherical or semi-spherical

1235   structure separated from the quadrate shaft by a narrow constriction. The ventral margin of the

1236   pterygoid flange attaches to the quadrate body just above the mandibular articulation, as in *S.*

1237   *samniticus* (Dal Sasso and Maganuco, 2011, figure 41) and *C. longipes* (pers. obs.), or at the

1238   same level than the mandibular condyles, as it seems to be the case in *S. prima* (Currie and

1239   Chen, 2001, figure 3f). The shape of the pterygoid flange cannot be determined with precision

1240   but seems to be roughly parabolic in *C. longipes* and sub-trapezoidal in *S. samniticus*. It is

1241   unknown whether the dorsal margin of the flange was reaching the quadrate head or not

1242   dorsally.

1243   The mandibular articulation includes two condyles in which the ectocondyle is smaller

1244   than the entocondyle in posterior view in *S. prima* (Currie and Chen, 2001, figure 3f).

1245   According to Peyer (2006), the reverse condition occurs in *C. longipes* but the mandibular

1246   articulation is not well-preserved enough to support this observation. A pneumatic quadrate is

1247   present at least in *S. prima* which shows a posterior pneumatopore centrally positioned on the

1248   quadrate body, at mid-height of the quadrate, and within the ventral part of a large posterior

1249   fossa (Currie and Chen, 2001).

1250

1251   Figure 13

1252   **Ornithomimosauria**

1253   *Garudimimus brevipes* (Kobayashi and Barsbold, 2005; Figure 13.6–13.7);

1254   *Sinornithomimus dongi* (Kobayashi and Lü, 2003; Figure 13.5); *Ornithomimus edmontonicus*

1255   (Tahara and Larsson, 2011; Figure 13.1–13.4); *Gallimimus bullatus* (IGM 100-1133);

1256   *Struthiomimus altus* (AMNH 5339); Ornithomimosauria gen. et sp. indet. (Makovicky and

1257   Norell, 1998).

1258   The quadrate has been described usually briefly for some ornithomimosaurs taxa such

1259   as *Gallimimus bullatus* (Osmólska et al., 1972), *Sinornithomimus dongi* (Kobayashi and Lü,

1260   2003), *Garudimimus brevipes* (Kobayashi and Barsbold, 2005), and an indeterminate

1261   ornithomimosaur from Mongolia (Makovicky and Norell, 1998).

1262   The quadrate is slender (ratio of less than 0.35) in posterior view with an expanded

1263   lateromedially mandibular articulation, the dorsal portion is particularly narrow and elongated

1264   (Figure 13.5–13.7), and both lateral and medial margins converge dorsally to the quadrate

1265   head. The quadrate of ornithomimosaurs is inclined posteriorly in the cranium so that the

1266   mandibular articulation is always anterior relative to the quadrate head.

1267   The quadrate foramen is present in *S. dongi* (Figure 13.5), *G. brevipes* (the

1268   'paraquadrate foramen' of Kobayashi and Lü 2003 and the 'paraquadrate foramen' or

1269   'paraquadratic foramen' of Kobayashi and Barsbold 2005 respectively; Figure 13.6–13.7), *O.*

1270   *edmontonicus* (Makovicky et al., 2004, figure 6.2A; Figure 13.3–13.4) and *S. Altus* (AMNH

1271   5339) and corresponds to a narrow and lenticular aperture positioned at two-fifths of the

1272   quadrate body. The quadrate foramen is equally delimited by the quadrate and quadratojugal

1273   in basal forms, and mostly bounded by the quadratojugal in derived forms like *O.*

1274   *edmontonicus*.

1275   The quadrate ridge of ornithomimosaurs is not well-defined except when delimited by

1276   the deep posterior fossa which forms a narrow rod-shaped structure subparallel to the long

1277   axis passing through the quadrate body (Figure 13.5–13.7). The pterygoid flange is well-

1278   visible in *G. brevipes* in lateral view (Kobayashi and Barsbold, 2005, figure 4A). The flange

1279   is parabolic in shape, with a rounded anterior margin in which the most anterior point occurs

1280   at mid-height of the quadrate body. The flange is moderately anteroposteriorly elongated

1281   (ratio of 0.58) but seems to be much larger than the pterygoid flange of *S. dongi* with a ratio

1282   of approximately 0.4 (Kobayashi and Lü, 2003). As *S. dongi*, the ventral margin of the

1283   pterygoid flange of *G. brevipes* seems to meet the quadrate body just above the mandibular

1284   condyles, and the dorsal margin reaches the quadrate head at its base. In *G. brevipes*, the

1285   quadrate head is single headed and fits in the quadrate head of the squamosal (Makovicky et

1286   al., 2004). The articulation with the squamosal is not exposed in lateral view in

1287 *Shenzhousaurus orientalis*, unlike the condition seen in *G. bullatus* and *O. edmontonicus* (Ji et

1288 al., 2003).

1289   One of the most diagnostic features of most ornithomimosaur quadrate is the deep,

1290 lanceolate and well-defined posterior fossa centrally positioned on the quadrate body and

1291 including a small pneumatic foramen (Makovicky et al., 2004; Figure 13.1, 13.3–13.7). Such

1292 fossa is present in *S. dongi* (the 'quadrate foramen' of Kobayashi and Lü (2003) and includes

1293 an ovoid pneumatopore divided by a vertical septum and located within the dorsal part of the

1294 fossa. It also exists in *G. brevipes* (the 'quadrate foramen' of Kobayashi and Barsbold (2005)

1295 whose the elliptical foramen is present ventrally in the depression, and an indeterminate

1296 ornithomimosaur (IGM 100-987) in which the deep and strongly elongated posterior fossa

1297 includes a tiny subcircular foramen at the most dorsal part of the fossa (Makovicky and

1298 Norell, 1998). A deep lanceolate posterior fossa is also present in *G. bullatus* and *S. altus* at

1299 two-thirds of the quadrate body (pers. obs.), yet it is unknown whether this depression was

1300 pneumatic or not. According to Makovicky and Norell (1998), a pneumatic and well-defined

1301 posterior fossa is not present in some ornithomimids such as *O. edmontonicus* (ROM 851,

1302 ROM 840). Yet, the specimen RTMP 95.110.1 of *O. edmontonicus* does possess a pneumatic

1303 foramen on the posteromedial surface of the quadrate, and leading to a vast pneumatic

1304 chamber inside the quadrate bone (Tahara and Larsson, 2011; Figure 13.3).

1305   The ventral quadratojugal contact of the quadrate has a unique morphology among

1306 ornithomimids. In *S. altus*, the ventral part of this contact corresponds to a hear-shape

1307 depression facing laterally and bounded by a prominent ridge along its ventral and posterior

1308 margin (Figure 13.1). The dorsal part of the ventral quadratojugal contact is, however, a line

1309 diminishing in width dorsally to meet the quadrate foramen. In *O. edmontonicus*, the

1310 quadratojugal display a dorsal projection which articulates along this articular surface, and

1311 delimits the quadrate foramen posteroventrally. The dorsal quadratojugal contact is located on

1312 the lateral surface of the quadrate body in *G. brevipes*, and on the anterior margin of the

1313 quadrate body in more derived ornithomimids like *S. altus* and *O. edmontonicus*. The

1314 quadrate of ornithomimids does not display a lateral process.

1315   The typical mandibular articulation structure of two condyles separated by an

1316 intercondylar sulcus is different in derived ornithomimosaurs. According to Kobayashi and

1317 Lü (2003) and Kobayashi and Barsbold (2005), the ecto- and entocondyles of *S. dongi* and *G.*

1318 *brevipes* are subequal in size and well-separated by an anteroposterior intercondylar sulcus.

1319 Yet the entocondyle is protuberant and projected medially in *S. dongi*, whereas there is an

1320 accessory condyle lateral to the ectocondyle and dorsally-positioned relative to the two

1321 mandibular condyles (Kobayashi and Lü, 2003). The examination of the quadrate of an

1322 undescribed skull of *Gallimimus bullatus* (IGM 100-1133) supports this morphology of the

1323 mandibular articulation of ornithomimids. The accessory condyle of Kobayashi and Lü (2003)

1324 corresponds in fact to a lateral extension of the ectocondyle, and the ecto- and entocondyle

1325 therefore differ significantly in their morphology (Figure 13.2). Indeed, the ectocondyle is

1326 parabolic and comma shaped, with a narrow diagonally elongated lateral part and a wide

1327 ovoid medial part, whereas the entocondyle is elliptical, almost spherical. This lateral

1328 extension of the ectocondyle articulates with a dorsolateral flange of the surangular, just

1329 anterior to the mandibular glenoid (Makovicky et al., 2004). Both mandibular condyles are

1330 separated by a wide, shallow and poorly delimited intercondylar sulcus which runs

1331 anteroposteriorly (Figure 13.2). In basal ornithomimids like *Nqwebasaurus thwazi*, the

1332 quadrate articulation is not as complex and consists of a lateromedially extended hemi-

1333 cylindrical ectocondyle and a hemispherical entocondyle (Choiniere et al., 2012).

1334

1335 Figure 14

1336 **Basal Maniraptora**

1337   *Ornitholestes hermanni* (AMNH FARB 619; Figure 14.7–14.11); *Mononykus*

1338   *olecranus* (Chiappe et al., 2002); *Shuvuuia deserti* (IGM 100-977, Figure 14.12–14.13; IGM

1339   100-1001, Figure 14.14–14.16; Dufeau, 2003).

1340   The quadrate was comprehensively described in the alvarezsaurids *Shuvuuia deserti*

1341   and *Mononykus olecranus* (Chiappe et al., 2002), but the cranial bone has not received any

1342   detailed description in *Ornitholestes hermanni*. Although all three taxa are basal members of

1343   the Maniraptora, *O. hermanni* is the most primitive maniraptoran (sensu Senter, 2011; Turner

1344   et al., 2012) whereas the two alvarezsaurids are derived forms of Alvarezsauroidea (Nesbitt et

1345   al., 2011; Xu et al., 2011; Choiniere et al., 2014), so that their quadrates significantly differ in

1346   their morphology.

1347   The left quadrate of *O. hermanni* is crushed and fragmented, and only the right

1348   quadrate provides data on the anatomy of this bone. The right quadrate is complete, slightly

1349   damaged but strongly deformed in its central part. It is preserved in articulation within the

1350   cranium, which is crushed and filled with sediment in its internal part so that few information

1351   can be extracted in anterior and medial views. Besides, only the ventral part of the bone is

1352   visible, the dorsal part other than the quadrate head, being obscured by the squamosal (Figure

1353   14.7).

1354   The quadrate of *O. hermanni* is tall (0.28). Despite some deformation in the central

1355   part of the quadrate body, the quadrate displays a quadrate foramen at one-third of the bone,

1356   lateral to the prominent quadrate ridge, and open laterally (Figure 14.8–14.10). The quadrate

1357   foramen was mostly bordered by the quadrate as a well-developed ventral projection of the

1358   dorsal quadratojugal contact seems to have delimited part of the lateral margin of the quadrate

1359   foramen (Figure 14.10). A lateral process with a parabolic outline is visible in lateral view.

1360   This process projects anteriorly, yet it is unknown whether it was extending mostly laterally

1361   or anteriorly before taphonomic deformation. The ventral quadratojugal contact extends along

1362   the ventral half of the quadrate body and was most likely anteriorly inclined. There is no

1363   quadratojugal process extending from the ventral quadratojugal contact. The quadrate head,

1364   only visible in lateral view, is single headed and has a rounded dorsal margin. It is weakly

1365   oriented anteriorly and the pterygoid flange is not attached to its dorsal margin. The quadrate

1366   ridge is prominent, rod-shaped, laterally inclined and reaches the ectocondyle in its medial

1367   section.

1368   In *O. hermanni*, the pterygoid flange only projects anteriorly and its anterior extension

1369   is relatively limited compared to other basal coelurosaurs. The anterior margin of the

1370   pterygoid flange is parabolic and almost subtriangular, and the anteriormost point of the

1371   flange is situated at mid-height of the quadrate body. A deep posterior fossa occupies most of

1372   the quadrate body in posterior view, and extends from the mandibular articulation ventrally to

1373   at least the quadrate foramen. The mandibular articulation encompasses two condyles

1374   subequal in shape, size and orientation, and separated by a wide shallowly concave

1375   intercondylar sulcus (Figure 14.11). Both ecto- and entocondyles are elliptical and the angle

1376   between the long axis of the mandibular articulation and the main axis passing through the

1377   condyles and the intercondylar sulcus is approximately 120°.

1378   *S. deserti* is the only alvarezsauroid preserving a complete quadrate that has been well-

1379   described in the literature. Both quadrates of the primitive alvarezsauroid *Haplocheirus*

1380   *sollers* (Choiniere, Xu, et al., 2010) seems to be preserved as well but neither illustrations nor

1381   a description have been provided for the quadrate in this taxon. As for *M. olecranus*, only the

1382   quadrate head, which is double headed and contacts both the squamosal and prootic (Perle et

1383   al., 1994; Chiappe et al., 2002), is preserved. Access to both articulated skulls of *S. deserti*

1384   (IGM 100-977; IGM 100-1001) allows to provide a list of unique features in this taxon.

1385   The quadrate is remarkably different from this of other theropods in many aspects.

1386   Both specimens have been interpreted as belonging to different ontogenetic stages (Dufeau,

1387   2003), yet the quadrate of each specimens strongly differ in their morphology so much so that

1388   the assignation of both specimens to a same species is questionable. The right quadrate of the

1389   largest specimen (IGM 100-977) is complete and well-preserved but only its posterior side is

1390   well-visible (Figure 14.12–14.13). The most striking features of this bone is the lateral

1391   orientation of the quadrate head, the short and parabolic pterygoid flange, and the notch on

1392   the dorsal margin of this flange. In this specimen, the quadrate head seems to be single headed

1393   and lateromedially wider than the mandibular articulation. There is a faint quadrate ridge in

1394   posterior view but the ridge is well-demarcated in medial view. The dorsal margin of the

1395   pterygoid flange is unique in possessing a deep notch which does not seem to result from the

1396   loss of a fragment. The mandibular articulation is just a prolongation of the quadrate shaft. It

1397   is subrectangular, flat and seems to be unicondylar in posterior view. Nonetheless, a fragment

1398   of bone lying on the ventrolateral surface of the pterygoid flange may correspond to the lateral

1399   part of the mandibular articulation.

1400   The mandibular articulation of IGM 100-1001 is much wider than the quadrate shaft,

1401   and the ventral part of the quadrate body is boot-shaped, i.e., the lateroventral margin is

1402   convex, almost pointed, and projects far anteriorly. The lateral process is subtriangular and

1403   anterolaterally directed. Its anterior corner contacts both the postorbital and the squamosal, a

1404   quadrate autapomorphy of *S. deserti* (Chiappe et al., 1998). A small corner marks the ventral

1405   limit of the lateral process. The dorsal quadratojugal contact typically extends to that level in

1406   many other theropods but the quadratojugal only articulates at the ventrolateral corner of the

1407   quadrate body. As a result, the quadrate foramen is merged with the infratemporal fenestra,

1408   which is a second quadrate autapomorphy of *S. deserti*. The quadrate head of IGM 100-1001

1409   clearly displays two condyles, the squamosal capitulum, directed dorsally to contact the

1410   squamosal, and the otic capitulum, oriented medially towards the braincase (Chiappe et al.,

1411   1998, 2002).

1412   The pterygoid flange of IGM 100-1001 extends anteromedially and forms a short

1413   subtrapezoidal ala in which the anterior margin is long and posteriorly inclined (Figure

1414   14.15). The anteriormost point of the pterygoid flange is located at one fifth of the quadrate

1415   body, and the ventral margin of the flange attaches the quadrate flange just above the

1416   mandibular articulation. The pterygoid articulates with the medioventral part of the pterygoid

1417   flange close to the quadrate body (Figure 14.16). The mandibular articulation clearly shows

1418   two condyles in posterior view, and the ectocondyle is lateromedially longer than the

1419   entocondyle. In ventral view, the distinction between the two condyles is more subtle, and

1420   both ecto- and entocondyles are elliptical and follows the same orientation than the long axis

1421   of the mandibular articulation (Figure 14.16), which is also an autapomorphical feature of *S.*

1422   *deserti.*

1423

1424   **Therizinosauria**

1425   *Falcarius utahensis* (Zanno, 2010; Figure 13.8–13.12); *Erlikosaurus andrewsi* (Clark

1426   et al., 1994).

1427   The quadrate of therizinosaurs has been well-described and illustrated in only two

1428   taxa: *Erlikosaurus andrewsi* (Clark et al., 1994) and *Falcarius utahensis* (Zanno, 2010). The

1429   quadrate morphology in these two specialized theropods is significantly different from other

1430   closely related coelurosaurs, and both taxa share a combination of apomorphic characters.

1431   Due to the large quadrate foramen, which is deeply positioned inside the quadrate

1432   bone, the quadrate body is constricted at mid-height (Figure 13.10). Both ventral and dorsal

1433   parts are lateromedially-expanded, roughly making an hourglass shape of the quadrate body

1434   in posterior view. The quadrate is a moderately elongated bone (ratio between 0.38-0.4)

1435   whose quadrate ridge is shallow in posterior view. It is very well delimited in medial view in

1436   *F. utahensis* but almost unnoticeable in *E. andrewsi*. As in many tetanurans, the quadrate

1437   ridge of *F. utahensis* is laterally-inclined and becomes marked just above the entocondyle and

1438   reaches the quadrate head (Figure 13.10). The medial margin of the quadrate body of these

1439   two therizinosaurs is biconcave, and the convexity separating the two concavities is situated at

1440   one third of the quadrate body in *E. andrewsi* and at two thirds in *F. utahensis*.

1441   The quadrate foramen is mostly delimited by the quadrate in therizinosaurs, and the

1442   ventral projection of the dorsal quadratojugal contacts delimits an important part of the

1443   foramen laterodorsally in *F. utahensis* (Figure 13.10). The shape of the quadrate foramen is

1444   lenticular in *E. andrewsi* and a reversed teardrop in *F. utahensis*.

1445   The lateral process is here considered as present in *F. utahensis* (Figure 13.9) and *E.*

1446 *andrewsi* because there is a short lateral projection of the quadrate body from above the

1447 quadrate foramen to the quadrate head in both taxa. The lateral process projects completely

1448 laterally in *F. utahensis* whereas it extends anterolaterally in *E. andrewsi*, and the lateral

1449 margin of this process is parabolic in outline in these two therizinosaurs.

1450   The pterygoid flange is short in therizinosaurs, particularly in *F. utahensis* (Figure

1451 S10K) whose ratio between the anteroposterior width and the ventrodorsal length of the

1452 quadrate body is significantly low (0.33). The anterior margin of the flange is M-shaped in *F.*

1453 *utahensis* (Figure S10K) while the pterygoid flange of *E. andrewsi* is parabolic with a small

1454 concavity at its anteroventral margin (Clark et al., 1994, figure 2). In both therizinosaurs, the

1455 pterygoid flange projects anteromedially but does not curve medially. In addition, the ventral

1456 margin of the pterygoid flange meets the quadrate body well-above the entocondyle and the

1457 dorsal margin reaches the ventral base of the pterygoid flange. Interestingly, in *E. andrewsi*

1458 the prootic and basipshenoid contact the pterygoid flange posterodorsally. Although the

1459 cranium of this taxon has been strongly deformed and this part of the skull has been badly

1460 preserved, a contact between the pterygoid flange and the braincase seems to be genuine. A

1461 similar contact between those bones also occurs in the oviraptorosaur *Avimimus portentosus*.

1462   In therizinosaurs, the dorsal quadratojugal contact is positioned on the anterior side of

1463   the short lateral process (Figure 13.8). This contact also possesses a ventral projection widely

1464   expanded in *F. utahensis* whereas such projection is absent in *E. andrewsi*. The dorsal

1465   quadratojugal contact corresponds to an elongated line in *F. utahensis* (Figure 13.8) and *E.*

1466   *andrewsi*. The ventral quadratojugal contact is elliptical and situated just above the

1467   ectocondyle in *F. utahensis* (Figure 13.9) and *E. andrewsi* but this suture with the

1468   quadratojugal is much broader anteroposteriorly in the former, and it is narrow and oblong in

1469   the latter.

1470   The mandibular articulation is formed by two condyles in *F. utahensis* (Figure S10L)

1471   and by three condyles in *E. andrewsi* (Clark et al., 1994). The mandibular condyles are ovoid

1472   to subcircular in both therizinosaurs. In *F. utahensis*, the ectocondyle is ovoid and the long

1473   axis passing through it is inclined laterally by an angle of 130° relative to the long axis of the

1474   mandibular articulation (Figure 13.12). The entocondyle is protuberant and separated from the

1475   ectocondyle by a very broad but shallow intercondylar sulcus, which is parallel to the long

1476   axis of the lateral condyle. The three mandibular condyles of *E. andrewsi* are well developed,

1477   with a larger ectocondyle, a medium entocondyle (two thirds of the size of the ectocondyle)

1478   and a third much smaller condyle (half of the size of the entocondyle) lying posteriorly

1479   between the two (Clark et al., 1994).

1480   A wide pneumatic recess appears in the ventromedial part of the flange in *F. utahensis*

1481   (Figure 13.11). This recess of *F. utahensis* penetrates deeply inside the pterygoid flange and

1482   quadrate body, and is strongly displaced laterally, contrarily to the medial pneumatopores of

1483   other theropods (Figure 13.8). This lateral displacement implies the fact that the ventralmost

1484   margin of the pterygoid flange meets the quadrate body at the same level than the

1485   intercondylar sulcus rather than close to the entocondyle. Although pneumaticity might have

1486   been present in the quadrate of *E. andrewsi*, it is not conspicuously expressed like in *F.*

1487   *utahensis*. Clark et al. (1994) inferred the possible existence of a pneumatic foramen in a

1488   posteromedial depression near the dorsal margin of the bone, which is not observable due to

1489   crushing. Nevertheless, a large medial pneumatic recess is not present in *E. andrewsi*.

1490

1491   Figure 15

1492   **Oviraptorosauria**

1493   *Incisivorosaurus gauthieri* (Balanoff et al., 2009); *Avimimus portentosus* (Kurzanov,

1494   1985; Vickers-Rich et al., 2002; Figure 15.1–15.4); *Citipati osmolskae* (IGM 100-978; Figure

1495   15.5–15.8); *Khaan mckennai* (IGM 100-1002; IGM 100-1127; Balanoff and Norell, 2012;

1496   Figure 15.9–15.12); *Heyuannia huangi* (Lü, 2003); *Conchoraptor gracilis* (Kundrát and

1497   Janáček, 2007); Oviraptoridae gen. et sp. indet. (Maryańska and Osmólska, 1997).

1498   The anatomy of the quadrates of some derived oviraptorids (*Oviraptor*? sp. and

1499   *Ingenia yanshini* or *Conchoraptor gracilis*) has been comprehensively investigated by

1500   Maryańska and Osmólska (1997) and the quadrate anatomy of more basal oviraptorosaurs and

1501   other oviraptorids is well-documented in the literature with only good descriptions of the bone

1502   in some taxa such as *Incisivorosaurus gauthieri* (Balanoff et al., 2009), *Avimimus portentosus*

1503   (Kurzanov, 1985; Vickers-Rich et al., 2002), *Citipati osmolskae* (Chiappe et al., 2002) and

1504   *Khaan mckennai* (Balanoff and Norell, 2012). As noticed by Maryańska and Osmólska

1505   (1997), the quadrate of oviraptorids, and to some extend oviraptorosaur theropods, is atypical

1506   because of the shape of its mandibular articulation, its contact with the pterygoid and,

1507   especially, its quadrate head. In the present paper, the quadrate of the basal oviraptorosaur *A.*

1508   *portentosus* (PIN 3907/1) will be described before summarizing the synapomorphic characters

1509   found in Oviraptoridae.

1510   In *A. portentosus*, the quadrate is uncommonly fused to the braincase and the

1511   pterygoid flange (Figure 15.1–15.3). The quadrate body is concave all along the bone and has

1512   subparallel lateral and medial margins ventrally. Dorsally, the quadrate body enlarges at about

1513   two-fifths of the bone height, where the pterygoid flange meets the quadrate body at its

1514   medial margin. The ventral part of the pterygoid flange, rather than projecting anteriorly or

1515   anteromedially as all nonavian theropods, curves medially to contact the braincase on its

1516   posterior side. In ventral view, the dorsal part of the pterygoid flange is oriented

1517   anteromedially and fuses to the pterygoid flange anteriorly and the endocranium

1518   anterodorsally (Figure 15.4). In lateral view, the anterior margin of the pterygoid flange is

1519   parabolic and the most anterior point is situated at one third of the quadrate (Figure 15.1–

1520   15.3).

1521   What is here interpreted as being a ventral projection of the pterygoid bone contacts

1522   the quadrate body on its anteroventral side just above the mandibular articulation (Figure

1523   15.4). If our interpretation is correct, this would be an autapomorphic character for *A.*

1524   *portentosus*. This elongated bone was interpreted by Kurzanov (1985) as being intergrown

1525   jugal and quadratojugal bones. However, the presence of a well-visible ventral quadratojugal

1526   contact on the lateral side of the left quadrate as well as a pterygoid contact on the

1527   anteroventral margin of the right quadrate makes this interpretation doubtful. Due to the

1528   absence of both quadratojugals in PIN 3907/1, it is hard to assume the presence of a quadrate

1529   foramen. However, the quadratojugal contact of the quadrate seems to form a unique suture

1530   along the lateral margin of the quadrate body. The ventral portion of the suture is

1531   anteroposteriorly widened and lanceolate, whereas the dorsal part is a very narrow, elongated

1532   contact receiving both the quadratojugal and the squamosal. A short anterior projection occurs

1533   on the anteroventral part of the quadrate body, at the level of the ectocondyle but just above it.

1534   The quadrate head is unfortunately not completely visible in PIN 3907/1, but close

1535   observation suggests that the quadrate head was in contact with the squamosal and the

1536   braincase (Figure 15.1). The mandibular articulation of *A. portentosus* is formed by two

1537   elliptical and subparallel condyles of the same size (Figure 15.4). These two condyles are

1538   delimited by a narrow and shallow intercondylar sulcus parallel to the main axis passing

1539   through the two condyles and inclined medially. There is no pneumatic foramen in *A.*

1540   *portentosus* and the quadrate is obviously apneumatic in this taxon.

1541   The quadrate of oviraptorid theropods is highly diagnostic given the combination of

1542   the following features, namely: an "Eiffel-tower" shape of the quadrate body in posterior

1543   view, terminating dorsally by a conical double-headed quadrate head formed by the

1544   squamosal and otic capitula; a pterygoid contact on the medial side of the quadrate body and

1545   touching the entocondyle (this might not however be the case in *C. gracili*s, see (Kundrát and

1546   Janáček, 2007, figure 2D), and a W-shaped mandibular articulation with a pointing

1547   ventromedial margin of the quadrate body in posterior view (Figure 15.6).

1548   The quadrate foramen is medium-sized, lenticular, equally formed by the quadrate and

1549   quadratojugal and visible in lateral view (Figure 15.6). The oviraptorid quadrate ridge is not

1550   well-delimited in posterior view, but it is strongly inclined laterally and has a biconcave

1551   medial margin. As most tetanurans, there is no lateral process projecting from the quadrate

1552   body (Figure 15.10). The double-headed quadrate head is tall and conical, with a rounded tip

1553   pointing dorsally, and a small constriction separates the head from the rest of the quadrate

1554   body.

1555   The pterygoid flange mostly projects anteriorly and slightly curves medially, and in *C.*

1556   *osmolskae* and *K. mckennai* the flange is subtrapezoidal in shape with a straight (and short in

1557   *K. mckennai*) anteriormost margin inclined posteriorly (Figure 15.9) like in most basal

1558   theropods. The ventral quadratojugal contact is broad, lanceolate and extends on the posterior

1559   side of the quadrate body. In some oviraptorids such as *C. osmolskae*, an ventral process

1560   projects laterally from the ventral part of this articulation to contact the quadratojugal dorsally

1561   (lateral process *sensu* Maryańska and Osmólska, 1997). Among nonavian theropods, such

1562 ventral process only exists in oviraptorids. The dorsal quadratojugal contact forms a narrow

1563 and elongated line for receiving the dorsal quadratojugal process. The ventral margin of the

1564 pterygoid flange meets the quadrate body close to the mandibular articulation, at the level of

1565 the entocondyle and just dorsal to the latter (Figure 15.7).

1566 A pneumatic quadrate has been reported in several troodontids, including *K. mckennai*

1567 (Balanoff and Norell, 2012), *Heyuannia huangi* (Lü, 2003), and *C. gracili*s (Kundrát and

1568 Janáček, 2007). No pneumatic foramen is visible in the posterior surface of *K. mckennai* and

1569 *C. gracilis*, however there is indication that the dorsal tympanic recess of *C. gracilis* invades

1570 the multichambered quadrate pneumatic sinus through an opening on the medial side of the

1571 otic capitulum (Kundrát and Janáček, 2007). In *H. huangi*, a pneumatic foramen is

1572 autapomorphically located on the ventrolateral surface of the pterygoid flange. On the other

1573 hand, an elliptical pneumatopore is present on the ventromedial surface of the pterygoid

1574 flange in some oviraptorid specimen of Mongolia (Maryańska and Osmólska, 1997). This

1575 large and ventrodorsally elongated pneumatic opening is subdivided into numerous hollow

1576 compartments and leads into a pneumatic chamber invading the quadrate shaft, mandibular

1577 articulation, and ventral part of the pterygoid flange (Maryańska and Osmólska, 1997).

1578

1579 Figure 16

1580 **Dromaeosauridae**

1581 *Buitreraptor gonzalezorum* (MPCA 245); *Bambiraptor feinbergi* (AMNH FARB

1582 30556; Figure 16.1–16.6); *Tsaagan mangas* (IGM 100-1015; Figure 16.7–16.11);

1583 *Dromaeosaurus albertensis* (AMNH FARB 5356; Figure 16.12–16.17); *Velociraptor*

1584 *mongoliensis* (AMNH 6415; Sues, 1977; Barsbold and Osmólska, 1999); *Sinornithosaurus*

1585 *millenii* (Xu and Wu, 2001).

1586   Isolated quadrates of dromaeosaurid theropods have been well-illustrated for *Tsaagan*

1587   *mangas* (Norell et al., 2006) and *Bambiraptor feinbergi* (Burnham, 2004), and a detailed

1588   description of the bone is given for *Tsaagan mangas* (Norell et al., 2006), *Dromaeosaurus*

1589   *albertensis* (Colbert and Russell, 1969; Currie, 1995), *Velociraptor mongoliensis* (Sues, 1977;

1590   Barsbold and Osmólska, 1999), and *Sinornithosaurus millenii* (Xu and Wu, 2001).

1591   As many other clades of theropods, the quadrate of Dromaeosauridae is highly

1592   diagnostic. The quadrate is particularly short (ratio of the elongation of the quadrate body

1593   higher than 0.5) due to an important lateromedial expanded mandibular articulation (Figure

1594   16.3–16.7). The quadrate body has a well-marked quadrate ridge laterally-inclined and getting

1595   marked from or right above the entocondyle to reach the quadrate head, as in *T. mangas*, *V.*

1596   *mongoliensis*, and *D. albertensis*. The quadrate head of derived dromaeosaurid such as *V.*

1597   *mongoliensis* (Barsbold and Osmólska, 1999), *D. albertensis* (Currie, 1995), *B. feinbergis*

1598   (Burnham, 2004) and *T. mangas* (Norell et al., 2006) is single-headed and articulates

1599   exclusively with the squamosal. A 'bistylic quadrate head' (sensu Turner et al., 2007) is

1600   present in the basal dromaeosaurid *Mahakala omnogovae* and may have been articulated with

1601   the squamosal and the prootic of the braincase (Turner et al., 2007, 2011). However, the

1602   quadrate head is not double-headed "but the compressed rectangular profile coupled with the

1603   abrupt change to a triangular cross section gives the articular portion of the quadrate a

1604   medially directed 'head'" (Turner et al., 2011, p.8).

1605   The quadrate foramen is well-visible in lateral view and typically large (Paul, 1988;

1606   Barsbold and Osmólska, 1999), forming a lanceolate fenestra equally delimited by the

1607   quadrate and quadratojugal. In some dromaeosaurids like *T. mangas* and *B. feinbergis*, the

1608   quadrate foramen is delimited ventrally by an elongated quadratojugal process, i.e., a well-

1609   developed projection of the ventral quadratojugal contact of the quadrate (Figure 16.2–16.8).

1610   This quadratojugal process is present in many theropods such as Spinosauridae and

1611 Allosauridae, yet the process does not extend much anteriorly, unlike the condition seen in

1612 dromaeosaurids. The quadratojugal process is short in the basal dromaeosaurid *Buitreraptor*

1613 *gonzalezorum*.

1614   The dorsomedial margin of the quadrate foramen is formed by a subtriangular or

1615 parabolic lateral process. This process is particularly well-developed in *Buitreraptor*

1616 *gonzalezorum* (MPCA 245), *B. feinbergi* (FIP 001; Figure 16.3), *T. mangas* (IGM 100-1015;

1617 Figure 16.8), and *V. mongoliensis* (Barsbold and Osmólska, 1999) and much shorter in *D.*

1618 *albertensis* (AMNH 5356; Figure 16.14) and *S. millenii* (Xu and Wu, 2001). The orientation

1619 of the lateral process is variable among dromaeosaurids, projecting laterally in *D. albertensis*,

1620 and *B. gonzalezorum*, and being anterolaterally oriented in *T. mangas* and *Adasaurus*

1621 *mongoliensis*. The lateral process of the latter is apomorphically displaced dorsally, with the

1622 anteriormost point of the process being situated at fourth fifth of the quadrate body, slightly

1623 below the quadrate head (Turner et al., 2012). A subtriangular lateral process was previously

1624 thought to be unique among Dromaeosauridae but, as noted by Agnolin and Novas (2011),

1625 this feature also exists in many basal theropods and basal Avialae such as *Archaeopteryx*

1626 *lithographica* (Walker, 1985). Nevertheless, the morphology of the lateral process of some

1627 dromaeosaurids can be apomorphic in possessing a subrectangular projection receiving the

1628 dorsal process of the quadratojugal, as in *T. mangas* (Figure 16.8).

1629   The atypical pterygoid flange in dromaeosaurid theropods corresponds to a

1630 subtriangular flange formed by two elongated sides meeting ventrally in the quadrate body, at

1631 one-third or one-fourth of the quadrate bone (Xu and Wu, 2001; Figure 16.4, 15.10, 15.13).

1632 The ventral margin of the pterygoid flange meets the quadrate body well-above the

1633 entocondyle, whilst the dorsal margin attaches to the quadrate body just beneath the

1634 articulating surface of the quadrate head. The dorsal margin of the pterygoid flange is

1635 apomorphically columnar in *S. millenii* (Xu and Wu, 2001), the margin being thickened and

1636 round along most of the flange, contrasting with the thin dorsal margin of the pterygoid flange

1637 of other theropods. However, a columnar posterior margin of the pterygoid flange has also

1638 been observed in an undescribed troodontid (IGM 100-1128). The flange can either be

1639 straight and projecting anteromedially like in *B. feinbergi* and *D. albertensis* (Colbert and

1640 Russell, 1969, figure 9), or slightly curved anteromedially as in *T. mangas*.

1641 The medial fossa, posteroventrally situated on the pterygoid flange, is shallow and

1642 does not host a pneumatic recess. A posterior fossa lies on the posterior side of the quadrate

1643 body at mid-height of the quadrate body in *T. mangas* (Norell et al., 2006) and *B. feinbergi*

1644 (FIP 001). The mandibular articulation consists of an ovoid to oblong entocondyle delimited

1645 from the elongated, narrow and sigmoid/parabolic ectocondyle by a deep intercondylar sulcus

1646 (Figure 16.6, 15.11, 15.17). The intercondylar sulcus is diagonally-oriented and its main axis

1647 is sometimes parallel to the main axis passing through the entocondyle. In posterior view,

1648 both ecto- and entocondyles are strongly lateromedially-elongated and shortly ventrodorsally-

1649 expanded. They are delimited by the shallow intercondylar sulcus giving sometimes to the

1650 mandibular articulation a convex form, rather than a well-marked biconvex shape like in most

1651 other nonavian theropods.

1652 A pneumatic quadrate is absent in *T. mangas* (Norell et al., 2006), *B. feinbergi*

1653 (Burnham, 2004), *V. mongoliensis* (Barsbold and Osmólska, 1999) and *D. albertensis* (Currie,

1654 1995) but present in the basal dromaeosaurid *B. gonzalezorum* (Makovicky et al., 2005)

1655 suggesting that the quadrate may have been pleisiomorphically pneumatic in dromaeosaurids.

1656 The pneumatopore of *B. gonzalezorum* is deep and subcircular, and the pneumatic opening is

1657 located on the posterolateral side of the quadrate body, at the level of the ventral part of the

1658 lateral process (Makovicky et al., 2005, figure 2E).

1659

1660 **Troodontidae**

1661   *Anchiornis huxleyi* (Hu et al., 2009); *Xiaotingia zhengi* (Xu et al., 2011); *Mei long* (Xu

1662   and Norell, 2004; Gao et al., 2012); *Sinovenator changii* (Xu et al., 2002); *Troodon formosus*

1663   (Currie and Zhao, 1993a); *Saurornithoides mongoliensis* (Norell and Hwang, 2004);

1664   Troodontidae gen. et sp. indet. (Barsbold et al., 1987); Undescribed Troodontidae (IGM 100-

1665   1128; IGM 100-1323).

1666   Information regarding quadrate anatomy of Troodontidae (sensu Turner et al., 2012

1667   and Godefroit et al., 2013) is very scarce in the literature because most troodontid taxa such as

1668   *Saurornithoides mongoliensis* (Russell, 1969; Barsbold, 1974; Norell et al., 2009), *Zanabazar*

1669   *junior* (Norell et al., 2009), *Byronosaurus jaffei* (Makovicky et al., 2003; Bever and Norell,

1670   2009), *Sinovenator changii* (Xu et al., 2002), *Xixiasaurus henanensis* (Lü et al., 2010), and

1671   *Troodon formosus* (Currie, 1985; Currie and Zhao, 1993a) either preserved just a small

1672   portion of the quadrate or did not have preserved the bone at all. Nevertheless, the quadrates

1673   of *Mei long*, *Anchiornis huxleyi* and *Xiaotingia zhengi* are visible in lateral view; the left

1674   quadrate of an indeterminate troodontid lacking the pterygoid flange (IGM 100-44) was

1675   briefly described and illustrated in posterior view by Barsbold et al. (1987), and a well-

1676   preserved ventral portion of a right quadrate probably belonging to *Saurornithoides*

1677   *mongoliensis* has been described by Norell and Hwang (2004). Likewise, the quadrate bone of

1678   two undescribed troodontid skulls (IGM 100-1128; IGM 100-1323) from the Upper

1679   Cretaceous of Mongolia are also preserved, yet only IGM 100-1128 shows undistorted and

1680   relatively complete left and right quadrates.

1681   The troodontid quadrate is moderately, almost strongly elongated (ratio of 0.353 in

1682   IGM 100-1128 and 0.4 in IGM 100-44). Both quadrates of IGM 100-1128 are found in

1683   articulation within an undistorted skull and their mandibular articulation lies at the same level

1684   than the alveolar margin of the upper jaw. This is, however, not the case in *M*. *long* and *A*.

1685   *huxleyi* in which the mandibular articulation projects well ventral from the ventral margin of

1686 the upper jaw. In IGM 100-1128, the ventral half of the quadrate body extends horizontally,

1687 perpendicular to the ventral margin of the cranium, whereas the dorsal half is strongly

1688 inclined posteriorly so that the quadrate is inclined posteriorly in the cranium and the

1689 mandibular articulation is always anterior relative to the quadrate head. A similar condition

1690 occurs in *A. huxleyi* (Hu et al., 2009, figure S2d). The dorsal margin of the quadrate body is

1691 parabolic in outline in lateral view in IGM 100-1128, and the medial margin is biconcave.

1692 The quadrate ridge is rod-shaped and prominent at one third of the quadrate and along the

1693 second third of the quadrate body. The quadrate ridge does not extends to the entocondyle but

1694 reaches the quadrate head in a fainted way.

1695 The quadrate head of IGM 100-1128 is clearly monostylic and contacts the braincase

1696 medially. This is the case of the quadrate heads of other troodontid taxa which are also single

1697 headed (Currie, 1985; Barsbold et al., 1987) and mostly contacts the squamosal (Currie and

1698 Zhao, 1993a) and other bones of the braincase (exoccipital/opisthotic and prootic), as noted in

1699 *T. formosus* (Currie and Zhao, 1993a), *S. mongoliensis* (Norell et al., 2009), the perinate

1700 *Byronosaurus* sp. (Bever and Norell, 2009) and *Sinornithoides youngi* (Russell and Dong,

1701 1993).

1702 The ventral quadratojugal contact of troodontids is ventro-dorsally elongated,

1703 lanceolate, and inclined medially in posterior view. The ventral quadratojugal contact faces

1704 posterolaterally in IGM 100-1083, and laterally in IGM 100-1128 and IGM 100-44 (Barsbold

1705 et al., 1987, plate 49 figure 4). There is no contact with the quadratojugal along the dorsal part

1706 of the quadrate body in *M. long* as the quadratojugal of this taxon only gets attached to the

1707 lower part of the quadrate body, at the level of the mandibular articulation. Both

1708 quadratojugal and lateral margin of the quadrate are incomplete in IGM 100-1128 and the

1709 presence of a quadrate foramen and a dorsal quadratojugal contact cannot be ruled out in this

1710 specimen. A large quadrate foramen similar to this of dromaeosaurids has been noted in *X.*

1711 *zhengi* (Xu et al., 2011). Likewise, the notched lateral margin of the quadrate has been

1712 interpreted as contributing to a large quadrate foramen in *A. huxleyi* (Hu et al., 2009, figure

1713 S2d). The quadrate foramen seems to be equally delimited by the quadrate and quadratojugal

1714 in these two taxa. However, there is no evidence of a quadrate foramen, nor a dorsal

1715 quadratojugal contact on the quadrate of more derived troodontids hitherto.

1716   The anterior margin of the pterygoid flange of *M. long* (Xu and Norell, 2004, figure

1717 1B) and IGM 100-1128 is parabolic in outline and almost subrectangular. The most anterior

1718 points is situated at one third of the quadrate body in both specimens. Similar to the condition

1719 seen in Dromaeosauridae, the ventral margin of the pterygoid flange contacts the quadrate

1720 body well-above the entocondyle, and the posterior margin of the flange is strongly inclined

1721 anteroventrally. The dorsal margin of the flange meets the quadrate head beneath the articular

1722 surface of the head, and the flange is straight and projects only anteriorly. Nevertheless, the

1723 pterygoid flange of Troodontidae is particularly short anteroposteriorly (ratio of 0.25-0.3; Xu

1724 et al., 2011), which is not the case in dromaeosaurids. Some troodontids such as *A. huxleyi*

1725 and *X. zhengi* possess a well-developed lateral process (Hu et al., 2009; Xu et al., 2011). It is

1726 however unknown whether this process is present in more derived troodontid taxa.

1727   The mandibular articulation of troodontid quadrates has only been well-illustrated and

1728 well-described in IGM 100-1083 by Norell and Hwang (2004). As in some oviraptorids and

1729 dromaeosaurids, the medial margin of the mandibular articulation of IGM 100-1083 is

1730 pointed in posterior view, but the medial corner is oriented medially. On the other hand, the

1731 medial margin of the entocondyle is rounded and does not show this medial corner in IGM

1732 100-44 and IGM 100-1128, yet the ventral margin of the ectocondyle is pointed in posterior

1733 view in both specimens. In ventral view, the mandibular articulation of IGM 100-1083 is

1734 composed of two condyles separated by a shallow and almost indistinct intercondylar sulcus.

1735 The condyles are roughly oval and the entocondyle is larger than the ectocondyle, as observed

1736   in IGM 100-44 (Barsbold et al., 1987, plate 49 figure 4) and IGM 100-1128 in posterior view.

1737   There is no quadratojugal process in IGM 100-1083 and IGM 100-1128.

1738   Quadrate pneumaticity in Troodontidae is well-known (Varricchio, 1997) and has

1739   been reported in a Jurassic troodontid (Hartman et al., 2005), *T. formosus* (Currie and Zhao,

1740   1993a), *S. changii* (Xu et al., 2002), *M. long* (Xu and Norell, 2004; Gao et al., 2012) and *X.*

1741   *zhengi* (Xu et al., 2011) where a posterior pneumatopore has been observed on the quadrate

1742   body in the two later taxa. This is also the case of the quadrate described by Barsbold et al.

1743   (1987) which displays a small pneumatic foramen positioned medially on the posterior

1744   surface of the quadrate body, at mid-height of the bone, and leading to a canal (Barsbold et

1745   al., 1987). However, all troodontids may not possess a pneumatic quadrate because no

1746   pneumatic chamber has been observed in the broken quadrate of IGM 100-1083 (Norell and

1747   Hwang, 2004).

1748

1749   **DISCUSSION**

1750   **Cladistic Analysis**

1751   This cladistic analysis performed based on a character datamatrix related to one single

1752   bone gives strikingly similar results to those from analyses using characters from the entire

1753   skeleton (Figures 1 & 2). The well-resolved tree follows the topology of the classification of

1754   nonavian theropods, thus demonstrating the phylogenetic value of the quadrate and offering

1755   more quadrate-related characters to be used in future cladistic analyses.

1756   Expectedly, when analyzed in a phylogenetic context, the morphology of the quadrate

1757   retrieves all major nonavian theropod clades (Neotheropoda, Ceratosauria, Tetanurae and

1758   Avetheropoda) as well as more restricted clades (e.g., Abelisauroidea, Abelisauridae,

1759   Megalosauridae, Spinosauridae, Carcharodontosauridae, Tyrannosauridae, Dromaeosauridae)

1760 supporting the idea that many quadrate synapomorphies contribute to clarifying nonavian

1761 theropod relationships.

1762   Although the major clades of nonavian theropods have been found resolved by this

1763 analysis, some important discrepancies with the current classification of theropods are

1764 apparent. The disparate position of basal and derived Allosauroidea is the most striking and

1765 can be explained by the following characters: the shape of the ventral part above the

1766 mandibular articulation on the posterior surface of the quadrate body (chars. 8) and the

1767 morphology of the mandibular articulation (char., 20, 28, 19) and the quadrate foramen (char.

1768 73, 76). In basal allosauroids (Allosauridae, Sinraptoridae and Neovenatoridae), the posterior

1769 surface of the quadrate body dorsal to the mandibular articulation is deeply concave whereas

1770 it is strongly convex in Carcharodontosauridae. In addition, the mandibular articulation of

1771 carcharodontosaurids is mediolaterally longer than those of basal allosauroids: the

1772 ectocondyle is elongated, parabolic and with a sigmoid anterior margin, convergent with the

1773 ectocondyle morphology of dromaeosaurids, whereas in other allosauroids, the ectocondyle is

1774 shorter, ovoid and with a convex anterior margin in ventral view. As in dromaeosaurids, the

1775 quadrate foramen of carcharodontosaurids is also equally delimited by the quadrate and

1776 quadratojugal and situated well ventral to the mid-height of the quadrate body. In basal

1777 allosauroids, and by convergence with therizinosaurs, the quadrate foramen is roughly

1778 positioned at mid-height of the quadrate, mostly delimited by the quadrate and elliptical or

1779 bean-shaped in shape.

1780   The results of the phylogenetic analysis allow the identification of evolutionary trends

1781 of the quadrate across the clade of Theropoda. Our intention is to propose simple hypotheses

1782 as a result of our phylogenetic results and anatomical overview, the understanding of the

1783 functional reasons and interdependence of anatomical sub-units will be reserved for another

1784 study. The major trends can be summarized as follows: decrease of the elongation of the

1785   quadrate body and enlargement of the mandibular articulation across the evolution of

1786   Theropoda and specifically across the evolution of Megalosauroidea and Tyrannosauroidea;

1787   increase of the quadrate ridge width across the evolution of Megalosauroidea and decrease of

1788   it in Tyrannosauroidea and Coelophysoidea; loss of the quadrate foramen in Ceratosauria and

1789   Megalosauridae; reduction of the size of the quadrate foramen during the evolution of the

1790   Spinosauridae and increase of the foramen size in Tyrannosauroidea; increase of the

1791   contribution of the quadratojugal in the quadrate foramen during the evolution of

1792   Allosauroidea and Coelurosauria; loss of the lateral process in Tetanurae; dorsal displacement

1793   of the anteriormost point of the pterygoid flange in Ceratosauria and Megalosauroidea, and

1794   ventral displacement of this point during the evolution of Dromaeosauridae and

1795   Therizinosauria; development of two capitula in the quadrate head during the evolution of

1796   Oviraptorosauria (and convergently in Avialae); lateromedial elongation of the mandibular

1797   articulation during the evolution of Megalosauroidea, Allosauroidea and Maniraptoriformes,

1798   and increase of the anteroposterior thickness during the evolution of Ceratosauria;

1799   development of a sigmoid ectocondyle in Dilophosauridae and Spinosauridae, and an ovoid

1800   ectocondyle in Abelisauroidea, Oviraptorosauria, basal Allosauroidea, Tyrannosauroidea and

1801   Therizinosauria; and pneumatization of the quadrate in some tetanuran clades.

1802

1803   **Major Trends in the Evolution of the Quadrate in Nonavian Theropods**

1804   The results of the phylogenetic analysis allow the identification of evolutionary

1805   transformations of the quadrate across the theropod clade which can be summarized as

1806   follows:

1807   **Quadrate body.** Decrease of the elongation of the quadrate body and enlargement of the

1808   mandibular articulation across the evolution of Theropoda and specifically across the

1809   evolution of Tyrannosauroidea and Megalosauroidea leading to Spinosauridae. Elongated

73

1810   quadrates with short mandibular articulation can be seen in ceratosaurs and ornithomimosaurs

1811   while short quadrates with broad mandibular articulation are present in spinosaurids,

1812   tyrannosaurids and dromaeosaurids.

1813   **Quadrate ridge.** Increase of the ridge width across the evolution of Megalosauroidea and

1814   decrease of it in Tyrannosauroidea and Coelophysoidea. Most of nonavian theropods have

1815   rod-shaped ridges but the Coelophysoidea, Tyrannosauridae and the neovenatorid *Aerosteon*

1816   have a narrow crest-like ridge, whereas the Spinosauridae possess a very broad stick-like

1817   ridge. The quadrate ridge is usually well delimited in nonavian theropods but a very shallow

1818   ridge can be observed in abelisauroids, *Eustreptospondylus*, ornithomimosaurs, therizinosaurs

1819   and oviraptorosaurs. In anterior view, the ridge is only visible in Abelisauridae.

1820   **Quadrate foramen.** 1) Loss of the quadrate foramen independently in Ceratosauria and

1821   Megalosauridae. 2) Reduction of the size of the foramen during the evolution of the

1822   Spinosauridae and increase of the foramen size in Tyrannosauroidea. A small quadrate

1823   foramen exists in non-tetanuran theropods, spinosaurines and basal Tyrannosauroidea while a

1824   large quadrate foramen (or quadrate fenestra) can be observed in some Baryonychinae,

1825   Tyrannosauroidea, Alvarezsauroidea and Dromaeosauridae. 3) Increase of the contribution of

1826   the quadratojugal in the quadrate foramen during the evolution of Coelurosauria. The

1827   quadrate foramen is mostly delimited by the quadrate in all nonavian theropods but

1828   Maniraptoriformes (except *Falcarius*) where the contribution of the quadrate and

1829   quadratojugal in the foramen is roughly equal.

1830   **Lateral process.** 1) Loss of the lateral process in Tetanurae. A lateral process is absent in

1831   basal tetanurans, megalosauroids, and some basal averostrans. A very well-developed

1832   subtriangular lateral process anterolaterally oriented exists in basal theropods and ceratosaurs

1833   but also in alvarezsaurids, derived therizinosauroids, and dromaeosaurids where this structure

1834   reappears. 2) Ventral displacement of the ventral margin of the lateral process during the

1835   evolution of Ceratosauria. In basal-most theropods, coelophysoids (Dilophosauridae +

1836   Coelophysidae), some ceratosaurs (Ceratosauridae + Noasauridae), derived therizinosauroids,

1837   alvarezsauroids, and dromaeosaurids, the lateral process extends ventrally at mid-height of the

1838   quadrate body, from the quadrate foramen when present. However, in Abelisauroidea the

1839   lateral process extends ventrally to the mandibular articulation or just above it.

1840   **Pterygoid flange.** 1) Dorsal displacement of the anteriormost point of the pterygoid flange in

1841   Ceratosauria and Megalosauroidea, and ventral displacement of this point during the

1842   evolution of Dromaeosauridae and Therizinosauria. The anteriormost point of the pterygoid

1843   flange of most nonavian theropod is situated at mid-height of the quadrate in lateral/medial

1844   views. On the other hand, this point is situated at two-thirds of the quadrate in ceratosaurs and

1845   megalosauroids, and at one-third of the quadrate in *Erlikosaurus*, *Zuolong* and some

1846   dromaeosaurids. 3) Appearance of a medial fold of the ventral margin of the pterygoid flange

1847   in Ceratosauria and disappearance of it in Megalosauridae, derived Carcharodontosauridae

1848   and Coelurosauria. A straight ventral margin of the pterygoid flange is present in basal

1849   theropods, megalosaurids, derived carcharodontosaurids and coelurosaurs. The ventral margin

1850   of this flange is folded medially in ceratosaurs, basal tetanurans, spinosaurids, sinraptorids

1851   and neovenatorids, and mediodorsally or dorsally folded in allosaurids and basal

1852   carcharodontosaurids.

1853   **Quadrate head.** 1) Dorsal displacement of the quadrate head to or close to the level of the

1854   dorsal margin of the orbit in Ceratosauria and Megalosauridae. A quadrate head at the level or

1855   slightly ventral to the dorsal margin of the orbit can be seen in most ceratosaurs and

1856   megalosaurids whereas all other nonavian theropods show a quadrate head well ventral to the

1857   dorsal margin of the orbit. 2) Decrease of quadrate head width (relative to the width of the

1858   mandibular articulation) across the evolution of Allosauroidea and Dromaeosauridae. 3)

1859   Development of two capitula in the quadrate head during the evolution of Oviraptorosauria

1860   and Alvarezsauridae (and convergently in Avialae). The quadrate head is single headed in

1861   most nonavian theropods other than oviraptosaurids and the derived alvarezsaurid *Shuvuuia*

1862   which possess two well-distinguished heads contacting the squamosal and the braincase.

1863   **Mandibular articulation.** 1) Ventral displacement of the mandibular articulation in

1864   Spinosauridae and Avetheropoda, and dorsal displacement of this articulation at the same

1865   level than the alveolar margin of the maxilla in Tyrannosauridae. A mandibular articulation at

1866   the level of the ventral margin of the maxilla can be seen in most basal Theropoda, most

1867   Ceratosauria, basal Tetanurae, Megalosauridae and Tyrannosauridae. On the other hand, a

1868   mandibular articulation projecting well-ventral of the alveolar margin of the cranium exists in

1869   *Irritator*, the coelophysoid *Zupaysaurus* and most avetheropods. 2) Lateromedial elongation

1870   of the mandibular articulation during the evolution of Megalosauroidea, Allosauroidea and

1871   Maniraptoriformes, and increase of the anteroposterior thickness during the evolution of

1872   Ceratosauria. A very mediolaterally broad mandibular articulation (ratio > 3) exits in

1873   Spinosauridae, Carcharodontosauridae and Deinonychosauria whereas a particularly

1874   anteroposteriorly broad mandibular articulation (ratio < 2) appears in Ceratosauria.

1875   **Entocondyle.** Increase of the entocondyle width during the evolution of Ceratosauria,

1876   Oviraptorosauria and some Megalosauridae. Among nonavian theropods, an entocondyle

1877   larger than the ectocondyle exists in Abelisauroidea, Oviraptoridae and the megalosaurid

1878   *Afrovenator*.

1879   **Ectocondyle.** Development of a sigmoid ectocondyle in Dilophosauridae and Spinosauridae,

1880   and an ovoid ectocondyle in Abelisauroidea, Oviraptorosauria, basal Allosauroidea,

1881   Tyrannosauroidea, and Therizinosauria.

1882   **Pneumacity.** 1) Pneumatization of the quadrate independently in Neovenatoridae,

1883   Carcharodontosauridae, Tyrannosauridae and Maniraptoriformes. 2) Reduction of the size of

1884   the medial pneumatopore in derived Carcharodontosauridae.

1885

1886   **Phylogenetic Morphometrics Analysis**

1887   Phylogenetic morphometrics characters are being proposed for the first time for

1888   Dinosauria. By exclusively analyzing the ventral view of the mandibular articulation of

1889   nonavian theropods (analysis 2, character 2; Figure 2.2) two distinct 'morphoclades' emerged

1890   from the analysis. This presents evidence of two fundamentally distinct morphotypes with

1891   possible functional implications.

1892   The first morphotype mandibular articulation (morphotype A) is characterized by: an

1893   anteroposteriorly broad mandibular articulation, two ovoid/subcircular ecto- and entocondyles

1894   roughly subequal in size, and an intercondylar sulcus in which the angle formed by the main

1895   axis of the sulcus and the long axis of mandibular articulation is relatively low (< 135°). This

1896   morphotype is present in all ceratosaurs but also in oviraptorosaurs, therizinosaurs,

1897   tyrannosaurids and some non-carcharodontosaurid allosauroids. Morphotype A is present in a

1898   large variety of nonavian theropods, from the small and slender oviraptorosaurs to the large

1899   and robust tyrannosaurids. However, all of these taxa share a roughly similar articulation with

1900   the lower jaw. In these theropods, the two rami of the mandibles are weakly displaced

1901   laterally when the mouth opened, due to the weakly elongated mandibular articulation latero-

1902   medially and the ectocondyle, and an angle of the intercondylar sulcus lower than in the

1903   second morphotype.

1904   On the other hand, the second morphotype (morphotype B) corresponds to: an

1905   elongate and anteroposteriorly narrow mandibular articulation, a long and parabolic/sigmoid

1906   ectocondyle much longer than the entocondyle, and an intercondylar sulcus in which the angle

1907   between the main axis passing through the sulcus also the long axis of the mandibular

1908   articulation is high (> 135°). This combination of features allows the lower jaw rami to be

1909   slightly to strongly displaced laterally when sliding along the intercondylar sulcus of the

1910   quadrate. Morphotype B can be seen in a large variety of theropods as they include all

1911   megalosauroids but *Afrovenator*, the dromaeosaurids and the carcharodontosaurids. Once

1912   again, although these theropods with morphotype B show some important morphological

1913   disparity in their skull and body, it seems that their mandibular articulation was

1914   morphofunctionally convergent. These theropods were able to enlarge the pharynx by opening

1915   the mouth like some ornithocheiroid pterosaurs and living pelecanid birds (Wellnhofer, 1980;

1916   Bennett, 2001; Hendrickx and Buffetaut, 2008).

1917   The presence of *Aerosteon* and *Acrocanthosaurus* at the base of each 'morphotypes'

1918   clearly demonstrates the transition from one morphotype to the other during the evolution of

1919   Allosauroidea. Likewise, the presence of *Allosaurus* in both morphotypes implies some

1920   important variability of the mandibular articulation among this particular taxon.

1921   Although their skull seem to be very disparate, morphotype A includes theropods with

1922   either relatively short and broad skulls resisting torsional bending like ceratosaurs, some

1923   allosauroids and tyrannosaurids (Rayfield, 2005; Sampson and Witmer, 2007), or beaked

1924   skulls like in the herbivorous oviraptorosaurs and therizinosaurs (Zanno et al., 2009). In both

1925   case, a broad and latero-medially short articulation of the quadrate was advantageous for

1926   either feeding on large prey or on hard plants thanks to a powerful and high efficiency biting

1927   (Therrien et al., 2005; Sakamoto, 2010). On the other hand, theropods with a latero-medially

1928   elongated mandibular articulation displaying a strongly diagonally oriented intercondylar

1929   sulcus where those favoring the deglutition of whole preys, or large chunk of food. They

1930   include weak/fast biter theropods with elongated skulls like the Dilophosauridae,

1931   Spinosauridae and Dromaeosauridae (Sakamoto, 2010). Those theropods were feeding on

1932   relatively small preys they were swallowing in one piece such as fishes (Charig and Milner,

1933   1997; Hendrickx and Buffetaut, 2008) and perhaps insects (Senter, 2009). Morphotype B also

1934   includes massive theropods with extremely powerful skulls like Carcharodontosauridae and

1935   *Torvosaurus* which must have swallowed large chunk of meet from preys they would easily

1936   disarticulate thanks to their strong bite force (Therrien et al., 2005; Sakamoto, 2010).

1937

1938   **CONCLUSION**

1939   The present study goes along the lines of other research efforts that recognize that a

1940   single bone can bear a wealth of phylogenetic information that cannot be dismissed, such as

1941   the quadrate of mosasaurs (Polcyn and Bell, 2005), the ilium of anura (Gardner et al., 2010),

1942   the coracoid of eosauropterygian (White, 1940) or the teeth of ornithopods (Araújo et al.,

1943   2008). To the eight characters on the quadrate bones used in the most recent publication on a

1944   phylogenetic context for nonavian theropod (Choiniere et al., 2014), we increased a number

1945   of characters that contribute to describe the disparity and evolutionary transformations of the

1946   bone. Many quadrate-related characters are synapomorphic to several major theropod clades

1947   such as Neotheropoda, Averostra, Ceratosauria, Tetanurae, Megalosauroidea and

1948   Avetheropoda and almost all families of nonavian theropods (e.g., Abelisauridae,

1949   Megalosauridae, Spinosauridae, Carcharodontosauridae, Tyrannosauridae, Oviraptoridae and

1950   Dromaeosauridae) are retrieved based on the combination of homologous and non-

1951   homologous quadrate related synapomorphies.

1952   The cladistic analysis performed on the datamatrix of 98 quadrate related characters

1953   allowed many evolutionary trends for this specific cranial bone to be drawn such as: 1) a

1954   decrease of the elongation of the quadrate body and enlargement of the mandibular

1955   articulation across the evolution of Theropoda, 2) the loss of the quadrate foramen

1956   independently in Ceratosauria and Megalosauridae, 3) the loss of the lateral process in

1957   Tetanurae and 4) a reduction of the quadrate ridge width in Tyrannosauridae.

1958   Phylogenetic morphometrics analysis on the quadrate bone in nonavian theropods also

1959   highlighted the existence of two different morphotypes in the mandibular articulation. These

1960   morphotypes are linked to the morphofunctional aspect of the articulation between the lower

1961   jaw and the cranium. In morphotype A, characterized by an anteroposteriorly broad

1962   mandibular articulation with two ovoid/subcircular condyles roughly subequal in size, the

1963   displacement of the mandible laterally was very weak or even inexistent. On the other hand,

1964   in morphotype B, characterized by an elongate and anteroposteriorly narrow mandibular

1965   articulation and a long and parabolic/sigmoid ectocondyle, the lower jaw rami was displaced

1966   laterally when the mouth opened.

1967

ACKNOWLEDGMENTS

1985   Chicago), N. Smith (Uni. Chicago), L. Zanno (FMNH), R. Tykoski (MNSD), D. Burnham

1986   (Uni. Kansas), M. Ezcurra (MACNBR), P. Asaroff (MACNBR), R. Irmis (UMNH), V.

1987   Shneider (NCMNS), C. Brochu (Uni. Iowa), S. Lautenschlager (Uni. Bristol), M. Mortimer

1988   and K. Peyer (MNHN), and the authors would like to address their sincere thanks to all of

1989   these people.

1990

1991   **REFERENCES**

1992   Agnolin, F.L. and Novas, F.E. 2011. Unenlagiid theropods: are they members of the

1993   Dromaeosauridae (Theropoda, Maniraptora)? *Anais da Academia Brasileira de*

1994   *Ciências* 83:117–162.

1995   Allain, R. 2002. Discovery of megalosaur (Dinosauria, Theropoda) in the middle Bathonian

1996   of Normandy (France) and its implications for the phylogeny of basal Tetanurae.

1997   *Journal of Vertebrate Paleontology* 22:548–563. doi:10.1671/0272-

1998   4634(2002)022[0548:DOMDTI]2.0.CO;2.

1999   Araújo, R., Castahinha, R. and Mateus, O. 2008. Major trends in the evolution of teeth and

2000   mandibles in ornithopod dinosaurs. *Tercer Congreso Latinoamericano de*

2001   *Paleontología de Vertebrados, Neuquén, Argentina* 18.

2002   Arcucci, A.B. and Coria, R.A. 2003. A new Triassic carnivorous dinosaur from Argentina.

2003   *Ameghiniana* 40:217–228.

2004   Averianov, A. and Sues, H.D. 2011. Skeletal remains of Tyrannosauroidea (Dinosauria:

2005   Theropoda) from the Bissekty Formation (Upper Cretaceous: Turonian) of

2006   Uzbekistan. *Cretaceous Research*.

2007   Bakker, R.T. 1998. Brontosaur killers: late Jurassic allosaurids as sabre-tooth cat analogues.

2008   *Gaia* 15:145–158.

2009   Balanoff, A.M. and Norell, M.A. 2012. Osteology of *Khaan mckennai* (Oviraptorosauria:

2010   Theropoda). *Bulletin of the American Museum of Natural History* 1–77.

2011   doi:10.1206/803.1.

2012   Balanoff, A.M., Xu, X., Kobayashi, Y., Matsufune, Y. and Norell, M.A. 2009. Cranial

2013   osteology of the theropod dinosaur *Incisivosaurus gauthieri* (Theropoda:

2014   Oviraptorosauria). *American Museum Novitates* 3651:1–35.

2015   Barsbold, R. 1974. Saurornithoididae, a new family of small theropod dinosaurs from central

2016   Asia and North America. *Palaeontologia Polonica* 30:5–22.

2017   Barsbold, R. 1981. Toothless carnivorous dinosaurs of Mongolia. *Trudy Sovmestnoi Sovetsko-*

2018   *Mongol'skoi Paleontologicheskoi Ekspeditsii* 15:28–39.

2019   Barsbold, R. 1986. Raubdinosaurier Oviraptoren, p. 210–223. In Vorobyeva, E.I. (ed.),

2020   *Gerpetologičeskie issledovaniâ v Mongol'skoi Narodnoj Respublike*. Moscow.

2021   Barsbold, R. and Osmólska, H. 1999. The skull of *Velociraptor* (Theropoda) from the Late

2022   Cretaceous of Mongolia. *Acta Palaeontologica Polonica* 44:189–219.

2023   Barsbold, R., Osmólska, H. and Kurzanov, S.M. 1987. On a new troodontid (Dinosauria,

2024   Theropoda) from the Early Cretaceous of Mongolia. *Acta Palaeontologica Polonica*

2025   32:121–132.

2026   Barsbold, R. and Perle, A. 1980. Segnosauria, a new infraorder of carnivorous dinosaurs. *Acta*

2027   *Palaeontologica Polonica* 25:187–195.

2028   Bennett, S.C. 2001. The osteology and functional morphology of the Late Cretaceous

2029   pterosaur *Pteranodon* Part I. General description of osteology. *Palaeontographica*

2030   *Abteilung A* 260:1–112.

2031   Benson, R., Carrano, M. and Brusatte, S. 2010. A new clade of archaic large-bodied predatory

2032   dinosaurs (Theropoda: Allosauroidea) that survived to the latest Mesozoic.

2033   *Naturwissenschaften* 97:71–78. doi:10.1007/s00114-009-0614-x.

2034 Benson, R.B.J. 2010. A description of *Megalosaurus bucklandii* (Dinosauria: Theropoda)

2035   from the Bathonian of the UK and the relationships of Middle Jurassic theropods.

2036   *Zoological Journal of the Linnean Society* 158:882–935.

2037 Bever, G.S. and Norell, M.A. 2009. The perinate skull of *Byronosaurus* (Troodontidae) with

2038   observations on the cranial ontogeny of paravian theropods. *American Museum*

2039   *Novitates* 3657:1–52.

2040 Bonaparte, J.F. 1985. A horned Cretaceous carnosaur from Patagonia. *National Geographic*

2041   *Research* 1:149–151.

2042 Bonaparte, J.F. 1991. The Gondwanian theropod families Abelisauridae and Noasauridae.

2043   *Historical Biology* 5:1–25.

2044 Bonaparte, J.F. and Novas, F.E. 1985. *Abelisaurus comahuensis*, n.g., Carnosauria del

2045   Crétacico Tardio de Patagonia. *Ameghiniana* 21:259–265.

2046 Bonaparte, J.F. and Powell, J.E. 1980. A continental assemblage of tetrapods from the Upper

2047   Cretaceous beds of El Brete, northwestern Argentina (Sauropoda-Coelurosauria-

2048   Carnosauria-Aves). *Mémoires de la Société Géologique de France, Nouvelle Série*

2049   139:19–28.

2050 Bookstein, F.L. 1997. *Morphometric Tools for Landmark Data: Geometry and Biology*.

2051   Cambridge University Press.

2052 Bremer, K. 1994. Branch support and tree stability. *Cladistics* 10:295–304.

2053 Britt, B.B. 1991. Theropods of Dry Mesa Quarry (Morrison Formation, Late Jurassic),

2054   Colorado, with emphasis on the osteology of *Torvosaurus tanneri*. *Brigham Young*

2055   *University Geology Studies* 37:1–72.

2056 Brochu, C.A. 2003. Osteology of *Tyrannosaurus rex*: Insights from a nearly complete

2057   skeleton and high-resolution computed tomographic analysis of the skull. *Journal of*

2058   *Vertebrate Paleontology* 22:1–138. doi:10.1080/02724634.2003.10010947.

2059   Brusatte, S.L. 2012. *Dinosaur Paleobiology*. Wiley-Blackwell.

2060   Brusatte, S.L., Benson, R.B.J., Chure, D.J., Xu, X., Sullivan, C. and Hone, D.W.E. 2009. The

2061   first definitive carcharodontosaurid (Dinosauria: Theropoda) from Asia and the

2062   delayed ascent of tyrannosaurids. *Naturwissenschaften* 96:1051–1058.

2063   Brusatte, S.L., Benson, R.B.J., Currie, P.J. and Xijin, Z. 2010. The skull of *Monolophosaurus*

2064   jiangi (Dinosauria: Theropoda) and its implications for early theropod phylogeny and

2065   evolution. *Zoological Journal of the Linnean Society* 158:573–607.

2066   Brusatte, S.L., Carr, T.D., Erickson, G.M., Bever, G.S. and Norell, M.A. 2009. A long-

2067   snouted, multihorned tyrannosaurid from the Late Cretaceous of Mongolia.

2068   *Proceedings of the National Academy of Sciences* 106:17261–17266.

2069   Brusatte, S.L., Carr, T.D. and Norell, M.A. 2012. The osteology of *Alioramus*, a gracile and

2070   long-snouted tyrannosaurid (Dinosauria: Theropoda) from the Late Cretaceous of

2071   Mongolia. *Bulletin of the American Museum of Natural History* 366:1–197.

2072   doi:10.1206/770.1.

2073   Brusatte, S.L., Chure, D.J., Benson, R.B.J. and Xu, X. 2010. The osteology of *Shaochilong*

2074   *maortuensis*, a carcharodontosaurid (Dinosauria: Theropoda) from the Late

2075   Cretaceous of Asia. *Zootaxa* 2334:1–46.

2076   Brusatte, S.L., Norell, M.A., Carr, T.D., Erickson, G.M., Hutchinson, J.R., Balanoff, A.M.,

2077   Bever, G.S., Choiniere, J.N., Makovicky, P.J. and Xu, X. 2010. Tyrannosaur

2078   paleobiology: new research on ancient exemplar organisms. *Science* 329:1481–1485.

2079   doi:10.1126/science.1193304.

2080   Burnham, D.A. 2004. New Information on *Bambiraptor feinbergi* (Theropoda:

2081   Dromaeosauridae) from the Late Cretaceous of Montana, p. 67–111. In Currie, P.J.,

2082   Koppelhus, E.B., Shugar, M.A., and Wright, J.L. (eds.), *Feathered Dragons: Studies*

2083   *on the Transition from Dinosaurs to Birds*. Indiana University Press, Bloomington,

2084   Indiana.

2085 Burnham, D.A., Derstler, K.L., Currie, P.J., Bakker, R.T., Zhou, Z. and Ostrom, J.H. 2000.

2086   Remarkable new birdlike dinosaur (Theropoda: Maniraptora) from the Upper

2087   Cretaceous of Montana. *The Paleontological Institute, The University of Kansas* 13:1–

2088   14.

2089 Carr, T.D. 1996. Cranial osteology and craniofacial ontogeny of Tyrannosauridae:

2090   Dinosauria: Theropoda from the Dinosaur Park Formation (Judith River Group, Upper

2091   Cretaceous, Campanian) of Alberta. MSc. Dissertation, University of Toronto,

2092   Toronto, Ontario, Canada.

2093 Carr, T.D. and Williamson, T.E. 2010. *Bistahieversor sealeyi*, gen. et sp. nov., a new

2094   tyrannosauroid from New Mexico and the origin of deep snouts in Tyrannosauroidea.

2095   *Journal of vertebrate Paleontology* 30:1–16.

2096 Carrano, M.T., Benson, R.B.J. and Sampson, S.D. 2012. The phylogeny of Tetanurae

2097   (Dinosauria: Theropoda). *Journal of Systematic Palaeontology* 10:211–300.

2098   doi:10.1080/14772019.2011.630927.

2099 Carrano, M.T., Loewen, M.A. and Sertich, J.J.W. 2011. New materials of *Masiakasaurus*

2100   *knopfleri* Sampson, Carrano, and Forster, 2001, and implications for the morphology

2101   of the Noasauridae (Theropoda: Ceratosauria). *Smithsonian Contributions to*

2102   *Paleobiology* 95:1–53.

2103 Carrano, M.T. and Sampson, S.D. 2008. The phylogeny of Ceratosauria (Dinosauria:

2104   Theropoda). *Journal of Systematic Palaeontology* 6:183–236.

2105   doi:10.1017/S1477201907002246.

2106   Catalano, S.A. and Goloboff, P.A. 2012. Simultaneously Mapping and Superimposing

2107   Landmark Configurations with Parsimony as Optimality Criterion. *Systematic Biology*

2108   61:392–400. doi:10.1093/sysbio/syr119.

2109   Catalano, S.A., Goloboff, P.A. and Giannini, N.P. 2010. Phylogenetic morphometrics (I): the

2110   use of landmark data in a phylogenetic framework. *Cladistics* 26:539–549.

2111   Charig, A.J. and Milner, A.C. 1986. *Baryonyx*, a remarkable new theropod dinosaur. *Nature*

2112   324:359–361.

2113   Charig, A.J. and Milner, A.C. 1990. The systematic position of *Baryonyx walkeri*, in the light

2114   of Gauthier's reclassification of the Theropoda, p. 127–140. In Carpenter, K. and

2115   Currie, P.J. (eds.), *Dinosaur Systematics: Approaches and Perspectives*. Cambridge

2116   University Press, New York, New York.

2117   Charig, A.J. and Milner, A.C. 1997. *Baryonyx walkeri*, a fish-eating dinosaur from the

2118   Wealden of Surrey. *Bulletin of the Natural History Museum* 53:11–70.

2119   Chiappe, L.M. and Göhlich, U.B. 2010. Anatomy of *Juravenator starki* (Theropoda:

2120   Coelurosauria) from the Late Jurassic of Germany. *Neues Jahrbuch für Geologie und*

2121   *Paläontologie Abhandlungen* 258:257–296. doi:10.1127/0077-7749/2010/0125.

2122   Chiappe, L.M., Norell, M.A. and Clark, J.M. 1998. The skull of a relative of the stem-group

2123   bird *Mononykus*. *Nature* 392:275–278. doi:10.1038/32642.

2124   Chiappe, L.M., Norell, M.A. and Clark, J.M. 2002. The Cretaceous, short-armed

2125   Alvarezsauridae: *Mononykus* and its kin, p. 87–120. In Chiappe, L.M. and Witmer,

2126   L.M. (eds.), *Mesozoic birds: above the heads of dinosaurs*. University of California

2127   Press.

2128   Choiniere, J.N., Clark, J.M., Forster, C.A., Norell, M.A., Eberth, D.A., Erickson, G.M., Chu,

2129   H. and Xu, X. 2014. A juvenile specimen of a new coelurosaur (Dinosauria:

2130   Theropoda) from the Middle–Late Jurassic Shishugou Formation of Xinjiang,

2131   People's Republic of China. *Journal of Systematic Palaeontology* 12:177–215.

2132   doi:10.1080/14772019.2013.781067.

2133 Choiniere, J.N., Clark, J.M., Forster, C.A. and Xu, X. 2010. A basal coelurosaur (Dinosauria:

2134   Theropoda) from the Late Jurassic (Oxfordian) of the Shishugou Formation in

2135   Wucaiwan, People's Republic of China. *Journal of Vertebrate Paleontology* 30:1773–

2136   1796. doi:10.1080/02724634.2010.520779.

2137 Choiniere, J.N., Forster, C.A. and de Klerk, W.J. 2012. New information on *Nqwebasaurus*

2138   *thwazi*, a coelurosaurian theropod from the Early Cretaceous Kirkwood Formation in

2139   South Africa. *Journal of African Earth Sciences* 71–72:1–17.

2140   doi:10.1016/j.jafrearsci.2012.05.005.

2141 Choiniere, J.N., Xu, X., Clark, J.M., Forster, C.A., Guo, Y. and Han, F. 2010. A basal

2142   alvarezsauroid theropod from the Early Late Jurassic of Xinjiang, China. *Science*

2143   327:571–574. doi:10.1126/science.1182143.

2144 Chure, D.J. 2000. A new species of *Allosaurus* from the Morrison Formation of Dinosaur

2145   National Monument (Utah-Colorado) and a revision of the theropod family

2146   Allosauridae. Ph.D. Dissertation, Columbia University, New York, New York.

2147 Clark, J.M., Norell, M.A. and Rowe, T. 2002. Cranial anatomy of *Citipati osmolskae*

2148   (Theropoda, Oviraptorosauria), and a reinterpretation of the holotype of *Oviraptor*

2149   *philoceratops*. *American Museum Novitates* 3364:1–24.

2150 Clark, J.M., Perle, A. and Norell, M. 1994. The skull of *Erlicosaurus andrewsi*, a late

2151   Cretaceous "Segnosaur" (Theropoda, Therizinosauridae) from Mongolia. *American*

2152   *Museum Novitates* 3115:1–39.

2153 Colbert, E.H. 1989. The Triassic dinosaur *Coelophysis*. *Museum of Northern Arizona Bulletin*

2154   57:1–174.

2155   Colbert, E.H. and Russell, D.A. 1969. The small Cretaceous dinosaur *Dromaeosaurus*.

2156   *American Museum Novitates* 2380:1–49.

2157   Coria, R.A., Chiappe, L.M. and Dingus, L. 2002. A new close relative of *Carnotaurus sastrei*

2158   Bonaparte 1985 (Theropoda: Abelisauridae) from the Late Cretaceous of Patagonia.

2159   *Journal of Vertebrate Paleontology* 22:460–465. doi:10.1671/0272-

2160   4634(2002)022[0460:ANCROC]2.0.CO;2.

2161   Coria, R.A. and Currie, P.J. 2006. A new carcharodontosaurid (Dinosauria, Theropoda) from

2162   the Upper Cretaceous of Argentina. *Geodiversitas* 28:71–118.

2163   Coria, R.A. and Salgado, L. 1995. A new giant carnivorous dinosaur from the Cretaceous of

2164   Patagonia. *Nature* 377:224–226. doi:10.1038/377224a0.

2165   Coria, R.A. and Salgado, L. 1998. A basal Abelisauria Novas, 1992 (Theropoda-Ceratosauria)

2166   from the Cretaceous of Patagonia, Argentina. *Gaia* 15:89–102.

2167   Currie, P.J. 1985. Cranial anatomy of *Stenonychosaurus inequalis* (Saurischia, Theropoda)

2168   and its bearing on the origin of birds. *Canadian Journal of Earth Sciences* 22:1643–

2169   1658. doi:10.1139/e85-173.

2170   Currie, P.J. 1995. New information on the anatomy and relationships of *Dromaeosaurus*

2171   *albertensis* (Dinosauria: Theropoda). *Journal of Vertebrate Paleontology* 15:576–591.

2172   doi:10.1080/02724634.1995.10011250.

2173   Currie, P.J. 2003. Cranial anatomy of tyrannosaurid dinosaurs from the Late Cretaceous of

2174   Alberta, Canada. *Acta Palaeontologica Polonica* 48:191–226.

2175   Currie, P.J. 2006. On the quadrate of *Sinraptor dongi* (Theropoda: Allosauroidea) from the

2176   Late Jurassic of China. *Mesozoic and Cenozoic Vertebrates and Paleoenvironments.*

2177   *Tributes to the career of Prof. Dan Grigorescu* 111–115.

2178   Currie, P.J. and Chen, P. 2001. Anatomy of *Sinosauropteryx prima* from Liaoning,

2179   northeastern China. *Canadian Journal of Earth Sciences* 38:1705–1727.

2180   doi:10.1139/e01-050.

2181   Currie, P.J. and Zhao, X.-J. 1993a. A new troodontid (Dinosauria, Theropoda) braincase from

2182   the Dinosaur Park Formation (Campanian) of Alberta. *Canadian Journal of Earth*

2183   *Sciences* 30:2231–2247. doi:10.1139/e93-194.

2184   Currie, P.J. and Zhao, X.-J. 1993b. A new carnosaur (Dinosauria, Theropoda) from the

2185   Jurassic of Xinjiang, People's Republic of China. *Canadian Journal of Earth Sciences*

2186   30:2037–2081. doi:10.1139/e93-179.

2187   Dufeau, D.L. 2003. The cranial anatomy of the theropod dinosaur *Shuvuuia deserti*

2188   (Coelurosauria: Alvarezsauridae), and its bearing upon coelurosaurian phylogeny.

2189   MSc. Dissertation, University of Texas, Austin, Texas.

2190   Eddy, D.R. and Clarke, J.A. 2011. New information on the cranial anatomy of

2191   *Acrocanthosaurus atokensis* and its implications for the phylogeny of Allosauroidea

2192   (Dinosauria: Theropoda). *PLoS ONE* 6:e17932. doi:10.1371/journal.pone.0017932.

2193   Elzanowski, A., Paul, G.S. and Stidham, T.A. 2001. An avian quadrate from the Late

2194   Cretaceous Lance formation of Wyoming. *Journal of Vertebrate Paleontology*

2195   20:712–719.

2196   Ezcurra, M.D. 2007. The cranial anatomy of the coelophysoid theropod *Zupaysaurus rougieri*

2197   from the Upper Triassic of Argentina. *Historical Biology* 19:185–202.

2198   Galton, P.M. and Jensen, J.A. 1979. A new large theropod dinosaur from the Upper Jurassic

2199   of Colorado. *Brigham Young University Geology Studies* 26:1–12.

2200   Gao, C., Morschhauser, E.M., Varricchio, D.J., Liu, J. and Zhao, B. 2012. A second soundly

2201   sleeping dragon: new anatomical details of the Chinese troodontid *Mei long* with

2202   implications for phylogeny and taphonomy. *PLoS ONE* 7:e45203.

2203   doi:10.1371/journal.pone.0045203.

2204   Gardner, J.L., Trueman, J.W.H., Ebert, D., Joseph, L. and Magrath, R.D. 2010. Phylogeny

2205   and evolution of the Meliphagoidea, the largest radiation of Australasian songbirds.

2206   *Molecular Phylogenetics and Evolution* 55:1087–1102.

2207   Gilmore, C.W. 1920. Osteology of the carnivorous Dinosauria in the United State National

2208   museum: with special reference to the genera *Antrodemus* (*Allosaurus*) and

2209   *Ceratosaurus*. *Bulletin of the United States National Museum* 110:1–159.

2210   Gilmore, C.W. 1924. On *Troodon validus*, an ornithopodus dinosaur from the Belly River

2211   Cretaceous of Alberta, Canada. *Bulletin of the Department of Geology, University of*

2212   *Alberta* 1:1–143.

2213   Godefroit, P., Demuynck, H., Dyke, G., Hu, D., Escuillié, F. and Claeys, P. 2013. Reduced

2214   plumage and flight ability of a new Jurassic paravian theropod from China. *Nature*

2215   *Communications* 4:1394. doi:10.1038/ncomms2389.

2216   Gold, M.E.L., Brusatte, S. and Norell, M. 2013. The cranial pneumatic sinuses of the

2217   tyrannosaurid *Alioramus* (Dinosauria, Theropoda) and the evolution of cranial

2218   pneumaticity in theropod dinosaurs. *American Museum Novitates* 3790:1–46.

2219   Goloboff, P.A. and Catalano, S.A. 2011. Phylogenetic morphometrics (II): algorithms for

2220   landmark optimization. *Cladistics* 27:42–51.

2221   Goloboff, P.A., Farris, J.S. and Nixon, K.C. 2008. TNT, a free program for phylogenetic

2222   analysis. *Cladistics* 24:774–786. doi:10.1111/j.1096-0031.2008.00217.x.

2223   Hammer, W.R. and Hickerson, W.J. 1994. A crested theropod dinosaur from Antarctica.

2224   *Science* 264:828–830.

2225   Hartman, S., Lovelace, D. and Wahl, W. 2005. Phylogenetic assessment of a maniraptoran

2226   from the Morrison Formation. *Journal of Vertebrate Paleontology* 25:67A–68A.

2227   Hendrickx, C. and Buffetaut, E. 2008. Functional interpretation of spinosaurid quadrates

2228   (Dinosauria: Theropoda) from the Mid-Cretaceous of Morocco. *56th Annual*

2229   *Symposium of Vertebrate Palaeontology and Comparative Anatomy. Dublin*

2230   *(September 2nd-6th 2008)* 25–26.

2231   Hendrickx, C. and Mateus, O. 2012. Ontogenetical changes in the quadrate of basal

2232   tetanurans, p. 20, 101–104. In Royo-Torres, R., Gascó, F., and Alcalá, L. (eds.), *10th*

2233   *Annual Meeting of the European Association of Vertebrate Palaeontologists.*

2234   *¡Fundamental!*

2235   Hendrickx, C. and Mateus, O. 2014. Abelisauridae (Dinosauria: Theropoda) from the Late

2236   Jurassic of Portugal and dentition-based phylogeny as a contribution for the

2237   identification of isolated theropod teeth. *Zootaxa* 3759:1–74.

2238   doi:10.11646/zootaxa.3759.1.1.

2239   Hone, D.W.E., Wang, K., Sullivan, C., Zhao, X., Chen, S., Li, D., Ji, S., Ji, Q. and Xu, X.

2240   2011. A new, large tyrannosaurine theropod from the Upper Cretaceous of China.

2241   *Cretaceous Research* 32:495.

2242   Hu, D., Hou, L., Zhang, L. and Xu, X. 2009. A pre-*Archaeopteryx* troodontid theropod from

2243   China with long feathers on the metatarsus. *Nature* 461:640–643.

2244   doi:10.1038/nature08322.

2245   Hu, S. 1993. A new theropoda (*Dilophosaurus sinensis* sp. nov.) from Yunnan, China.

2246   *Vertebrata PalAsiatica* 31:65–69.

2247   Von Huene, F.R. 1926. LX.—On several known and unknown reptiles of the order Saurischia

2248   from England and France. *Journal of Natural History Series 9* 17:473–489.

2249   doi:10.1080/00222932608633437.

2250   Von Huene, F.R. 1934. Ein neuer Coelurosaurier in der thüringischen Trias. *Paläontologische*

2251   *Zeitschrift* 16:145–170. doi:10.1007/BF03042684.

2252   Hutt, S., Naish, D., Martill, D.M., Barker, M.J. and Newbery, P. 2001. A preliminary account

2253   of a new tyrannosauroid theropod from the Wessex Formation (Early Cretaceous) of

2254   southern England. *Cretaceous Research* 22:227–242. doi:10.1006/cres.2001.0252.

2255   Hwang, S.H. 2007. Phylogenetic patterns of enamel microstructure in dinosaur teeth. Ph.D.

2256   Dissertation, Columbia University, New York, New York.

2257   Hwang, S.H., Norell, M.A., Qiang, J. and Keqin, G. 2004. A large compsognathid from the

2258   Early Cretaceous Yixian Formation of China. *Journal of Systematic Palaeontology*

2259   2:13–30. doi:10.1017/S1477201903001081.

2260   Ji, Q., Ji, S., Lü, J. and Yuan, C. 2007. A new giant compsognathid dinosaur with long

2261   filamentous integuments from lower Cretaceous of Northeastern China. *Acta*

2262   *Geologica Sinica* 81:8–15.

2263   Ji, Q., Ji, S.A. and Zhang, L.J. 2009. First large tyrannosauroid theropod from the Early

2264   Cretaceous Jehol Biota in northeastern China. *Geological Bulletin of China* 28:1369–

2265   1374.

2266   Ji, Q., Norell, M.A., Makovicky, P.J., Gao, K.-Q., Ji, S. and Yuan, C. 2003. An early ostrich

2267   dinosaur and implications for ornithomimosaur phylogeny. *American Museum*

2268   *Novitates* 3420:1–19. doi:10.1206/0003-0082(2003)420<0001:AEODAI>2.0.CO;2.

2269   Kirkland, J.I., Zanno, L.E., Sampson, S.D., Clark, J.M. and DeBlieux, D.D. 2005. A primitive

2270   therizinosauroid dinosaur from the Early Cretaceous of Utah. *Nature* 435:84–87.

2271   Kobayashi, Y. and Barsbold, R. 2005. Reexamination of a primitive ornithomimosaur,

2272   *Garudimimus brevipes* Barsbold, 1981 (Dinosauria: Theropoda), from the Late

2273   Cretaceous of Mongolia. *Canadian Journal of Earth Sciences* 42:1501–1521.

2274   doi:10.1139/e05-044.

2275   Kobayashi, Y. and Lü, J.-C. 2003. A new ornithomimid dinosaur with gregarious habits from

2276   the Late Cretaceous of China. *Acta Palaeontologica Polonica* 48:235–259.

2277   Kundrát, M. and Janáček, J. 2007. Cranial pneumatization and auditory perceptions of the

2278   oviraptorid dinosaur *Conchoraptor gracilis* (Theropoda, Maniraptora) from the Late

2279   Cretaceous of Mongolia. *Naturwissenschaften* 94:769–778. doi:10.1007/s00114-007-

2280   0258-7.

2281   Kurzanov, S.M. 1981. An unusual theropod from the Upper Cretaceous of Mongolia. *Joint*

2282   *Soviet-Mongolian Paleontological Expedition* 15:39–49.

2283   Kurzanov, S.M. 1985. The skull structure of the dinosaur *Avimimus*. *Paleontological Journal*

2284   1985:92–99.

2285   Larson, P.L. 2008. Atlas of the skull bones of *Tyrannosaurus rex*, p. 233–243. In Larson, P.L.

2286   and Carpenter, K. (eds.), *Tyrannosaurus rex, the Tyrant King*. Indiana University

2287   Press, Bloomington, Indiana.

2288   Lavocat, R. 1955. Sur une portion de mandibule de théropode provenant du Crétacé supérieur

2289   de Madagascar. *Bulletin du Muséum National d'Histoire Naturelle* 27:256–259.

2290   Li, D., Norell, M.A., Gao, K.Q., Smith, N.D. and Makovicky, P.J. 2010. A longirostrine

2291   tyrannosauroid from the Early Cretaceous of China. *Proceedings of the Royal Society*

2292   *B: Biological Sciences* 277:183–190.

2293   Loewen, M.A., Irmis, R.B., Sertich, J.J.W., Currie, P.J. and Sampson, S.D. 2013. Tyrant

2294   dinosaur evolution tracks the rise and fall of Late Cretaceous oceans. *PLoS ONE*

2295   8:e79420. doi:10.1371/journal.pone.0079420.

2296   Lü, J. 2003. A new oviraptorosaurid (Theropoda: Oviraptorosauria) from the Late Cretaceous

2297   of southern China. *Journal of Vertebrate Paleontology* 22:871–875.

2298   doi:10.1671/0272-4634(2002)022[0871:ANOTOF]2.0.CO;2.

2299   Lü, J., Xu, L., Liu, Y., Zhang, X., Jia, S. and Ji, Q. 2010. A new troodontid theropod from the

2300   Late Cretaceous of central China, and the radiation of Asian troodontids. *Acta*

2301   *Palaeontologica Polonica* 55:381–388.

2302 Madsen, J.H. 1976a. A second new theropod dinosaur from the Late Jurassic of east central

2303   Utah. *Utah geology* 3:51–60.

2304 Madsen, J.H. 1976b. *Allosaurus fragilis*: A Revised Osteology. *Utah Geological Survey*

2305   *Bulletin* 109:1–177.

2306 Madsen, J.H. and Welles, S.P. 2000. *Ceratosaurus* (Dinosauria, Theropoda): a revised

2307   osteology. *Utah Geological Survey, Miscellaneous Publication* 00-2:1–89.

2308 Makovicky, P.J., Apesteguía, S. and Agnolín, F.L. 2005. The earliest dromaeosaurid theropod

2309   from South America. *Nature* 437:1007–1011. doi:10.1038/nature03996.

2310 Makovicky, P.J., Kobayashi, Y. and Currie, P.J. 2004. Ornithomimosauria, p. 137–150. In

2311   Weishampel, D.B., Dodson, P., and Osmólska, H. (eds.), *The Dinosauria, Second*

2312   *Edition*. University of California Press, Berkeley/Los Angeles/London.

2313 Makovicky, P.J. and Norell, M. 1998. A partial ornithomimid braincase from Ukhaa Tolgod

2314   (Upper Cretaceous, Mongolia). *American Museum Novitates* 3247:1–16.

2315 Makovicky, P.J., Norell, M.A., Clark, J.M. and Rowe, T. 2003. Osteology and relationships

2316   of *Byronosaurus jaffei* (Theropoda: Troodontidae). *American Museum Novitates*

2317   3402:1–32. doi:10.1206/0003-0082(2003)402<0001:OAROBJ>2.0.CO;2.

2318 Marsh, O.C. 1877. Notice of new dinosaurian reptiles from the Jurassic Formation. *American*

2319   *Journal of Science* 14:14–516.

2320 Marsh, O.C. 1884. Principal characters of the American Jurassic dinosaurs. Part VIII. The

2321   order Theropoda. *American Journal of Science, Series 3* 27:329–340.

2322 Martill, D.M., Cruickshank, A.R.I., Frey, E., Small, P.G. and Clarke, M. 1996. A new crested

2323   maniraptoran dinosaur from the Santana Formation (Lower Cretaceous) of Brazil.

2324   *Journal of the Geological Society* 153:5–8. doi:10.1144/gsjgs.153.1.0005.

2325 Martinez, R.N. and Alcober, O.A. 2009. A basal sauropodomorph (Dinosauria: Saurischia)

2326   from the Ischigualasto Formation (Triassic, Carnian) and the early evolution of

2327   Sauropodomorpha. *PLoS ONE* 4:e4397. doi:10.1371/journal.pone.0004397.

2328 Martinez, R.N., Sereno, P.C., Alcober, O.A., Colombi, C.E., Renne, P.R., Montañez, I.P. and

2329   Currie, B.S. 2011. A basal dinosaur from the dawn of the dinosaur era in southwestern

2330   Pangaea. *Science* 331:206–210. doi:10.1126/science.1198467.

2331 Maryańska, T. and Osmólska, H. 1997. The quadrate of oviraptorid dinosaurs. *Acta*

2332   *Palaeontologica Polonica* 42:361–371.

2333 Mateus, O., Walen, A. and Antunes, M.T. 2006. The large theropod fauna of the Lourinhã

2334   Formation (Portugal) and its similarity to the Morrison Formation, with a description

2335   of a new species of *Allosaurus*. *New Mexico Museum of Natural History and Science*

2336   *Bulletin* 36:123–129.

2337 Matthew, W.D. and Brown, B. 1922. The family Deinodontidae, with notice of a new genus

2338   from the Cretaceous of Alberta. *Bulletin of the American Museum of Natural History*

2339   46:367–385.

2340 Molnar, R.E. 1991. The cranial morphology of *Tyrannosaurus rex*. *Palaeontographica*

2341   *Abteilung A* 217:137–176.

2342 Nesbitt, S.J. 2011. The early evolution of archosaurs: relationships and the origin of major

2343   clades. *Bulletin of the American Museum of Natural History* 1–292.

2344   doi:10.1206/352.1.

2345 Nesbitt, S.J., Clarke, J.A., Turner, A.H. and Norell, M.A. 2011. A small alvarezsaurid from

2346   the eastern Gobi Desert offers insight into evolutionary patterns in the

2347   Alvarezsauroidea. *Journal of Vertebrate Paleontology* 31:144–153.

2348   doi:10.1080/02724634.2011.540053.

2349 Nesbitt, S.J., Smith, N.D., Irmis, R.B., Turner, A.H., Downs, A. and Norell, M.A. 2009. A

2350 complete skeleton of a Late Triassic saurischian and the early evolution of dinosaurs.

2351 *Science* 326:1530–1533. doi:10.1126/science.1180350.

2352 Nixon, K.C. 2002. WinClada, version 1.00.08. *Published by the author, Ithaca, New York*.

2353 Norell, M.A., Clark, J.M., Turner, A.H., Makovicky, P.J., Barsbold, R. and Rowe, T. 2006. A

2354 new dromaeosaurid theropod from Ukhaa Tolgod (Ömnögov, Mongolia). *American*

2355 *Museum Novitates* 3545:1–51. doi:10.1206/0003-

2356 0082(2006)3545[1:ANDTFU]2.0.CO;2.

2357 Norell, M.A. and Hwang, S.H. 2004. A troodontid dinosaur from Ukhaa Tolgod (Late

2358 Cretaceous Mongolia). *American Museum Novitates* 3446:1–9.

2359 Norell, M.A., Makovicky, P.J., Bever, G.S., Balanoff, A.M., Clark, J.M., Barsbold, R. and

2360 Rowe, T. 2009. A review of the Mongolian Cretaceous dinosaur *Saurornithoides*

2361 (Troodontidae: Theropoda). *American Museum Novitates* 3654:1–63.

2362 doi:10.1206/648.1.

2363 Novas, F.E. 1994. New information on the systematics and postcranial skeleton of

2364 *Herrerasaurus ischigualastensis* (Theropoda: Herrerasauridae) from the Ischigualasto

2365 Formation (Upper Triassic) of Argentina. *Journal of Vertebrate Paleontology* 13:400–

2366 423. doi:10.1080/02724634.1994.10011523.

2367 Novas, F.E., Ezcurra, M.D., Agnolin, F.L., Pol, D. and Ortíz, R. 2012. New Patagonian

2368 Cretaceous theropod sheds light about the early radiation of Coelurosauria. *Revista del*

2369 *Museo Argentino de Ciencias Naturales* 14:57–81.

2370 Osborn, H.F. 1903. *Ornitholestes hermanni*, a new compsognathoid dinosaur from the Upper

2371 Jurassic. *Bulletin of the American Museum of Natural History* 19:459–464.

2372 Osborn, H.F. 1905. *Tyrannosaurus* and other Cretaceous carnivorous dinosaurs. *Bulletin of*

2373 *the American Museum of Natural History* 21:259–265.

2374   Osborn, H.F. 1912. Crania of *Tyrannosaurus* and *Allosaurus*. *Memoirs of the American*

2375   *Museum of Natural History. New Series* 1:1–30.

2376   Osmólska, H., Roniewicz, E. and Barsbold, R. 1972. A new dinosaur, *Gallimimus bullatus* n.

2377   gen., n. sp.(Ornithomimidae) from the Upper Cretaceous of Mongolia. *Palaeontologia*

2378   *Polonica* 27:103–143.

2379   Ostrom, J.H. 1978. The osteology of *Compsognathus longipes* Wagner. *Zitteliana* 4:73–118.

2380   Paul, G.S. 1988. *Predatory Dinosaurs of the World: A Complete Illustrated Guide*. Simon &

2381   Schuster.

2382   Perle, A., Chiappe, L.M. and Barsbold, R. 1994. Skeletal morphology of *Mononykus*

2383   *olecranus* (Theropoda: Avialae) from the Late Cretaceous of Mongolia. *American*

2384   *Museum Novitates* 3105:1–29.

2385   Peyer, K. 2006. A reconsideration of *Compsognathus* from the upper Tithonian of Canjuers,

2386   southeastern France. *Journal of Vertebrate Paleontology* 26:879–896.

2387   doi:10.1671/0272-4634(2006)26[879:AROCFT]2.0.CO;2.

2388   Pol, D. and Rauhut, O.W.M. 2012. A Middle Jurassic abelisaurid from Patagonia and the

2389   early diversification of theropod dinosaurs. *Proceedings of the Royal Society B:*

2390   *Biological Sciences* 279:3170–3175. doi:10.1098/rspb.2012.0660.

2391   Polcyn, M.J. and Bell, G.L. 2005. *Russellosaurus coheni* n. gen., n. sp., a 92 million-year-old

2392   mosasaur from Texas (USA), and the definition of the parafamily Russellosaurina.

2393   *Netherlands Journal of Geosciences* 84:321–333.

2394   Raath, M.A. 1977. The anatomy of the Triassic theropod *Syntarsus rhodesiensis* (Saurischia:

2395   Podokesauridae) and a consideration of its biology. Ph.D. Dissertation, Department of

2396   Zoology and Entomology, Rhodes University, Salisbury, Rhodesia.

2397   Rauhut, O.W.M., Milner, A.C. and Moore-Fay, S. 2010. Cranial osteology and phylogenetic

2398   position of the theropod dinosaur *Proceratosaurus bradleyi* (Woodward, 1910) from

2399   the Middle Jurassic of England. *Zoological Journal of the Linnean Society* 158:155–

2400   195. doi:10.1111/j.1096-3642.2009.00591.x.

2401   Rayfield, E.J. 2005. Aspects of comparative cranial mechanics in the theropod dinosaurs

2402   *Coelophysis*, *Allosaurus* and *Tyrannosaurus*. *Zoological Journal of the Linnean*

2403   *Society* 144:309–316. doi:10.1111/j.1096-3642.2005.00176.x.

2404   Reig, O.A. 1963. La presencia de dinosaurios saurisquios en los "Estratos de Ischigualasto"

2405   (Mesotriásico Superior) de las provincias de San Juan y La Rioja (República

2406   Argentina). *Ameghiniana* 3:3–20.

2407   Rohlf, F.J. and Slice, D. 1990. Extensions of the procrustes method for the optimal

2408   superimposition of landmarks. *Systematic Biology* 39:40–59. doi:10.2307/2992207.

2409   Rowe, T. 1989. A new species of the theropod dinosaur *Syntarsus* from the Early Jurassic

2410   Kayenta Formation of Arizona. *Journal of Vertebrate Paleontology* 9:125–136.

2411   doi:10.1080/02724634.1989.10011748.

2412   Russell, D.A. 1969. A new specimen of *Stenonychosaurus* from the Oldman Formation

2413   (Cretaceous) of Alberta. *Canadian Journal of Earth Sciences* 6:595–612.

2414   doi:10.1139/e69-059.

2415   Russell, D.A. 1970. Tyrannosaurs from the Late Cretaceous of western Canada. *National*

2416   *Museum of Natural Sciences Publications in Paleontology* 1:1–34.

2417   Russell, D.A. and Dong, Z.-M. 1993. A nearly complete skeleton of a new troodontid

2418   dinosaur from the Early Cretaceous of the Ordos Basin, Inner Mongolia, People's

2419   Republic of China. *Canadian Journal of Earth Sciences* 30:2163–2173.

2420   doi:10.1139/e93-187.

2421   Sadleir, R., Barrett, P.M. and Powell, H.P. 2008. The anatomy and systematics of

2422   *Eustreptospondylus oxoniensis*, a theropod dinosaur from the Middle Jurassic of

2423   Oxfordshire, England. *Monograph of the Palaeontographical Society, London* 160:1–

2424   82.

2425   Sakamoto, M. 2010. Jaw biomechanics and the evolution of biting performance in theropod

2426   dinosaurs. *Proceedings of the Royal Society B: Biological Sciences* 277:3327–3333.

2427   doi:10.1098/rspb.2010.0794.

2428   Sampson, S.D. and Witmer, L.M. 2007. Craniofacial anatomy of *Majungasaurus*

2429   *crenatissimus* (Theropoda: Abelisauridae) from the Late Cretaceous of Madagascar.

2430   *Journal of Vertebrate Paleontology* 27:32–104. doi:10.1671/0272-

2431   4634(2007)27[32:CAOMCT]2.0.CO;2.

2432   Dal Sasso, C. and Maganuco, S. 2011. *Scipionyx samniticus* (Theropoda: Compsognathidae)

2433   from the Lower Cretaceous of Italy: osteology, ontogenetic assessment, phylogeny,

2434   soft tissue anatomy, taphonomy and palaeobiology. *Memorie della Società Italiana di*

2435   *Scienze Naturali e del Museo Civico di Storia Naturale di Milano* 37:1–281.

2436   Dal Sasso, C. and Signore, M. 1998. Exceptional soft-tissue preservation in a theropod

2437   dinosaur from Italy. *Nature* 392:383–387. doi:10.1038/32884.

2438   Senter, P. 2009. Pedal function in deinonychosaurs (Dinosauria: Theropoda): a comparative

2439   study. *Bulletin of the Gunma Museum of Natural History* 13:1–14.

2440   Senter, P. 2011. Using creation science to demonstrate evolution 2: morphological continuity

2441   within Dinosauria. *Journal of Evolutionary Biology* 24:2197–2216.

2442   doi:10.1111/j.1420-9101.2011.02349.x.

2443   Sereno, P.C., Beck, A.L., Dutheil, D.B., Gado, B., Larsson, H.C.E., Lyon, G.H., Marcot, J.D.,

2444   Rauhut, O.W.M., Sadleir, R.W., Sidor, C.A., Varricchio, D.D., Wilson, G.P. and

2445   Wilson, J.A. 1998. A long-snouted predatory dinosaur from Africa and the evolution

2446   of spinosaurids. *Science* 282:1298–1302. doi:10.1126/science.282.5392.1298.

2447   Sereno, P.C., Dutheil, D.B., Larochene, M., Larsson, H.C.E., Lyon, G.H., Magwene, P.M.,

2448   Sidor, C.A., Varricchio, D.J. and Wilson, J.A. 1996. Predatory dinosaurs from the

2449   Sahara and Late Cretaceous faunal differentiation. *Science* 272:986–991.

2450   doi:10.1126/science.272.5264.986.

2451   Sereno, P.C., Forster, C.A., Rogers, R.R. and Monetta, A.M. 1993. Primitive dinosaur

2452   skeleton from Argentina and the early evolution of Dinosauria. *Nature* 361:64–66.

2453   doi:10.1038/361064a0.

2454   Sereno, P.C., Martínez, R.N. and Alcober, O.A. 2013. Osteology of *Eoraptor lunensis*

2455   (Dinosauria, Sauropodomorpha). *Journal of Vertebrate Paleontology* 32:83–179.

2456   doi:10.1080/02724634.2013.820113.

2457   Sereno, P.C., Martinez, R.N., Wilson, J.A., Varricchio, D.J., Alcober, O.A. and Larsson,

2458   H.C.E. 2008. Evidence for avian intrathoracic air sacs in a new predatory dinosaur

2459   from Argentina. *PLoS ONE* 3:e3303. doi:10.1371/journal.pone.0003303.

2460   Sereno, P.C. and Novas, F.E. 1994. The skull and neck of the basal theropod *Herrerasaurus*

2461   *ischigualastensis*. *Journal of Vertebrate Paleontology* 13:451–476.

2462   doi:10.1080/02724634.1994.10011525.

2463   Sereno, P.C., Tan, L., Brusatte, S.L., Kriegstein, H.J., Zhao, X. and Cloward, K. 2009.

2464   Tyrannosaurid skeletal design first evolved at small body size. *Science* 326:418–422.

2465   doi:10.1126/science.1177428.

2466   Sereno, P.C., Wilson, J.A., Larsson, H.C.E., Dutheil, D.B. and Sues, H.-D. 1994. Early

2467   Cretaceous dinosaurs from the Sahara. *Science* 266:267–271.

2468   doi:10.1126/science.266.5183.267.

2469   Siegel, A.F. and Benson, R.H. 1982. A Robust Comparison of Biological Shapes. *Biometrics*

2470   38:341. doi:10.2307/2530448.

2471   Smith, N.D., Makovicky, P.J., Hammer, W.R. and Currie, P.J. 2007. Osteology of

2472   *Cryolophosaurus ellioti* (Dinosauria: Theropoda) from the Early Jurassic of Antarctica

2473   and implications for early theropod evolution. *Zoological Journal of the Linnean*

2474   *Society* 151:377–421. doi:10.1111/j.1096-3642.2007.00325.x.

2475   Stovall, J.W. and Langston Jr, W. 1950. *Acrocanthosaurus atokensis*, a new genus and

2476   species of Lower Cretaceous Theropoda from Oklahoma. *American Midland*

2477   *Naturalist* 696–728.

2478   Sues, H.-D. 1977. The skull of *Velociraptor mongoliensis*, a small Cretaceous theropod

2479   dinosaur from Mongolia. *Paläontologische Zeitschrift* 51:173–184.

2480   doi:10.1007/BF02986567.

2481   Sues, H.-D., Frey, E., Martill, D.M. and Scott, D.M. 2002. *Irritator challengeri*, a spinosaurid

2482   (Dinosauria: Theropoda) from the Lower Cretaceous of Brazil. *Journal of Vertebrate*

2483   *Paleontology* 22:535–547. doi:10.1671/0272-

2484   4634(2002)022[0535:ICASDT]2.0.CO;2.

2485   Sues, H.-D., Nesbitt, S.J., Berman, D.S. and Henrici, A.C. 2011. A late-surviving basal

2486   theropod dinosaur from the latest Triassic of North America. *Proceedings of the Royal*

2487   *Society B: Biological Sciences* 278:3459–3464. doi:10.1098/rspb.2011.0410.

2488   Tahara, R. and Larsson, H.C.E. 2011. Cranial pneumatic anatomy of *Ornithomimus*

2489   *edmontonicus* (Ornithomimidae: Theropoda). *Journal of Vertebrate Paleontology*

2490   31:127–143. doi:10.1080/02724634.2011.539646.

2491   Therrien, F., Henderson, D.M. and Ruff, C.B. 2005. Bite me: biomechanical models of

2492   theropod mandibles and implications for feeding behavior, p. 179–237. In Carpenter,

2493   K. (ed.), *The Carnivorous Dinosaurs*. Indiana University Press, Bloomington, Indiana.

2494   Turner, A.H., Hwang, S.H. and Norell, M.A. 2007. A small derived theropod from Öösh,

2495   Early Cretaceous, Baykhangor Mongolia. *American Museum Novitates* 3557:1–27.
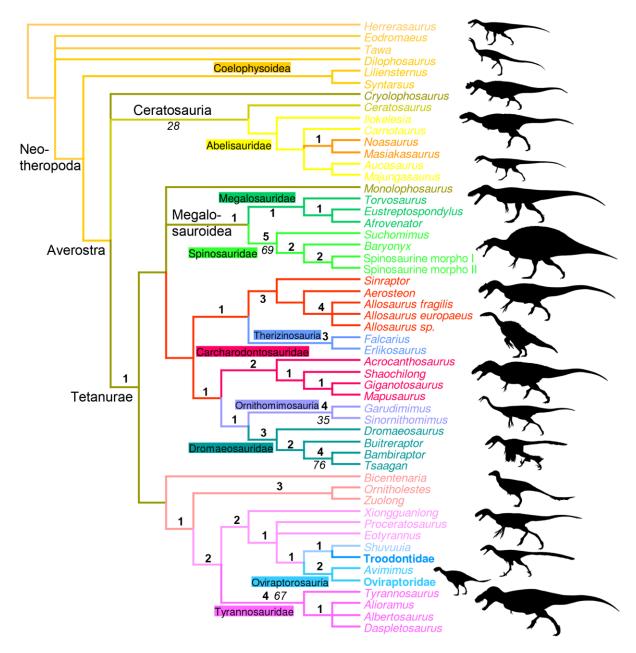
2496 Turner, A.H., Makovicky, P.J. and Norell, M. 2012. A review of dromaeosaurid systematics

2497 and paravian phylogeny. *Bulletin of the American Museum of Natural History* 371:1–

2498 206.

2499 Turner, A.H., Pol, D. and Norell, M.A. 2011. Anatomy of *Mahakala omnogovae* (Theropoda:

2500 Dromaeosauridae), Tögrögiin Shiree, Mongolia. *American Museum Novitates* 3722:1–

2501 66. doi:10.1206/3722.2.

2502 Tykoski, R.S. 2005. Anatomy, ontogeny, and phylogeny of coelophysoid theropods. Ph.D.

2503 Dissertation, The University of Texas, Austin, Texas.

2504 Varricchio, D.J. 1997. Troodontidae, p. 749–754. In Currie, P.J. and Padian, K. (eds.),

2505 *Encyclopedia of Dinosaurs*. Academic Press, San Diego, California.

2506 Vickers-Rich, P., Chiappe, L.M. and Kurzanov, S. 2002. The enigmatic birdlike dinosaur

2507 *Avimimus portentosus*, p. 65–86. In Chiappe, L.M. and Witmer, L.M. (eds.), *Mesozoic*

2508 *birds: above the heads of dinosaurs*. University of California Press, Berkeley/Los

2509 Angeles/London.

2510 Walker, A.D. 1964. Triassic reptiles from the Elgin Area: *Ornithosuchus* and the origin of

2511 carnosaurs. *Philosophical Transactions of the Royal Society of London. Series B,*

2512 *Biological Sciences* 248:53–134. doi:10.1098/rstb.1964.0009.

2513 Walker, A.D. 1985. The braincase of *Archaeopteryx*, p. 123–134. In Hecht, M.K., Ostrom,

2514 J.H., Viohl, G., and Wellnhofer, P. (eds.), *The Beginnings of Birds*. Freunde des Jura-

2515 Museums Eichstätt, Germany.

2516 Welles, S.P. 1954. New Jurassic Dinosaur from the Kayenta Formation of Arizona.

2517 *Geological Society of America Bulletin* 65:591–598. doi:10.1130/0016-

2518 7606(1954)65[591:NJDFTK]2.0.CO;2.

2519 Welles, S.P. 1984. *Dilophosaurus wetherilli* (Dinosauria, Theropoda). Osteology and

2520 comparisons. *Palaeontographica Abteilung A* 185:85–180.

2521   Wellnhofer, P. 1980. Flugsaurierreste aus der Gosau-Kreide von Muthmannsdorf

2522   (Niederösterreich)–ein Beitrag zur Kiefermechanik der Pterosaurier. *Mitteilungen der*

2523   *Bayerischen Statssammlung fur Paleontologie und historische Geologie* 20:95–

2524   112.

2525   White, T.E. 1940. Holotype of *Plesiosaurus longirostris* Blake and classification of the

2526   plesiosaurs. *Journal of Paleontology* 451–467.

2527   Xing, L. 2012. *Sinosaurus* from southwestern China. MSc. Dissertation, University of

2528   Alberta, Edmonton, Alberta, Canada.

2529   Xing, L., Bell, P.R., Rothschild, B.M., Ran, H., Zhang, J., Dong, Z., Zhang, W. and Currie,

2530   P.J. 2013. Tooth loss and alveolar remodeling in *Sinosaurus triassicus* (Dinosauria:

2531   Theropoda) from the Lower Jurassic strata of the Lufeng Basin, China. *Chinese*

2532   *Science Bulletin* 58:1931–1935. doi:10.1007/s11434-013-5765-7.

2533   Xu, X., Clark, J.M., Forster, C.A., Norell, M.A., Erickson, G.M., Eberth, D.A., Jia, C. and

2534   Zhao, Q. 2006. A basal tyrannosauroid dinosaur from the Late Jurassic of China.

2535   *Nature* 439:715–718. doi:10.1038/nature04511.

2536   Xu, X. and Norell, M.A. 2004. A new troodontid dinosaur from China with avian-like

2537   sleeping posture. *Nature* 431:838–841. doi:10.1038/nature02898.

2538   Xu, X., Norell, M.A., Kuang, X., Wang, X., Zhao, Q. and Jia, C. 2004. Basal tyrannosauroids

2539   from China and evidence for protofeathers in tyrannosauroids. *Nature* 431:680–684.

2540   doi:10.1038/nature02855.

2541   Xu, X., Norell, M.A., Wang, X., Makovicky, P.J. and Wu, X. 2002. A basal troodontid from

2542   the Early Cretaceous of China. *Nature* 415:780–784. doi:10.1038/415780a.

2543   Xu, X. and Wu, X.-C. 2001. Cranial morphology of *Sinornithosaurus millenii* Xu et al. 1999

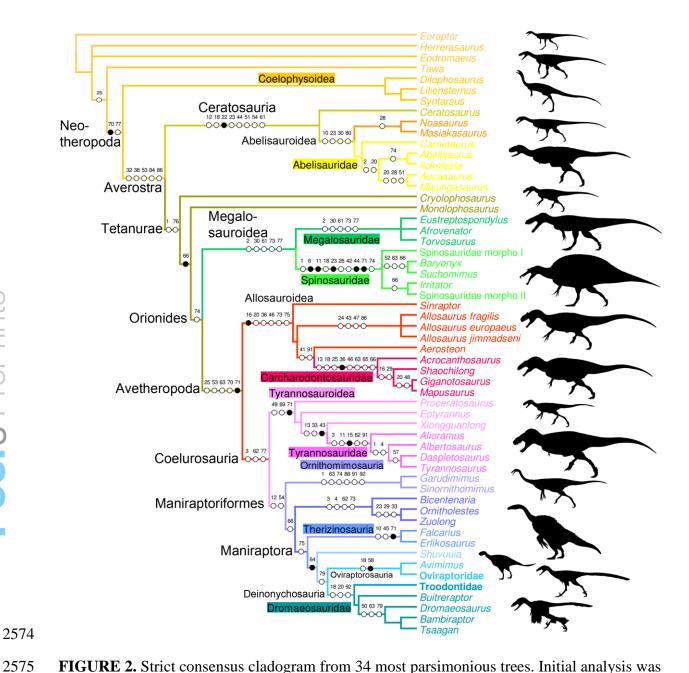2544   (Dinosauria: Theropoda: Dromaeosauridae) from the Yixian Formation of Liaoning,

2545   China. *Canadian Journal of Earth Sciences* 38:1739–1752. doi:10.1139/e01-082.

2546 Xu, X., You, H., Du, K. and Han, F. 2011. An *Archaeopteryx*-like theropod from China and

2547   the origin of Avialae. *Nature* 475:465–470. doi:10.1038/nature10288.

2548 Yates, A.M. 2005. A new theropod dinosaur from the Early Jurassic of South Africa and its

2549   implications for the early evolution of theropods. *Palaeontologia Africana* 41:105–

2550   122.

2551 Zanno, L.E. 2010. Osteology of *Falcarius utahensis* (Dinosauria: Theropoda): characterizing

2552   the anatomy of basal therizinosaurs. *Zoological Journal of the Linnean Society*

2553   158:196–230. doi:10.1111/j.1096-3642.2009.00464.x.

2554 Zanno, L.E., Gillette, D.D., Albright, L.B. and Titus, A.L. 2009. A new North American

2555   therizinosaurid and the role of herbivory in "predatory" dinosaur evolution.

2556   *Proceedings of the Royal Society B: Biological Sciences* 276:3505–3511.

2557   doi:10.1098/rspb.2009.1029.

2558 Zelditch, M.L., Wood, A.R. and Swiderski, D.L. 2009. Building Developmental Integration

2559   into Functional Systems: Function-Induced Integration of Mandibular Shape.

2560   *Evolutionary Biology* 36:71–87. doi:10.1007/s11692-008-9034-7.

2561 Zhao, X.-J. and Currie, P.J. 1993. A large crested theropod from the Jurassic of Xinjiang,

2562   People's Republic of China. *Canadian Journal of Earth Sciences* 30:2027–2036.

2563   doi:10.1139/e93-178.

2564

2565

FIGURE CAPTIONS

2567

FIGURE 1. Strict consensus cladogram from 13 most parsimonious trees. Initial analysis was a New Technology Search using TNT v.1.1 of a data matrix comprising 98 quadrate based characters for one outgroup (*Herrerasaurus ischigualastensis*) and 54 nonavian theropod taxa. Tree length = 589 steps; CI = 0.282; RI = 0.556. Bremer support values are in bold and bootstrap values are in italic.

2573

FIGURE 2. Strict consensus cladogram from 34 most parsimonious trees. Initial analysis was

a New Technology Search using TNT v.1.1 of a supermatrix comprising 98 quadrate based

characters combined with six recent datasets based on the whole skeleton (Choiniere, Xu, et

al., 2010; Brusatte, Norell, et al., 2010; Martinez et al., 2011; Carrano et al., 2012; Pol and

Rauhut, 2012) for one outgroup (*Eoraptor lunensis*) and 54 nonavian theropod taxa. Tree

length = 3616 steps; CI = 0.562; RI = 0.63113. Bremer support values are in bold and
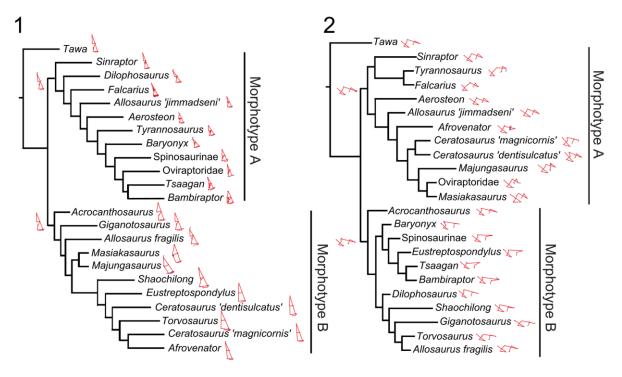
bootstrap values are in italic.

FIGURE 3. 1, Cladogram resulting from the phylogenetic morphometrics analysis of the
quadrate body shape in posterior view using 12 landmarks (tree score: 3.25, by using RFTRA)
and revealing two morphotypes: low and stout quadrate with well-delimited and relatively
broad lateromedially quadrate foramen (morphotype A; Spinosauridae and Coelurosauria)
versus tall and slender quadrate with a lateromedially narrow or completely absent quadrate
foramen (morphotype B; Ceratosauria and Megalosauridae); **2**, Cladogram resulting from the
phylogenetic morphometrics analysis of the mandibular articulation in ventral view using 8
landmarks (tree score: 2.92; by using RFTRA) and revealing two morphotypes:
anteroposteriorly broad mandibular articulation with two ovoid/subcircular condyles roughly
subequal in size (morphotype A; Ceratosauria, Tyrannosauroidea and Oviraptorosauria)
versus elongate and anteroposteriorly narrow mandibular articulation with a long and
parabolic/sigmoid ectocondyle (morphotype B; Megalosauroidea, Carcharodontosauridae and
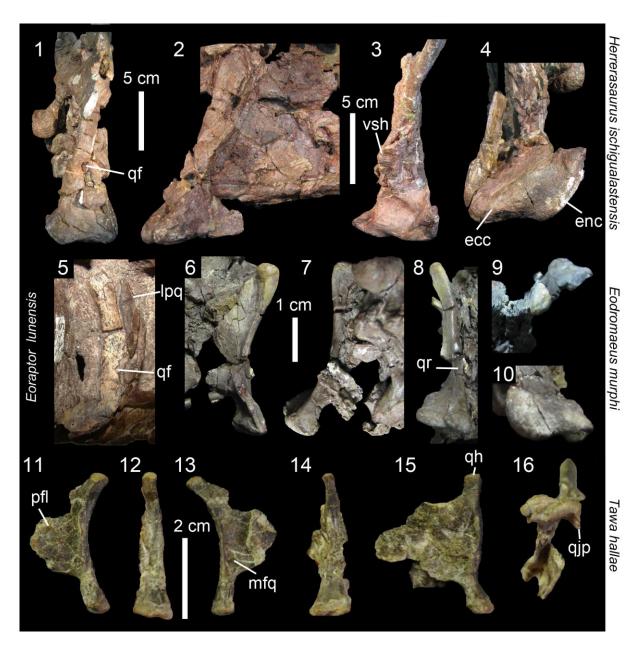Dromaeosauridae).

FIGURE 4. Quadrate diversity in non-neotheropod Theropoda. Right quadrate (**1–4**) of

Herrerasaurus ischigualastensis (PVSJ 53, formerly *Frenguellisaurus ischigualastensis*) in

(**1**) posterior, (**2**) medial, (**3**) anterior and (**4**) ventral views. Right quadrate (**5**) of *Eoraptor*

lunensis (PVSJ 512) in posterolateral view. Left quadrate (**5–10**) of *Eodromaeus murphi*

(PVSJ 562) in (**6**) lateral, (**7**) medial, (**8**) posterior, (**9**) dorsal, and (**10**) ventral views. Left

(**11–13**) and right (1**4–16**) quadrates of *Tawa hallae* (GR 241) in (**11**) lateral, (**12, 14**)

posterior, (**13, 15**) medial and (**16**) ventral views (courtesy of Sterling Nesbitt).

Abbreviations: **ecc**, ectocondyle; **enc**, entocondyle; **lpq**, lateral process; **mfq**, medial fossa;

2607 **pfl**, pterygoid flange; **pfq**, posterior fossa; **qf**, quadrate foramen; **qjp**, quadratojugal process;

2608 **qr** quadrate ridge; **vsh**, ventral shelf of the pterygoid flange.
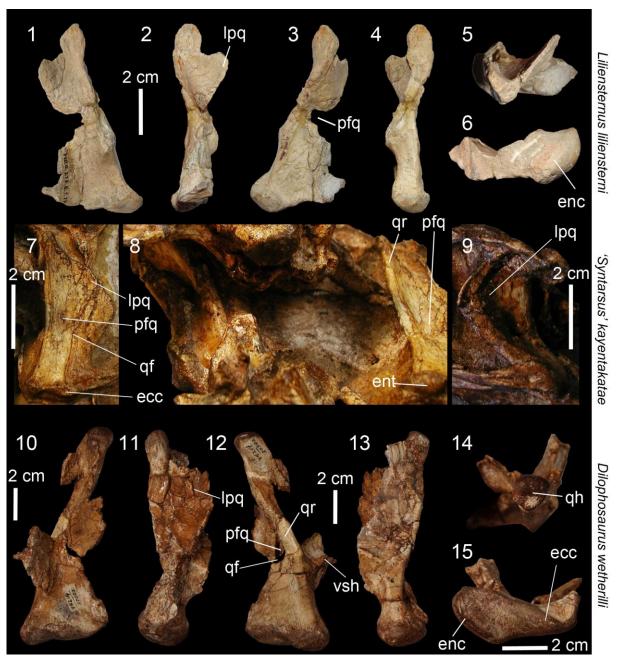
2609

2610

2611 **FIGURE 5**. Quadrate diversity in Coelophysoidea. Right quadrate (**1–6**) of *Liliensternus*

2612 *liliensterni* (MB R.2175) in (**1**) anterior, (**2**) lateral, (**3**) posterior, (**4**) medial, (**5**) dorsal, and

2613 (**6**) ventral views (courtesy of Martín Ezcurra). Right (**7–8**) and left (**8–9**) quadrates of

2614 '*Syntarsus*' *kayentakatae* (MNA V2623) in (**9**) lateral and (**7, 8**) posterior views (courtesy of

2615   Ronald Tykoski). Left (**10, 12, 15**) and right (**11, 13–14**) quadrates of *Dilophosaurus*

2616   *wetherilli* (UCMP 37302) in (**10**) anterior, (**11**) lateral, (**12**) posterior, (**13**) medial, (**14**) dorsal

2617   and (**15**) ventral views (courtesy of Randall Irmis). Abbreviations: **ecc**, ectocondyle; **enc**,

2618   entocondyle; **lpq**, lateral process; **mfq**, medial fossa; **pfl**, pterygoid flange; **pfq**, posterior

2619   fossa; **qf**, quadrate foramen; **qh**, quadrate head; **qjp**, quadratojugal process; **qr** quadrate ridge;

2620   **vsh**, ventral shelf of the pterygoid flange.

2621

The figure shows quadrate specimens labeled 1–17 with anatomical annotations (lpq, pfq, vsh, enc, ecc, qr, ptf, qjc, ics, pfl), scale bars (10 cm, 2 cm), and taxon labels (*Ceratosaurus nasicornis*, *Masiakasaurus knopfleri*, *Noasaurus leali*).
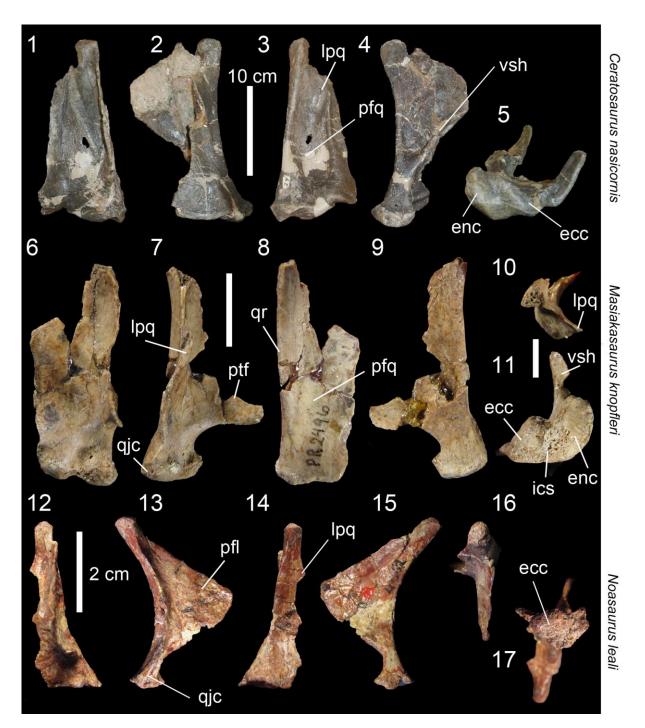
2622

FIGURE 6. Quadrate diversity in Ceratosauridae and Noasauridae. Coosified right (**1, 3**) and left (**2, 4–5**) quadrates and quadratojugals of *Ceratosaurus nasicornis* (MWC 1; formerly known as *C.* '*magnicornis*') in (**1**) anterior, (**2**) lateral, (**3**) posterior, (**4**) medial and (**5**) ventral views. Right quadrate (**6–9**) of *Masiakasaurus knopfleri* (FMNH PR 2496) in (**6**) lateral, (**7**) posterior, (**8**) medial and (**9**) ventral views (courtesy of Matthew Carrano). Right quadrate (**10–15**) of *Noasaurus leali* (PVL 4061) in (**10**) anterior, (**11**) lateral, (**12**) posterior, (**13**)

2629 medial, dorsal (**14**), and (**15**) ventral views. Abbreviations: **ecc**, ectocondyle; **enc**,

2630 entocondyle; **ics**, intercondylar sulcus; **lpq**, lateral process; **mfq**, medial fossa; **ptf**, pterygoid

2631 flange; **qh**, quadrate head; **qjc**, quadratojugal contact; **qr** quadrate ridge; **vsh**, ventral shelf of

2632 the pterygoid flange; **pfq**, posterior fossa.
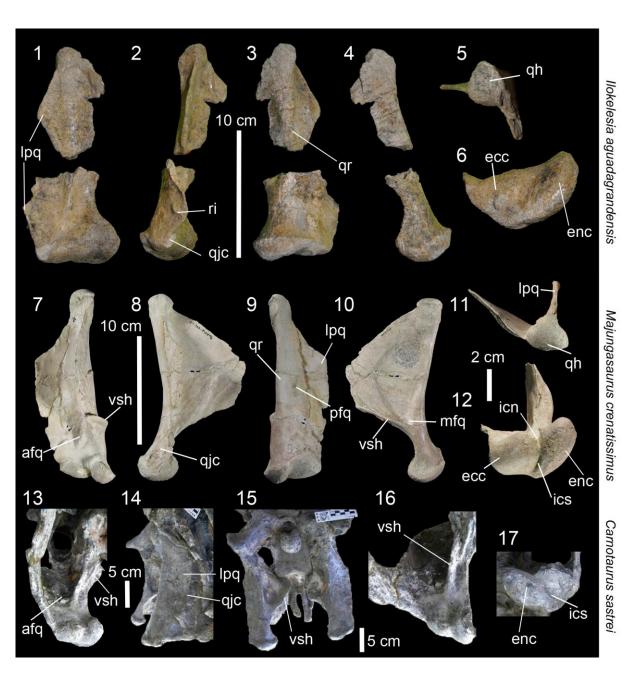
2633

2634

2635 **FIGURE 7**. Quadrate diversity in Abelisauridae. Right quadrate (**1–6**) of *Ilokelesia*

2636 *aguadagrandensis* (PVPH 35) in (**1**) anterior, (**2**) lateral, (**3**) posterior, (**4**) medial, (**5**) dorsal

2637 and (**6**) ventral views (courtesy of Matthew Lamanna). Right quadrate (**7–12**) of

2638   *Majungasaurus crenatissimus* (FMNH PR 2100) in (**7**) anterior, (**8**) lateral, (**9**) posterior, (**10**)

2639   medial, (**11**) dorsal and (**12**) ventral views (courtesy of Lawrence Witmer). Right (**13**, **14**, **15**,

2640   **16**) and left (**15**, **17**) quadrates of *Carnotaurus sastrei* (MACN CH 894) in (**13**) anteroventral,

2641   (**14**) lateral, (**15**) posterior, (**16**) anteromedial and (**17**) ventral views (courtesy of Pablo

2642   Asaroff). Abbreviations: **ecc**, ectocondyle; **enc**, entocondyle; **icn**, intercondylar notch; **ics**,

2643   intercondylar sulcus; **lpq**, lateral process; **mfq**, medial fossa; **pfq**, posterior fossa; **qh**,

2644   quadrate head; **qjc**, quadratojugal contact; **qr** quadrate ridge; **ri**, ridge on the ventrolateral

2645   surface of the quadrate body; **vsh**, ventral shelf of the pterygoid flange.

2646

FIGURE 8. Quadrate diversity in Megalosauridae. Right quadrate (**1–5**) of

Eustreptospondylus oxoniensis (OUMNH J.13558) in (**1**) anterior, (**2**) lateral, (**3**) posterior,

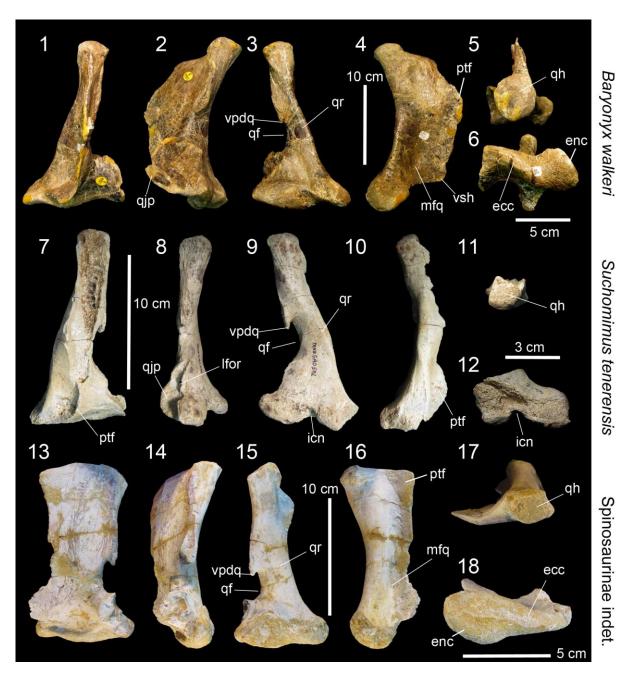(**4**) medial and (**5**) ventral views (courtesy of Paul Barrett). Right quadrate (**6–11**) of

Torvosaurus tanneri (BYUVP 9246) in (**6**) anterior, (**7**) lateral, (**8**) posterior, (**9**) medial, (**10**)

dorsal and (**11**) ventral views (courtesy of Matthew Lamanna). Left quadrates (**12–17**) of

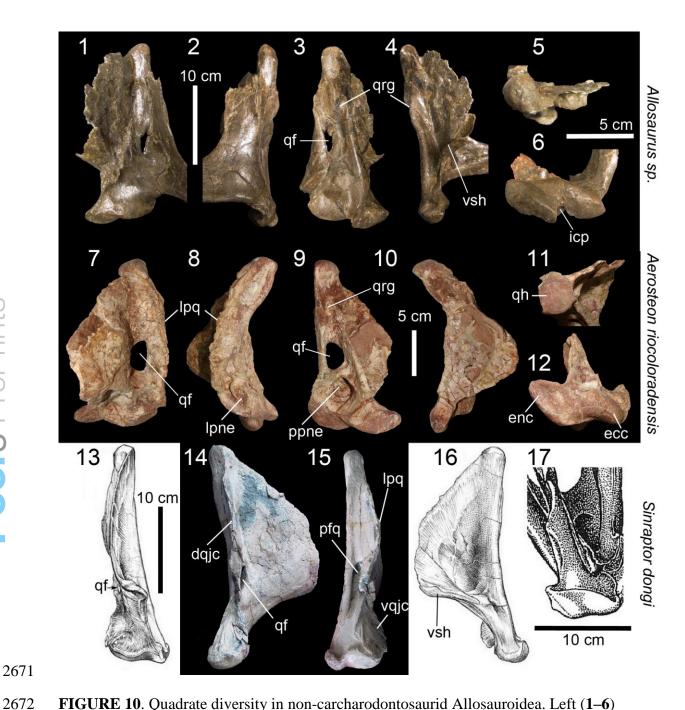*Afrovenator abakensis* (UC OBA1) in (**12**) anterior, (**13**) lateral, (**14**) posterior, (**15**) medial,

(**16**) dorsal and (**17**) ventral views (courtesy of Roger Benson). Abbreviations: **ecc**,

2655 ectocondyle; **enc**, entocondyle; **fo1**, medial foramen 1; **fo2**, medial foramen 2; **ics**,

2656 intercondylar sulcus; **mfq**, medial fossa; **pfq**, posterior fossa; **qh**, quadrate head; **qjc**,

2657 quadratojugal contact; **qjp**, quadratojugal process; **vmfo**, ventromedial foramen.

2658

2659

2660 **FIGURE 9**. Quadrate diversity in Spinosauridae. Left quadrate (**1–6**) of *Baryonyx walkeri*

2661 (BMNH R9951) in (**1**) anterior, (**2**) lateral, (**3**) posterior, (**4**) medial, (**5**) dorsal and (**6**) ventral

2662 views. Left quadrate (**7–12**) of *Suchomimus tenerensis* (MNN GAD 502) in (**7**) anterior, (**8**)

2663 lateral, (**9**) posterior, (**10**) medial, (**11**) dorsal and (**12**) ventral views. Left quadrate (**13**–**18**) of

2664 and indeterminate Spinosaurinae from the Kem Kem beds (MSNM V6896) in (**13**) anterior,

2665 (**14**) lateral, (**15**) posterior, (**16**) medial, (**17**) dorsal and (**18**) ventral views. Abbreviations:

2666 **ecc**, ectocondyle; **enc**, entocondyle; **icp**, intercondylar pit; **lfo**, lateral foramen; **mfq**, medial

2667 fossa; **ptf**, pterygoid flange; **qf**, quadrate foramen; **qh**, quadrate head; **qjp**, quadratojugal

2668 process; **qr**, quadrate ridge; **vpdq**, ventral projection of the dorsal quadratojugal contact; **vsh**,
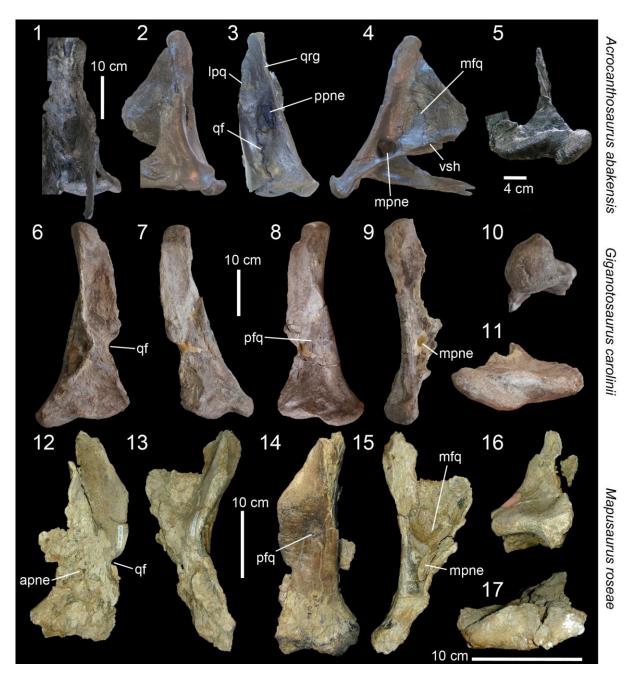
2669 ventral shelf of the pterygoid flange.

2670

FIGURE 10. Quadrate diversity in non-carcharodontosaurid Allosauroidea. Left (**1–6**) coosified quadrate and quadratojugal of *Allosaurus 'jimmadseni'*. (SMA 005/02) in (**1**) anterior, (**2**) lateral, (**3**) posterior, (**4**) medial, (**5**) dorsal, and (**6**) ventral views. Left quadrate (**7–12**) of *Aerosteon riocoloradensis* (MCNA-PV-3137) in (**7**) anterior, (**8**) lateral, (**9**) posterior, (**10**) medial, (**11**) dorsal, and (**12**) ventral views (courtesy of Martin Ezcurra). Right quadrate (**13–17**) of *Sinraptor dongi* (IVPP 10600) in (**13**) anterior, (**14**) lateral, (**15**) posterior, (**16**) medial, and (**17**) ventral views (Currie, 2005 for 13, 16–17; courtesy of Philip

2679 Currie for 14–15). Abbreviations: **ecc**, ectocondyle; **enc**, entocondyle; **dqjc**, dorsal

2680 quadratojugal contact; **icp**, intercondylar pit; **lpq**, lateral process; **pfq,** posterior fossa; **ppne**,

2681 posterior pneumatopore; **qf**, quadrate foramen; **qr**, quadrate ridge; **qrg**, quadrate ridge

2682 groove; **vqjc**, ventral quadratojugal contact; **vsh**, ventral shelf of the pterygoid flange.

2683

2684

2685 **FIGURE 11**. Quadrate diversity in Carcharodontosauridae. Right (**1, 5**) and left (**2–4**)

2686 coosified quadrate and quadratojugal of *Acrocanthosaurus atokensis* (NCSM 14345) in (**1**)

2687   anterior, (**2**) lateral, (**3**) posterior, (**4**) medial, and (**5**) ventral views (courtesy of Drew Eddy

2688   and Vince Shneider). Right quadrate (**6–11**) of *Shaochilong moartuensis* (IVPP V2885.3) in

2689   (**6**) anterior, (**7**) lateral, (**8**) posterior, (**9**) medial, (**10**) dorsal and (**11**) ventral views (courtesy

2690   of Steve Brusatte). Left quadrate (**12–17**) of *Mapusaurus rosea* (MCFPVPH-108.102) in (**12**)

2691   anterior, (**13**) lateral, (**14**) posterior, (**15**) medial, (**16**) dorsal, and (**17**) ventral views (courtesy

2692   of Matthew Lamanna). Abbreviations: **apne**, anterior pneumatopore; **lpq**, lateral process;

2693   **mfq**, medial fossa; **mpne**, medial pneumatopore; **pfq**, posterior fossa; **ppne**, posterior

2694   pneumatopore; **qf**, quadrate foramen; **qrg**, quadrate ridge groove; **vsh**, ventral shelf of the
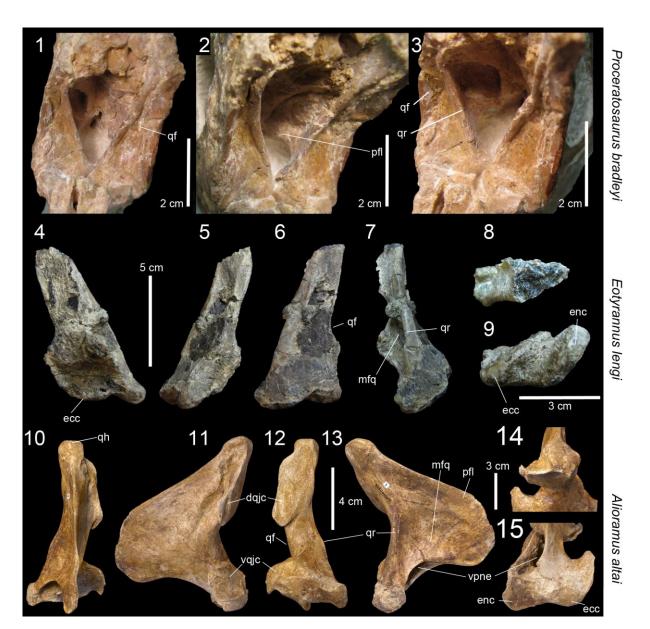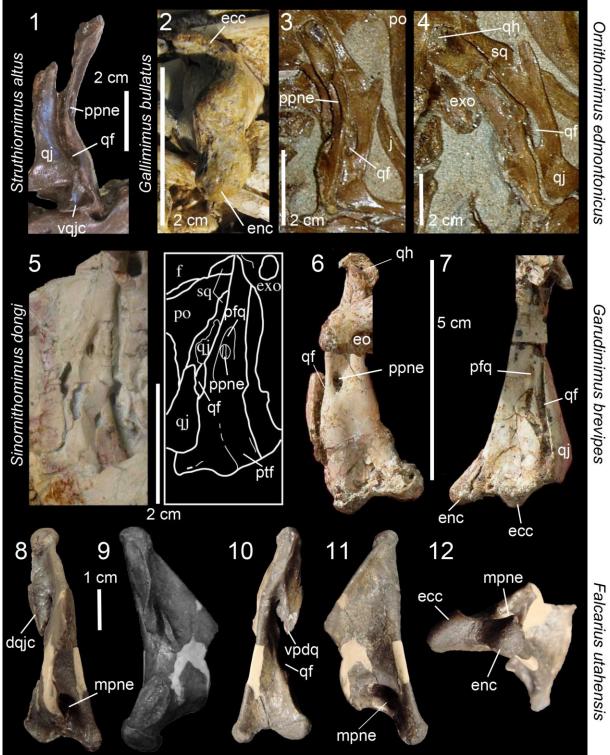
2695   pterygoid flange.

2696

FIGURE 12. Quadrate diversity in Tyrannosauroidea. Left and right (**1–3**) quadrates of

Proceratosaurus bradleyi (NHM R 4860) in (**1**) posterior and (**2–3**) posteromedial views.

Ventral part of the right quadrate (**4–9**) of *Eotyrannus lengi* (MIWG 1997.550) in (**4**) anterior,

(**5**) lateral, (**6**) posterior, (**7**) medial, (**8**) dorsal and (**9**) ventral views. Left quadrate (**10–15**) of

Alioramus altai (IGM 100-1844) in (**10**) anterior, (**11**) lateral, (**12**) posterior, (**13**) medial, (**14**)

dorsal, and (**15**) ventral views (courtesy of Mike Ellison © AMNH). Abbreviations: **dqjc**,

dorsal quadratojugal contact; **ecc**, ectocondyle; **enc**, entocondyle; **mfq**, medial fossa; **pfl**,

pterygoid flange; **pfq**, posterior fossa; **qf**, quadrate foramen; **qh**, quadrate head; **qr**, quadrate

ridge; **vqjc**, ventral quadratojugal contact; **vpne**, ventral pneumatopore.

2708

FIGURE 13. Quadrate diversity in basal Coelurosauria and Alvarezsauroidea. Right (**1–2**, **6**)

and left (**3–5**) quadrates of *Bicentenaria argentina* (MPCA 865) in (**1**) anterior, (**2**) lateral, (**3**)

posterior, (**4**) medial, (**5**) dorsal, and (**6**) ventral views. Right quadrate (**7–8**) of *Ornitholestes*

2712 *hermanni* (AMNH FARB 619) in (**7**) lateral, (**8, 10**) posterior, (**9**) posterolateral, and (**11**)

2713 ventral views, (**10**) with details of the central part of the quadrate body (photo courtesy shared

2714 by Mickey Mortimer). Right (**12**–**13**) and left (**14**–**16**) quadrates of *Shuvuuia deserti* (**12**–**13**:

2715 IGM 100-977; **14**–**16**: IGM 100-1001) in (**12**, **14**) posterior, (**13**) posteromedial, (**15**) lateral,

2716 and (**16**) ventral views. Abbreviations: **dpvq**, dorsal projection of the ventral quadratojugal

2717 contact; **ecc**, ectocondyle; **enc**, entocondyle; **ics**, intercondylar sulcus; **lpr**, lateral process;

2718 **mfq**, medial fossa; **oca**, ootic capitulum; **pfl**, pterygoid flange; **pfq**, posterior fossa; **po**,

2719 postorbital; **poc**, postorbital contact; **pt**, pterygoid; **ptc**, pterygoid contact; **qf**, quadrate

2720 foramen; **qh**, quadrate head; **qj**, quadratojugal; **qjc**, quadratojugal contact; **qr**, quadrate ridge;

2721 **sca**, squamosal capitulum; **sq**, squamosal; **vpdq**, ventral projection of the dorsal quadratojugal

2722 contact; **vpne**, ventral pneumatopore; **vqjc**, ventral quadratojugal contact; **vsh**, ventral shelf.
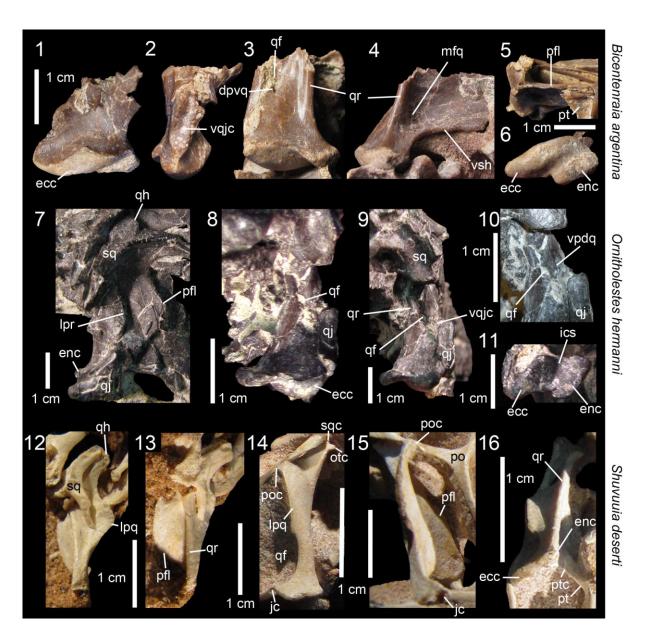
2723

FIGURE 14. Quadrate diversity in Ornithomimosauria and Therizinosauria. Left quadrate (**1**)

of *Struthiomimus altus* (AMNH 5339) in lateral view. Left quadrate (**2**) of *Gallimimus*

bullatus (IGM 100-1133) in ventral view. Right coosified quadrates and quadratojugal (**3–4**)

of *Ornithomimus edmontonicus* (RTMP 95.110.1) in (**1, 3**) lateral and (**2, 4**) lateroposterior

views (courtesy of Rui Tahara and Yoshitsugu Kobayashi). Left coosified quadrate and

quadratojugal (**5**) of *Sinornithomimus dongi* (IVPP−V11797−10) in posterior view (courtesy

of Yoshitsugu Kobayashi, modified). Left (**6**) and right (**7**) coosified quadrates and

quadratojugals of *Garudimimus brevipes* (IGM 100-13) in (**6–7**) posterior view (courtesy of

Yoshitsugu Kobayashi, modified). Right quadrate (**8–12**) of *Falcarius utahensis* (UMNH VP

2734 14559) in (**8**) anterior, (**9**) lateral, (**10**) posterior, (**11**) medial, and (**12**) ventral views (courtesy

2735 of Lindsay Zanno). Abbreviations: **dqjc**, dorsal quadratojugal contact; **ecc**, ectocondyle; **enc**,

2736 entocondyle; **exo**, exoccipital; **j**, jugal; **la**, lacrimal; **mpne**, medial pneumatopore; **pfq**,

2737 posterior fossa; **po**, postorbital; **ppne**, posterior pneumatopore; **qf**, quadrate foramen; **qh**,

2738 quadrate head; **qj**, quadratojugal; **pfq**, posterior fossa; **ppne**, posterior pneumatopore; **sq**,

2739 squamosal; **vqjc**, ventral quadratojugal contact.
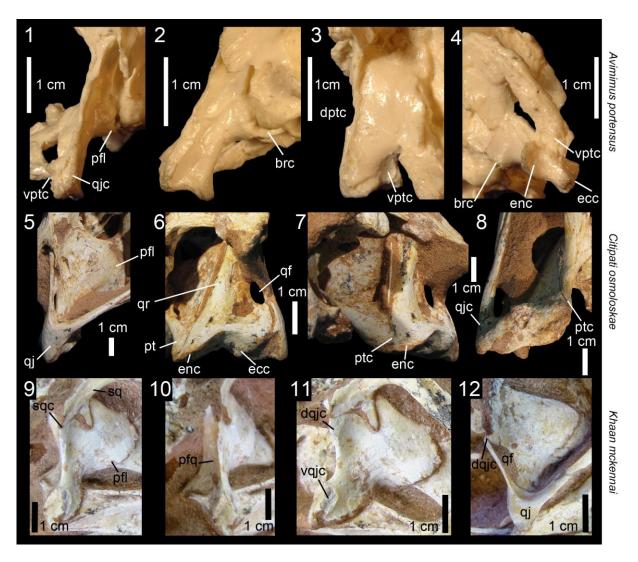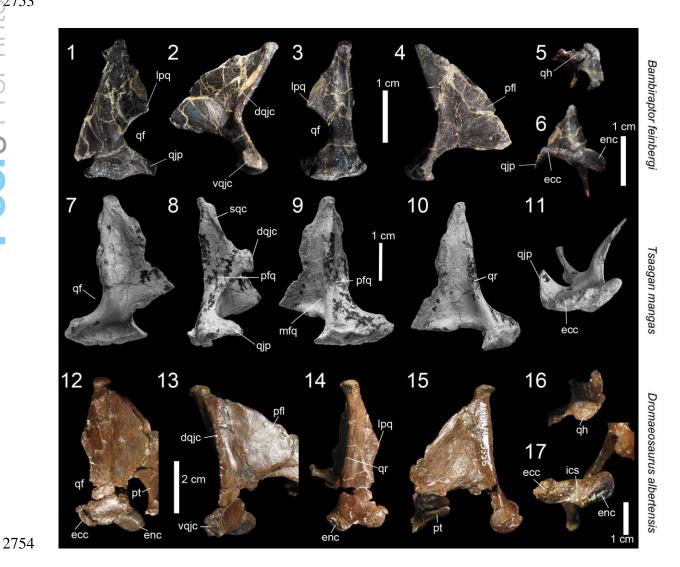
2740

2741

2742 **FIGURE 15.** Quadrate diversity in Oviraptorosauria. Occipital part of the cranium (**1–4**) of

2743 *Avimimus portentosus* (cast of PIN 3907/1) in (**1**) lateral, (**2**) posterior, (**3**) anterolateral, and

2744 (**4**) ventral views (courtesy of Lawrence Witmer). Right quadrate (**5–8**) of *Citipati osmolskae*

2745 (IGM 100-978) in (**5**) lateral, (**6**) posterior, (**7**) medioposterior, and (**8**) ventral views. Right

quadrate (**9–12**) of *Khaan mckennai* (IGM 100-1127 for 9–11, IGM 100-1002 for 12) in (**9, 12**) lateral, (**10**) posterolateral, and (**11**) anterolateral views. Abbreviations: **brc**, braincase contact; **dptc**, dorsal pterygoid contact; **dqjc**, dorsal quadratojugal contact; **ecc**, ectocondyle; **enc**, entocondyle; **pfl**, pterygoid flange; **pfq**, posterior fossa; **pt**, pterygoid; **ptc**, pterygoid contact; **qf**, quadrate foramen; **qj**, quadratojugal; **qjc**, quadratojugal contact; **qr**, quadrate ridge; **sq**, squamosal; **sqc**, squamosal contact; **vptc**, ventral pterygoid contact; **vqjc**, ventral quadratojugal contact.

FIGURE 16. Quadrate diversity in Dromaeosauridae. Left quadrate (**1–6**) of *Bambiraptor feinbergi* (AMNH 30556) in (**1**) anterior, (**2**) lateral, (**3**) posterior, (**4**) medial, (**5**) dorsal, and (**6**) ventral views. Right quadrate (**7–11**) of *Tsaagan mangas* (IGM 100-1015) in (**7**) anterior,

2758   (**8**) lateral, (**9**) posterior, (**10**) medial, and (**11**) ventral views (courtesy of Mick Ellison). Right

2759   quadrate (**12–17**) of *Dromaeosaurus albertensis* (AMNH 5356) in (**12**) anterior, (**13**) lateral,

2760   (**14**) posterior, (**15**) medial, (**16**) dorsal, and (**17**) ventral views. Abbreviations: **dqjc**, dorsal

2761   quadratojugal contact; **ecc**, ectocondyle; **enc**, entocondyle; **ics**, intercondylar sulcus; **lpq**,

2762   lateral process; **mfq**, medial fossa; **pfl**, pterygoid flange; **pfq**, posterior fossa; **pt**, pterygoid;

2763   **qf**, quadrate foramen; **qh**, quadrate head; **qjp**, quadratojugal process; **qr**, quadrate ridge; **sqc**,

2764   squamosal contact; **vqjc**, ventral quadratojugal contact; **vptc**, anteroventral pterygoid contact.

2765

2767 **TABLE 1.** Nonavian theropod specimens and clades examined and scored in the cladistic

2768 analysis. Taxa and clades with an asterisk were used in the phylogenetic morphometric

2769 analysis. Abbreviations: **Y**, Yes; **N**, No.

Taxon	Specimens	Examined	Photo credits	Literature
Eoraptor lunensis Sereno et al., 1993	PVSJ 512	Y	Martín Ezcurra	Sereno et al., 2013
Herrerasaurus ischigualastensis Reig, 1963	PVSJ 53, 407	Y	Martín Ezcurra	
Eodromaeus murphi Martinez et al., 2011	PVSJ 562	Y		
Tawa hallae* Nesbitt et al., 2009	GR 241	N	Sterling Nesbitt	Nesbitt et al., 2009
'*Syntarsus*' *kayentakatae* Rowe, 1989	MNA V2623	N	Ronald Tykoski; Randall Irmis	Rowe, 1989
Liliensternus liliensterni von Huene, 1934	MB R.2175	N	Martín Ezcurra	von Huene, 1934
Dilophosaurus wetherilli* Welles, 1954	UCMP 37302	N	Randall Irmis; Martín Ezcurra; Mathew Carrano	Welles, 1984
Ceratosaurus nasicornis* Marsh, 1884	USNM 4735; MWC 1	Y	Mathew Carrano	(Madsen and Welles, 2000)

Noasaurus leali Bonaparte and Powell, 1980	PVL 4061	Y		
Masiakasaurus knopfleri* Sampson et al. 2001	FMNH PR 2496	Y	Mathew Carrano	
Abelisaurus comahuensis Bonaparte and Novas, 1985	MPCA 11098	Y		
Ilokelesia aguadagrandensis Coria and Salgado, 1998	MCF PVPH 35	Y	Matthew Lamanna	
Carnotaurus sastrei Bonaparte, 1985	MACN CH 894	Y	Pablo Asaroff	
Aucasaurus garridoi Coria et al., 2002	MCF-PVPH-236	Y		
Majungasaurus crenatissimus* Lavocat, 1955	FMNH PR 2100	Y	Lawrence Witmer	
Cryolophosaurus ellioti Hammer and Hickerson, 1994	FMNH PR1821	N	Nathan Smith	Smith et al., 2007
Monolophosaurus jiangi Zhao and Currie, 1993	IVPP 84019	N		Zhao and Currie 1993; Brusatte, et al. 2010a
Eustreptospondylus oxoniensis* Walker, 1964	OUMNH J.13558	N	Paul Barrett	
Afrovenator abakensis*	UC OBA1	N	Roger Benson;	

Sereno et al., 1994			Juan Canale;	
			Mathew Carrano	
Torvosaurus tanneri Galton and Jensen, 1979	BYUVP 9246	Y	Matthew Lamanna	
Baryonyx walkeri* Charig and Milner, 1986	BMNH R9951	Y	Eric Buffetaut	
Suchomimus tenerensis Sereno et al., 1998	MNN GAD 502	Y	Steve Brusatte	
Irritator challengeri Martill et al., 1996	SMNS 58022	Y		
Spinosaurinae morphotype I*	MSNM V6896; WDC-CSG uncatalogued	Y		
Spinosaurinae morphotype II	WDC-CSG uncatalogued	Y		
Allosaurus fragilis* Marsh, 1877	BYU VP8901	Y		Osborn, 1912; Gilmore, 1920; Madsen, 1976b; Chure, 2000
Allosaurus europaeus Mateus et al., 2006	ML 415	Y		
Allosaurus 'jimmadseni'*	SMA	Y		

Chure, 2000	005/02			
*Aerosteon riocoloradensis** Sereno et al., 2008	MCNA-PV-3137	N	Martin Ezcurra	
*Sinraptor dongi** Currie and Zhao, 1993b	IVPP 10600	N	Philip Currie	Currie, 2006
*Acrocanthosaurus atokensis** Stovall and Langston Jr, 1950	NCSM 14345	Y	Drew Eddy; Vince Shneider	
*Shaochilong maortuensis** Brusatte, Benson, et al., 2009	IVPP V2885.3	N	Steve Brusatte	Brusatte, Benson, et al., 2009; Brusatte, Chure, et al., 2010
Mapusaurus roseae Coria and Currie, 2006	MCF PVPH 108.102	Y	Matthew Lamanna	
*Giganotosaurus carolinii** Coria and Salgado, 1995	MUCPv-CH-1	Y	Matthew Lamanna	
Ornitholestes hermanni Osborn, 1903	AMNH FARB 619	Y	Mickey Mortimer	
Bicentenaria argentina Novas et al., 2012	MPCA 865	Y		
Zuolong salleei Choiniere, Clark, et al., 2010	IVPP V15912	N		Choiniere, Clark, et al., 2010
Proceratosaurus bradleyi von Huene, 1926	NHM R 4860	Y		Rauhut et al., 2010

Eotyrannus lengi Hutt et al., 2001	MIWG 1997.550	Y	Darren Naish	
Xionggualong baimoensis Li et al., 2010	FRDC-GS JB16-2-1	N		Li et al., 2010
Alioramus altai Brusatte, Carr, et al., 2009	IGM 100-1844	N	Mick Ellison	Brusatte et al., 2012; Gold et al., 2013
Albertosaurus sarcophagus Osborn, 1905	RTMP 81.10.1; FMNH PR308; CMN 12; CMN 2120	N		Carr, 1996; Currie, 2003
Daspletosaurus sp. Russell, 1970	RTMP 94.143.1	N		Currie, 2003
Tyrannosaurus rex* Osborn, 1905	AMNH 5027; FMNH PR2081	Y	Mickey Mortimer	Molnar, 1991; Brochu, 2003; Larson, 2008
Garudimimus brevipes Barsbold, 1981	IGM 100-13	N	Yoshitsugu Kobayashi	Kobayashi and Barsbold, 2005
Sinornithomimus dongi Kobayashi and Lü, 2003	IVPP−V11 797−10	N	Yoshitsugu Kobayashi	Kobayashi and Lü, 2003
Shuvuuia deserti Chiappe et al., 1998	IGM 100-977, 100-	Y		Dufeau, 2003

	1001			
Falcarius utahensis* Kirkland et al., 2005	UMNH VP 14559	N	Lindsay Zanno	Zanno, 2010
Erlikosaurus andrewsi Barsbold and Perle, 1980	PST 100-111	N	Stephan Lautenschlager	Clark et al., 1994
Avimimus portentosus Kurzanov, 1981	PIN 3907/1	N	Lawrence Witmer	Kurzanov, 1985; Vickers-Rich et al., 2002
Oviraptoridae* Barsbold, 1986	AMNH FARB 6517; IGM 100-1002; IGM 100-1127; IGM 100-978	Y		Maryańska and Osmólska, 1997; Clark et al., 2002; Kundrát and Janáček, 2007; Balanoff and Norell, 2012
Buitreraptor gonzalezorum Makovicky et al., 2005	MPCA 245	Y	Martín Ezcurra	
Bambiraptor feinbergi* Burnham et al., 2000	FIN 001	Y	David Burnham	
Tsaagan mangas* Norell et al., 2006	IGM 100-1015	Y	Mick Ellison	
Dromaeosaurus albertensis Matthew and Brown, 1922	AMNH 5356	Y		
Troodontidae Gilmore, 1924	IGM 100-1083; IGM	Y	Rui Pei	Barsbold et al., 1987; Norell and

100-1128;

IGM 100-

1323

Hwang, 2004; Xu

and Norell, 2004;

Hu et al., 2009;

Xu et al., 2011;

Gao et al., 2012

2770